Quantum gas microscopy (Lecture I): Nuts & bolts of microscopy, correlations in half-filled systems

Waseem Bakr

PRINCETON UNIVERSITY

Boulder Summer School 2021

Quantum simulations with ultracold atoms

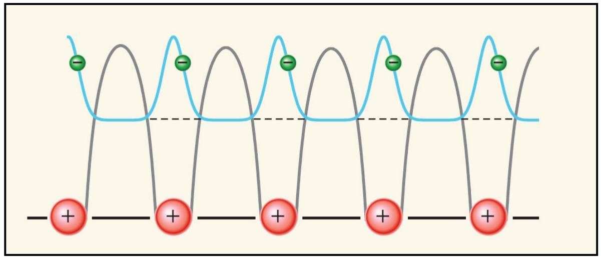

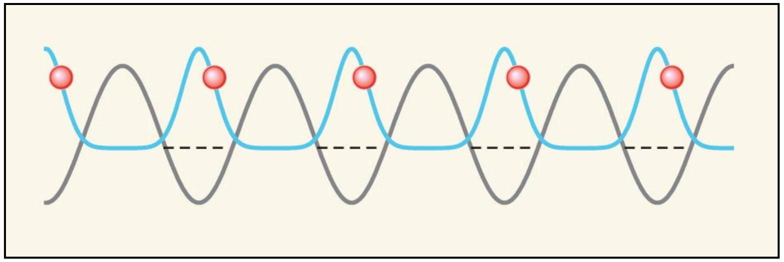

Why use ultracold atoms for quantum simulations?

- Complete control of microscopic parameters
- Clean systems, no impurities
- Dynamics on observable timescales (typically milliseconds)
- Understood from first principles
- Large interparticle spacing makes optical imaging/manipulation possible

Outline of talks

- Lecture 1: Nuts & bolts of quantum gas microscopy, microscopy of Bose-Hubbard systems, Fermi-Hubbard at half-filling.
- Lecture 2: Exploring doped Fermi-Hubbard systems with conventional probes: transport, ARPES, etc.
- Lecture 3: Microscopy of doped Fermi-Hubbard systems, new directions.

Probing ultracold gases: absorption imaging

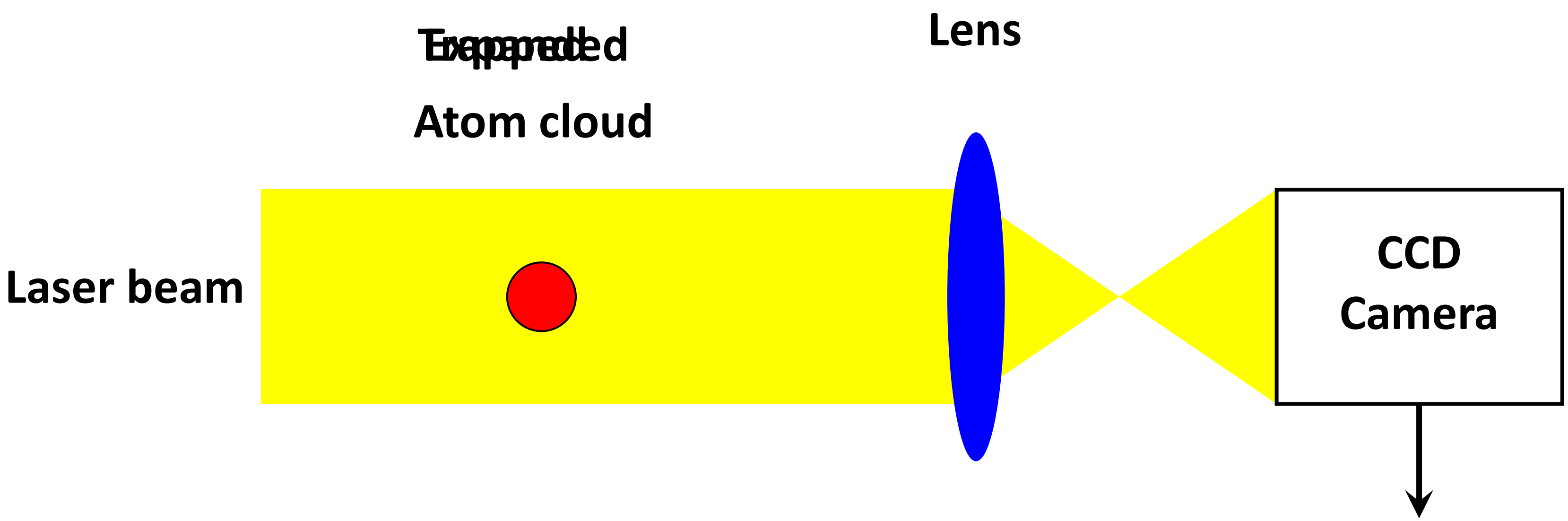

Analyzing shadow of cloud on beam, can extract:

- Total number of atoms in cloud.
- Temperature from the rate of expansion of the cloud.

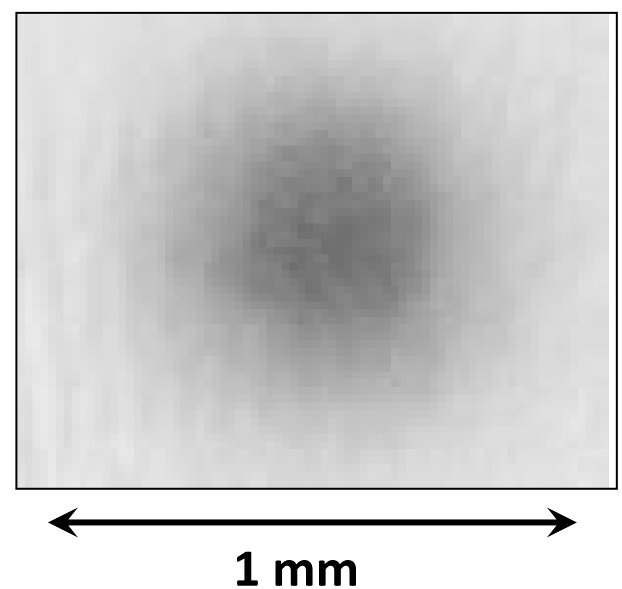

New possibilities with single-atom/single-site microscopy

- Imaging local density/spin fluctuations and correlations

- Local manipulation of atoms (e.g. dynamics after a spin flip, quantum gates)

- Patterning potential landscapes for Hamiltonian engineering.

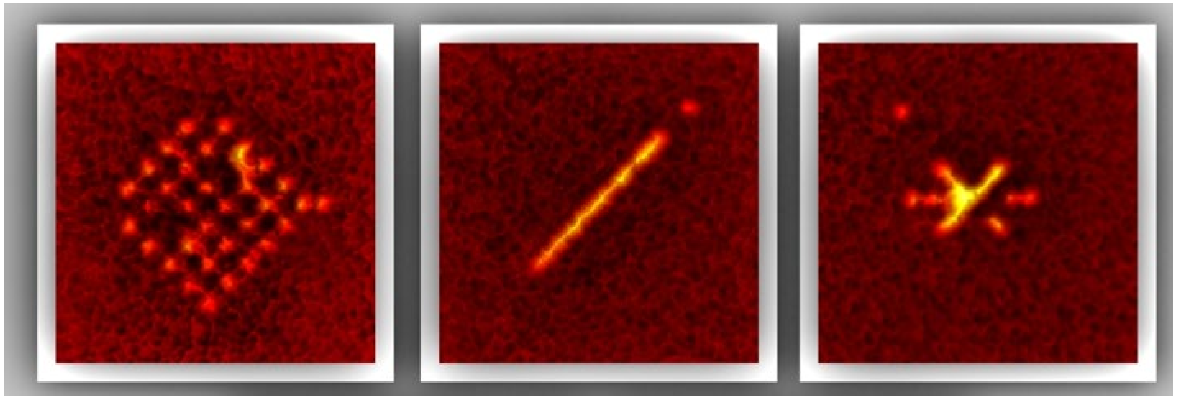

Bloch group (Munich)

Requirements for single-site microscopy

1. High-resolution optics

Length-scales:

Lattice spacing & thermal de Broglie wavelength: $\sim 0.5\ \mu$m
Size of atom: $\sim$ 1 Angstrom
Wavefunction size on a lattice site: $\sim$ 100 nm
Imaging resolution: given by Rayleigh criterion.

$$\delta x = 0.61\ \lambda/NA$$

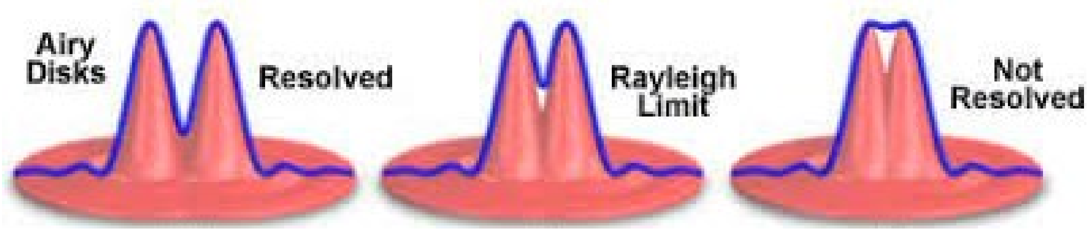

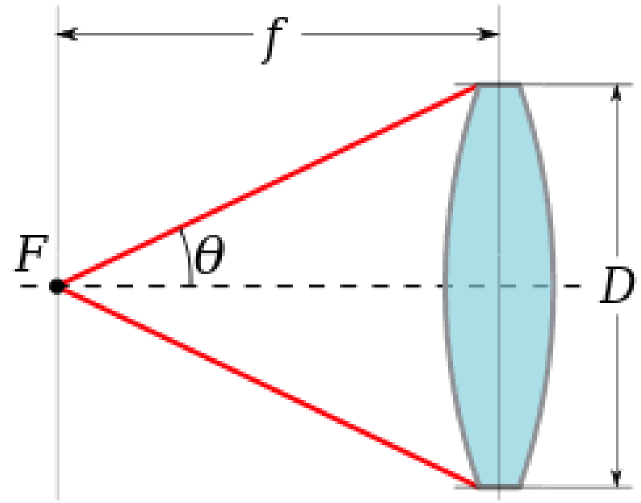

Requirements for single-site microscopy

1. High-resolution optics: typical NA 0.5 to 0.9, ``solid immersion” used to reach highest numerical apertures.

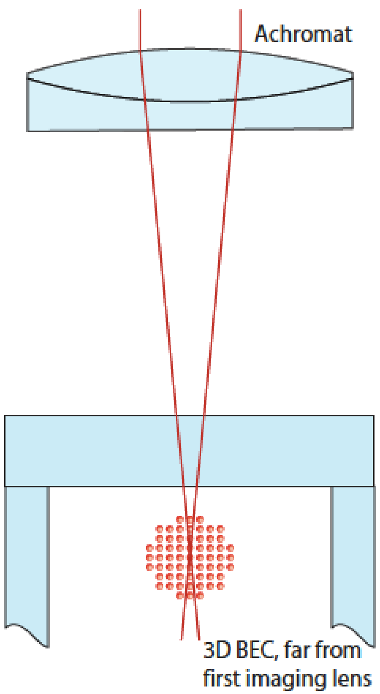

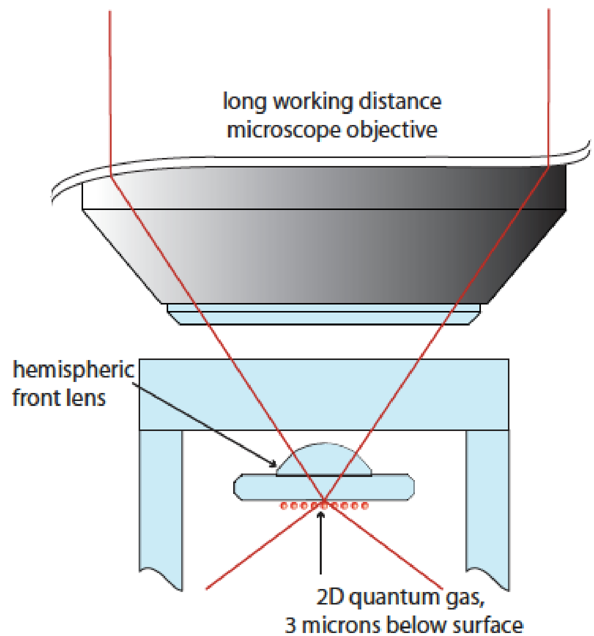

Greiner group

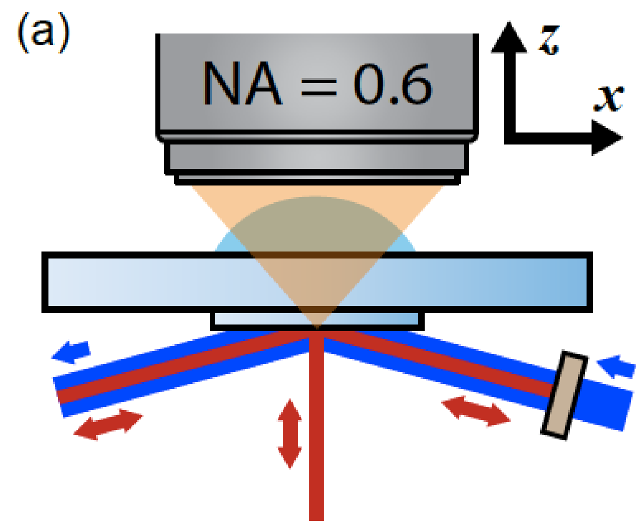

Zwierlein group

Requirements for single-site microscopy

1. High-resolution optics: special care to reach diffraction limit (correction for vacuum window thickness, careful alignment of optics)

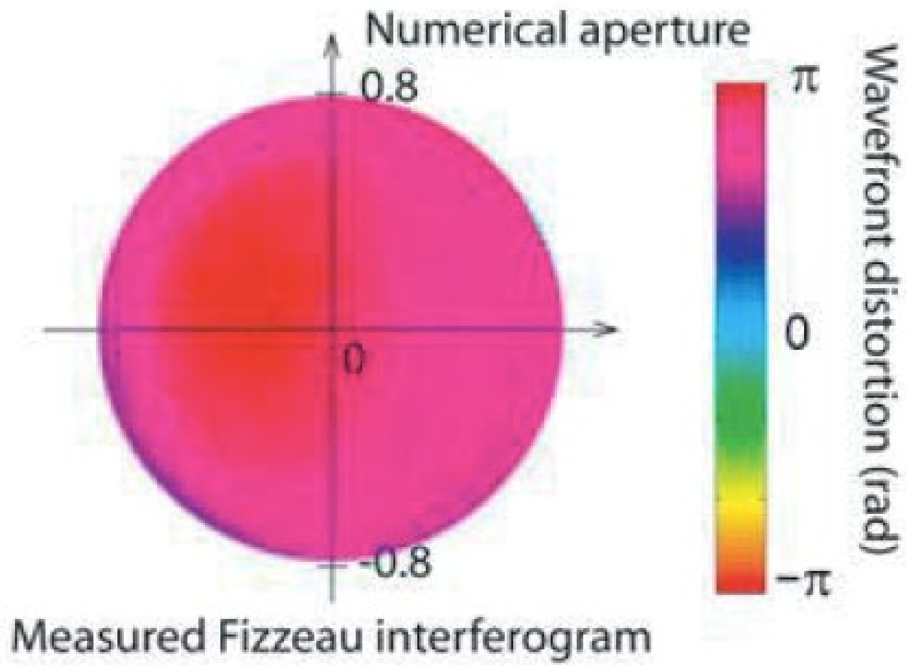

Greiner group

Requirements for single-site microscopy

2. Preparation of a single layer quantum gas.

Depth of focus $\sim 1\ \mu$m

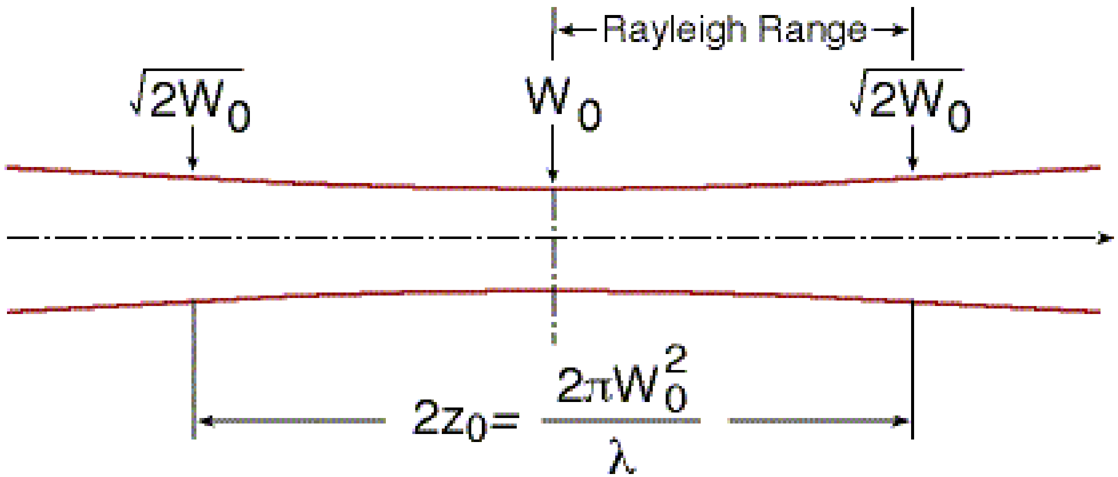

Requirements for single-site microscopy

2. Radiofrequency selection of a single layer.

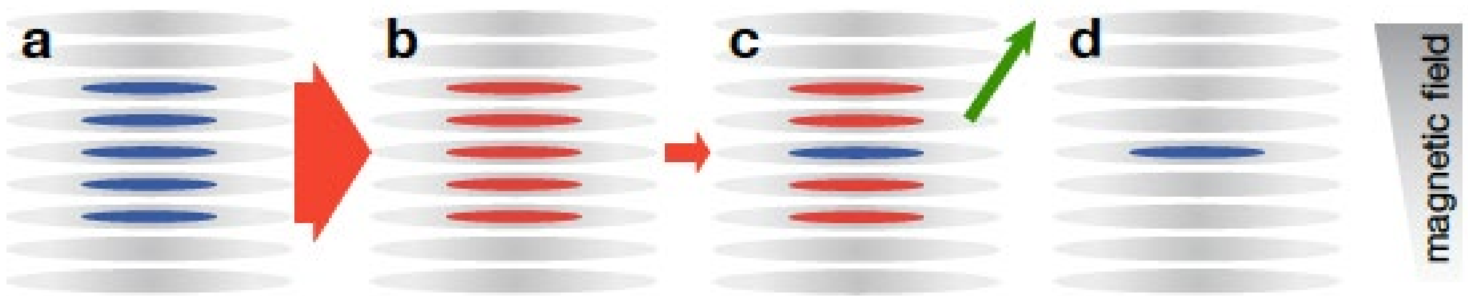

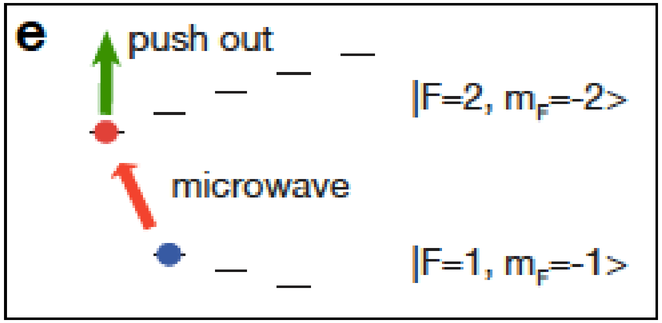

Bloch group

Requirements for single-site microscopy

2. Compress 3D cloud into 2D.

Evanescent wave trap

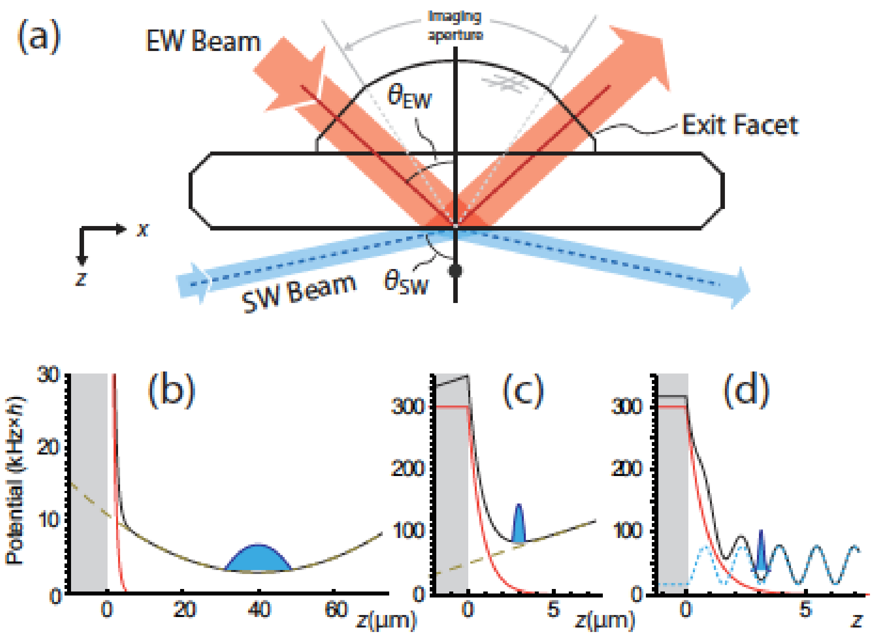

Accordion lattice

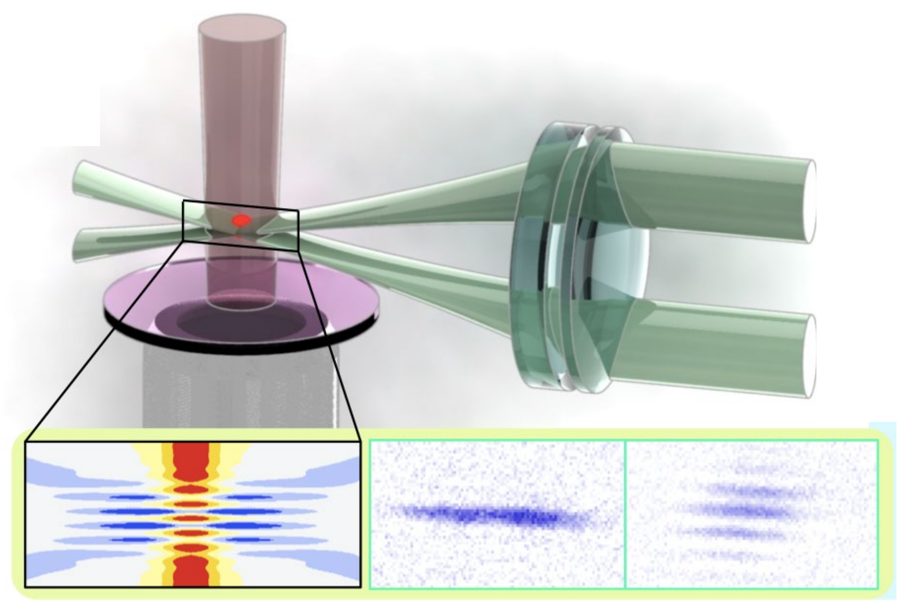

Greiner group

Bakr group

Requirements for single-site microscopy

3. Achieving sufficient signal to noise.

Noise sources: camera dark counts, readout noise, photon shot noise.
The bad: PSF ~ lattice spacing
The good: atoms are on a known grid
Bottomline: need around 1000 photons collected per atom
High NA helps with collection efficiency (typically around 5-10%)

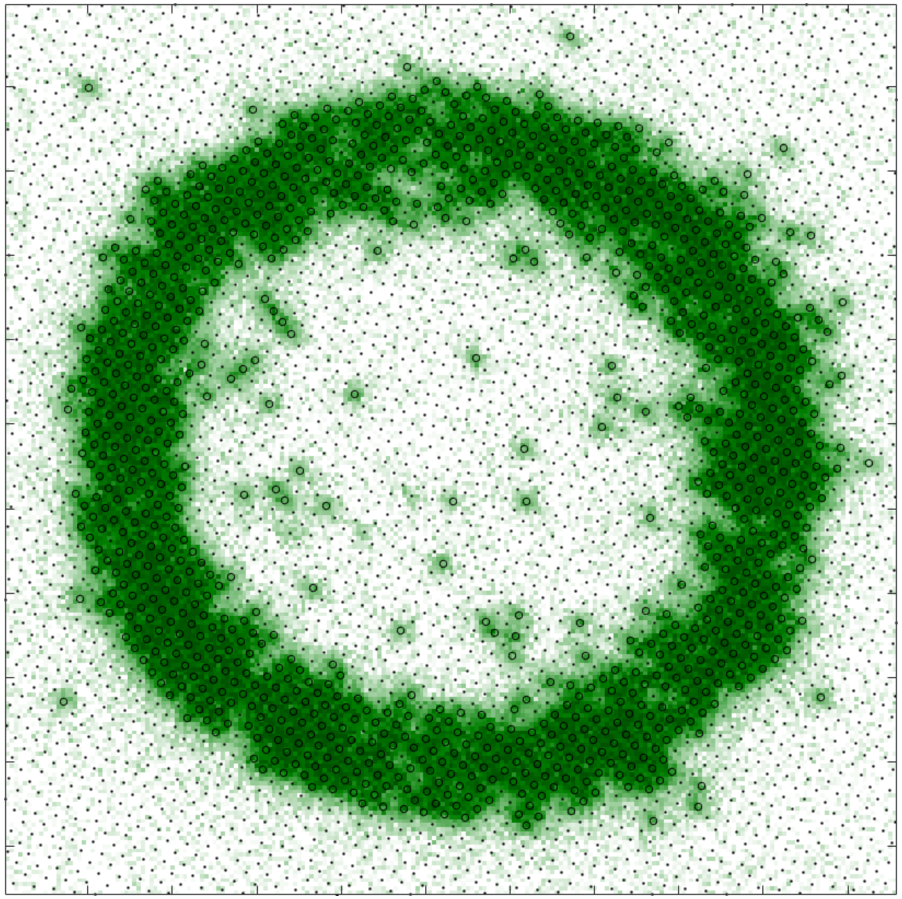

Requirements for single-site microscopy

3. Achieving sufficient signal to noise.

Use a deep lattice (0.3 – 1 mK, few thousand recoil energies)

Helps less than you might think … stochastic heating is a problem.

Options for deep lattice:
- High power
- (tens of W in 100 um)
- Near resonant lattices.

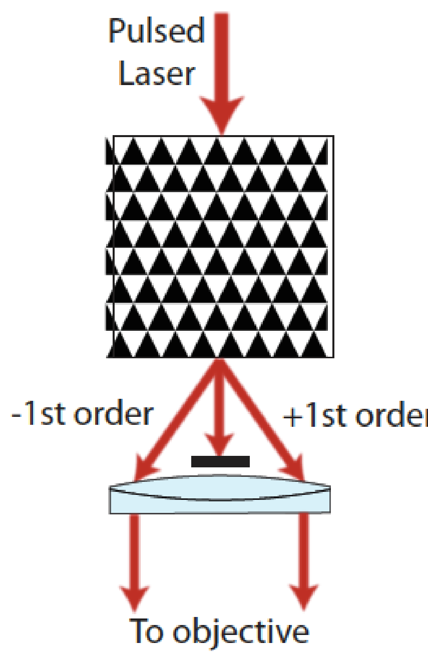

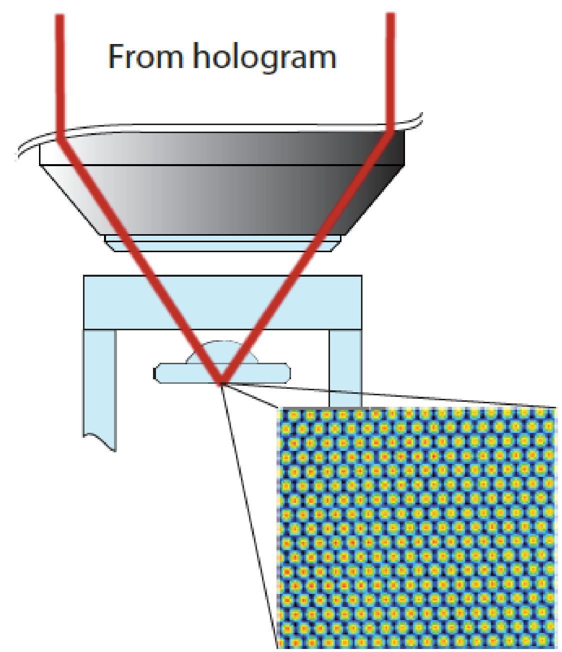

Greiner group

Requirements for single-site microscopy

3. Achieving sufficient signal to noise.

Start with quantum gas at nK temperatures.
Pin in deep lattice.
Shine near resonant light in cooling configuration -> gas heats up.
Need equilibrium temperature < ~1/10 of lattice depth to avoid hopping / loss.

Some options:
1. Polarization gradient cooling.
2. Raman-sideband cooling.

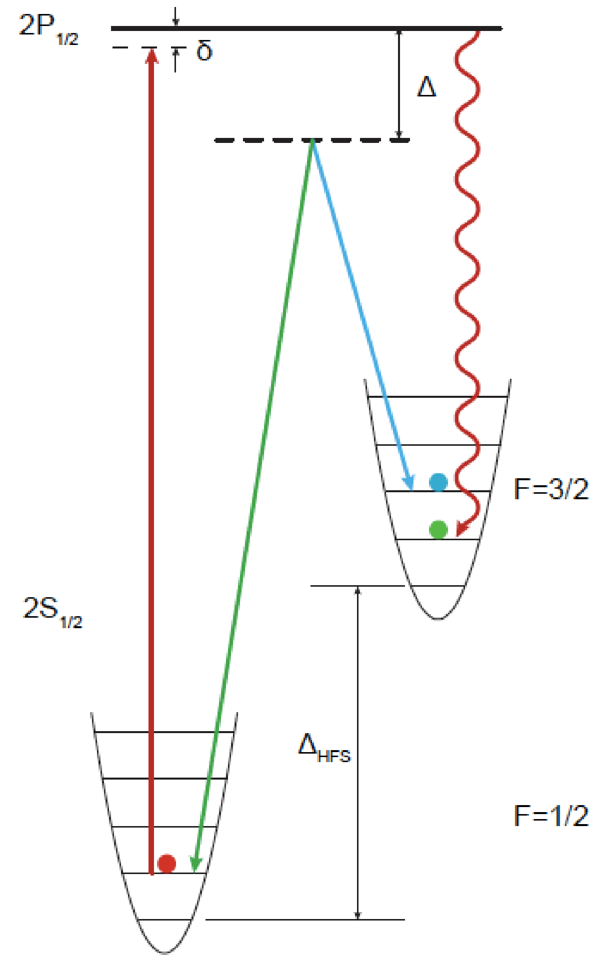

$$F_{n\to n'} = \langle n' | \exp(ik_z z) | n\rangle = \langle n' | \exp(i\eta(\hat{a}+\hat{a}^\dagger)) | n\rangle$$

$$\eta = k_z z_0 \qquad \exp(i\eta(\hat{a}+\hat{a}^\dagger)) = 1 + i\eta(\hat{a}+\hat{a}^\dagger) + O(\eta^2)$$

Atoms hopping in a lattice

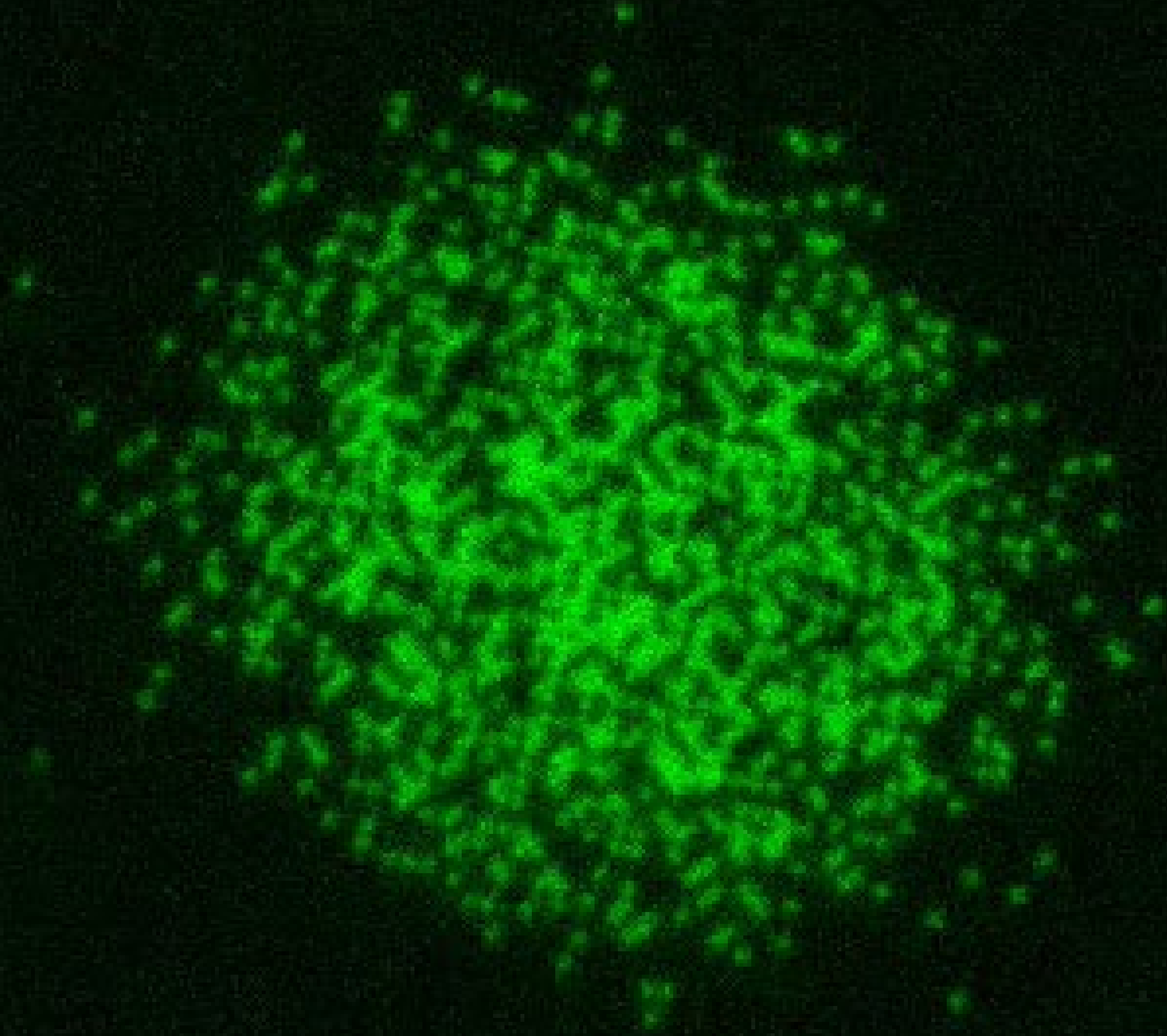

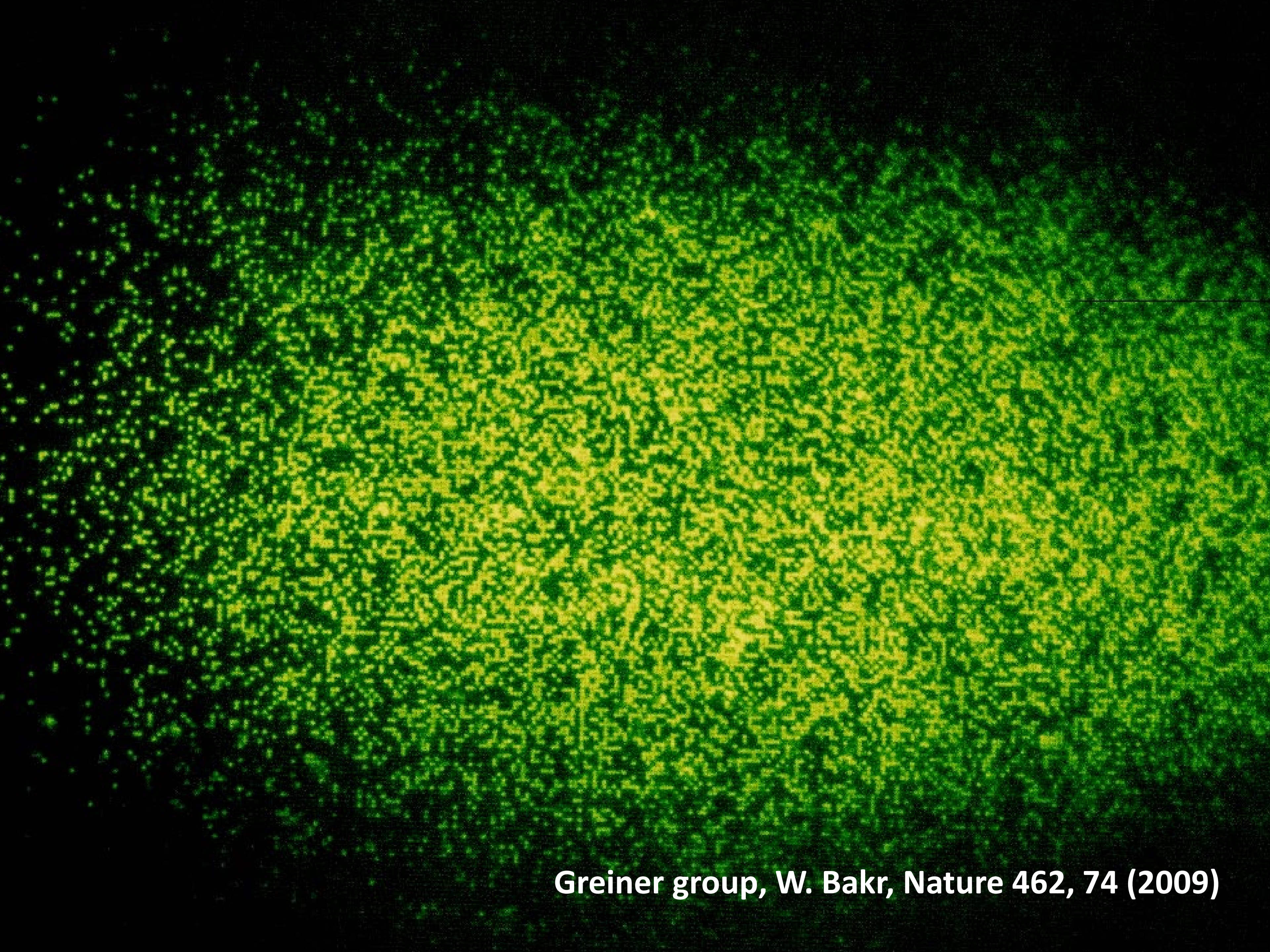

Greiner group, W. Bakr, Nature 462, 74 (2009)

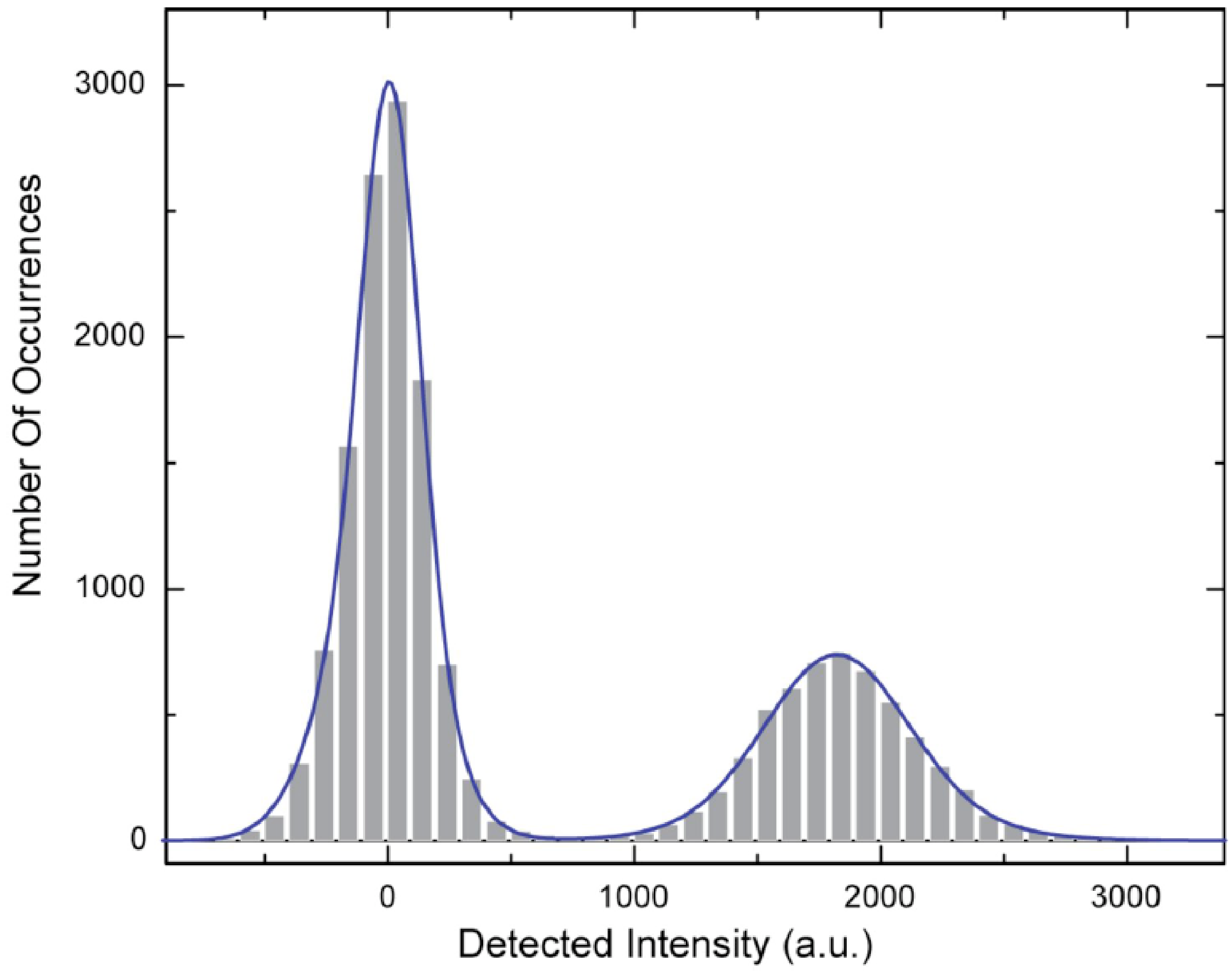

Typical exposure: 1 s, around 1000 photons collected per atom
Typical probability of hopping/loss during exposure: ~ 1%.

Quantum gas microscopy: what can it detect?

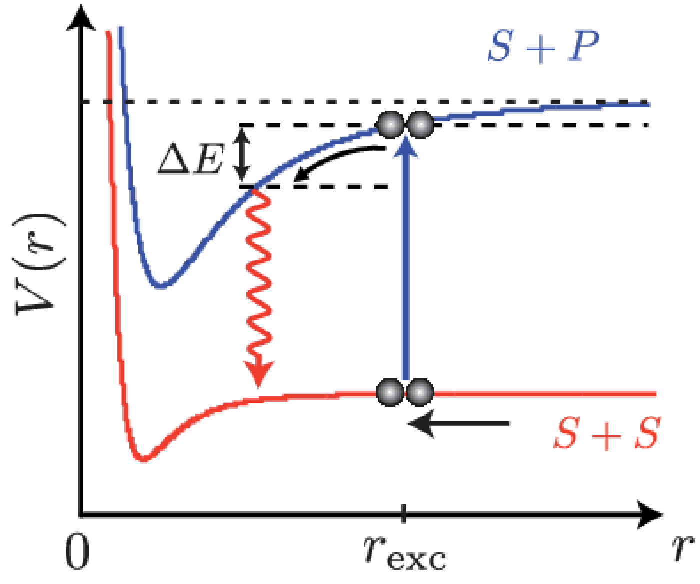

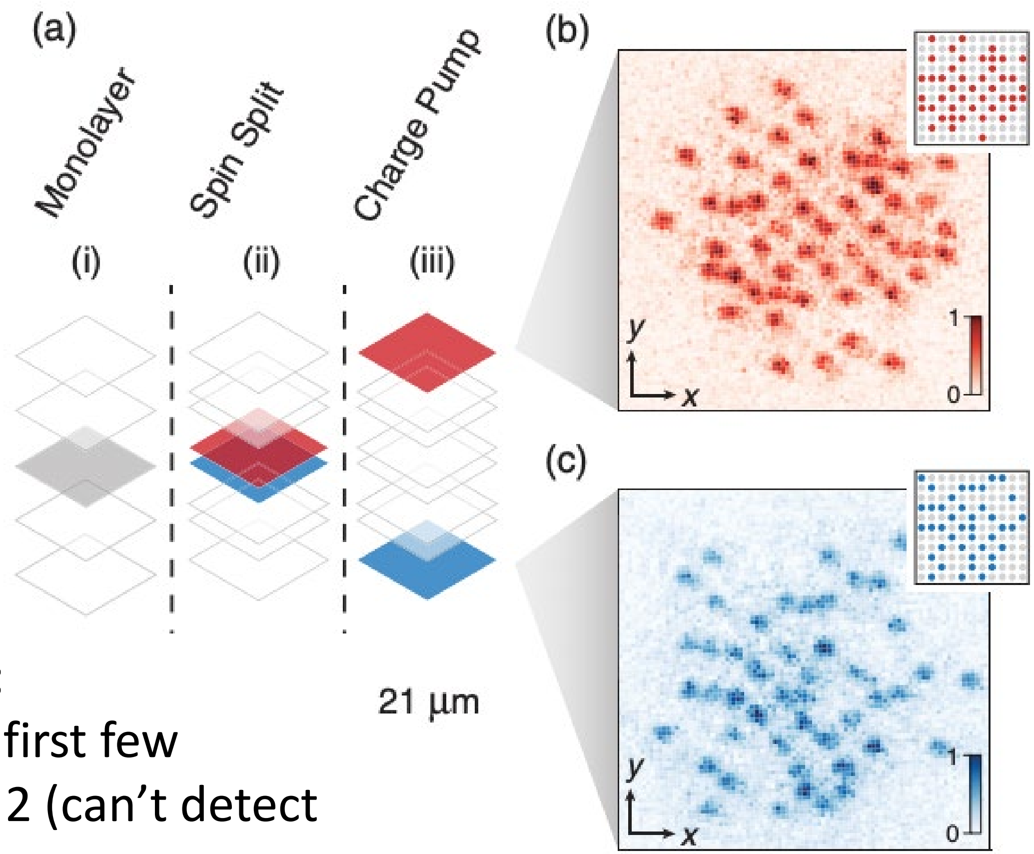

"Standard" quantum gas microscopy:

- Pairwise ejection of atoms within first few photons -> atom number modulo 2 (can't detect Fermi-Hubbard doublons).
- Spin jumbled up due to optical pumping processes.

Koepsell .. Gross, PRL 125, 010403 (2020)

Less standard: Bilayers + Stern-Gerlach circumvent these issues.

Single spin addressing

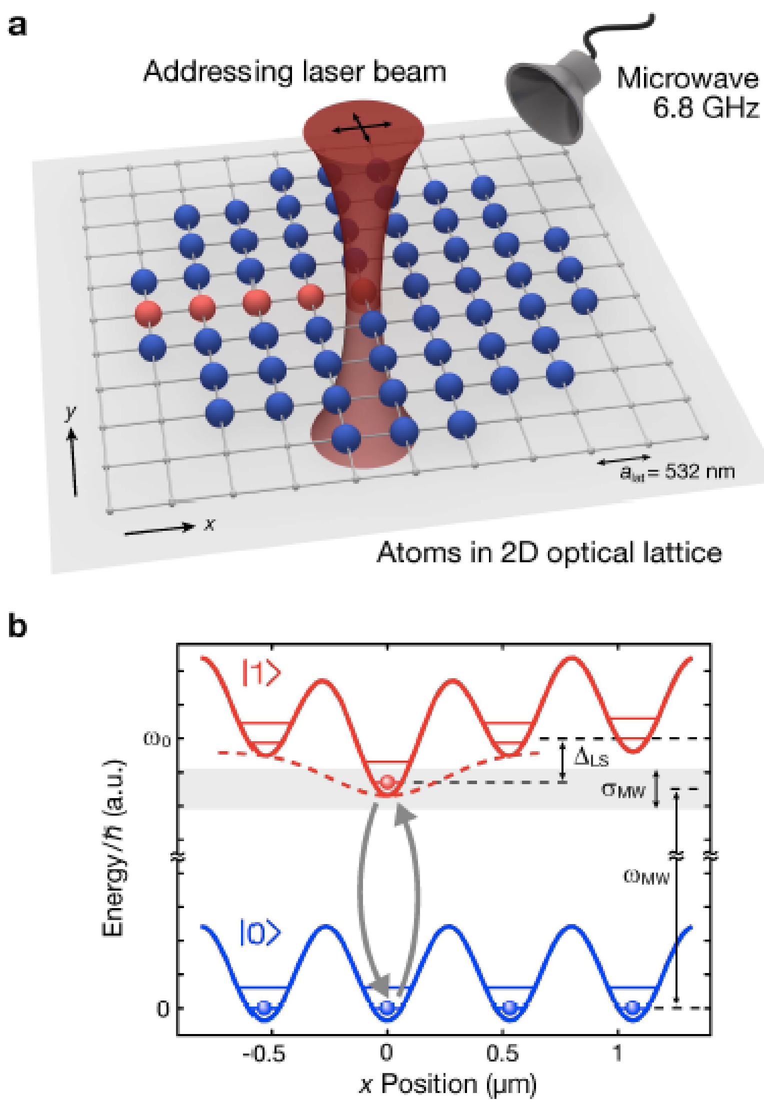

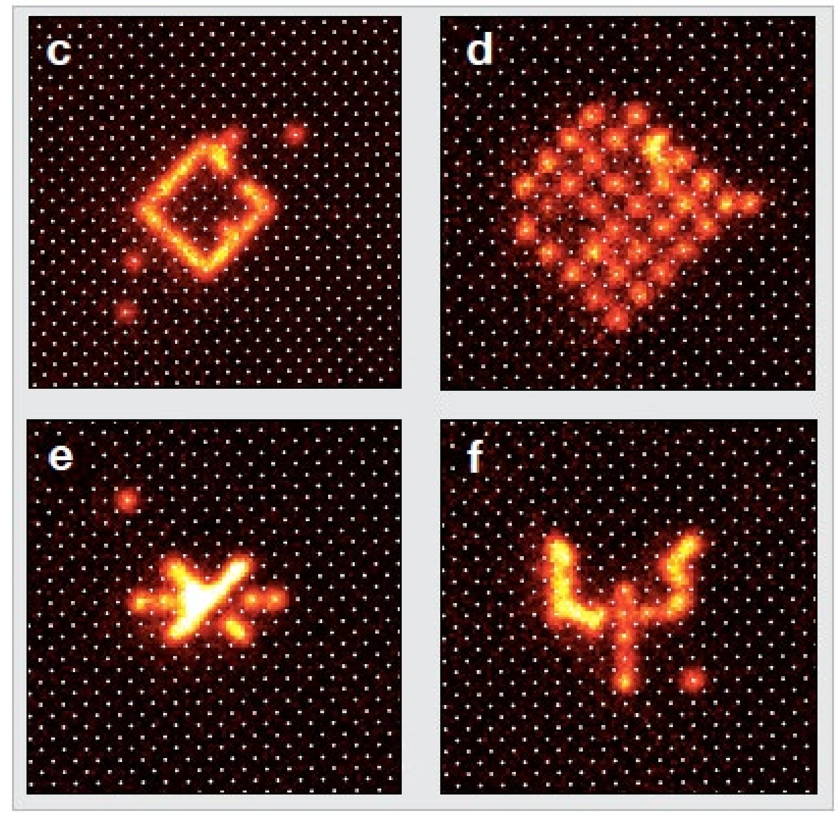

C. Weitenberg … S. Kuhr,
Nature 471, 319 (2011)


QUESTIONS

Bose-Hubbard Hamiltonian

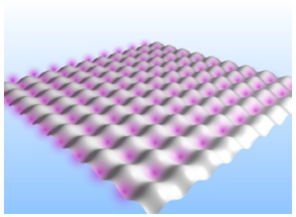

$$H = -J\sum_{\langle i,j\rangle}\hat{a}_i^\dagger\hat{a}_j + \frac{1}{2}U\sum_i\hat{n}_i(\hat{n}_i-1)$$

Tunneling term:

J: *tunneling matrix element*

$\hat{a}_i^\dagger\hat{a}_j$: *tunneling from site j to site i*

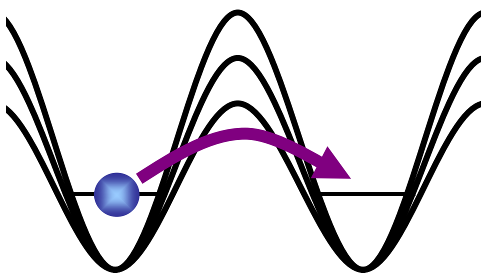

Interaction term:

U : *on-site interaction matrix element*

$\hat{n}_i(\hat{n}_i-1)$: *n atoms collide with n-1 atoms on same site*

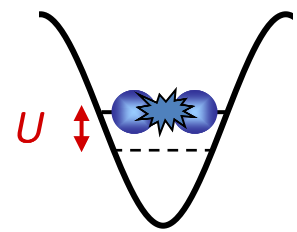

Ratio between tunneling J and interaction U can be widely varied by changing depth of 3D lattice potential!

M.P.A. Fisher et al, PRB 40, 546 (1989), D. Jaksch et al., PRL 81, 3108 (1998)

Superfluid – Mott insulator phase transition

Superfluid:

$$H = -J\sum_{\langle i,j\rangle}\hat{a}_i^\dagger \hat{a}_j + \cancel{\frac{1}{2}U\sum_i \hat{n}_i(\hat{n}_i - 1)}$$

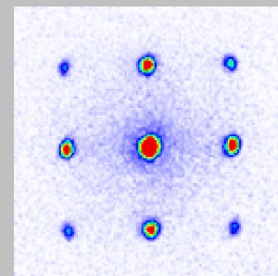

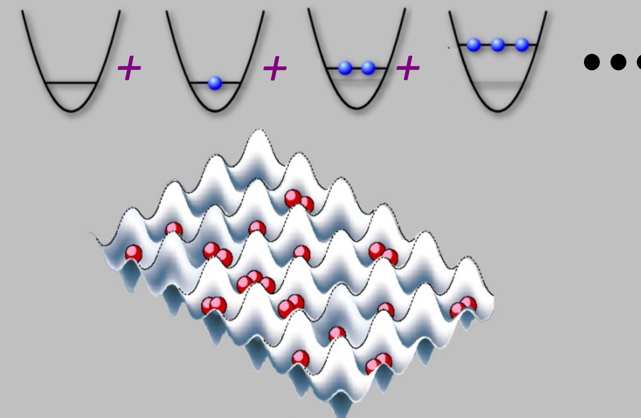

Atoms are delocalized over the entire lattice !

Mott Insulator:

$$H = \cancel{-J\sum_{\langle i,j\rangle}\hat{a}_i^\dagger \hat{a}_j} + \frac{1}{2}U\sum_i \hat{n}_i(\hat{n}_i - 1)$$

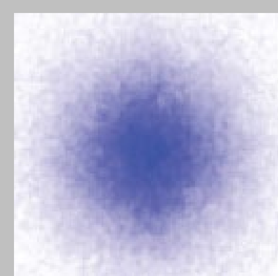

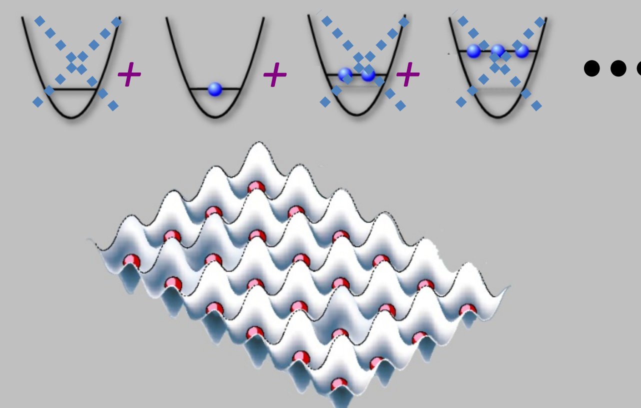

Atoms are localized to lattice sites !

Greiner et al., Nature 415 (2002)

Atom number squeezing across the transition

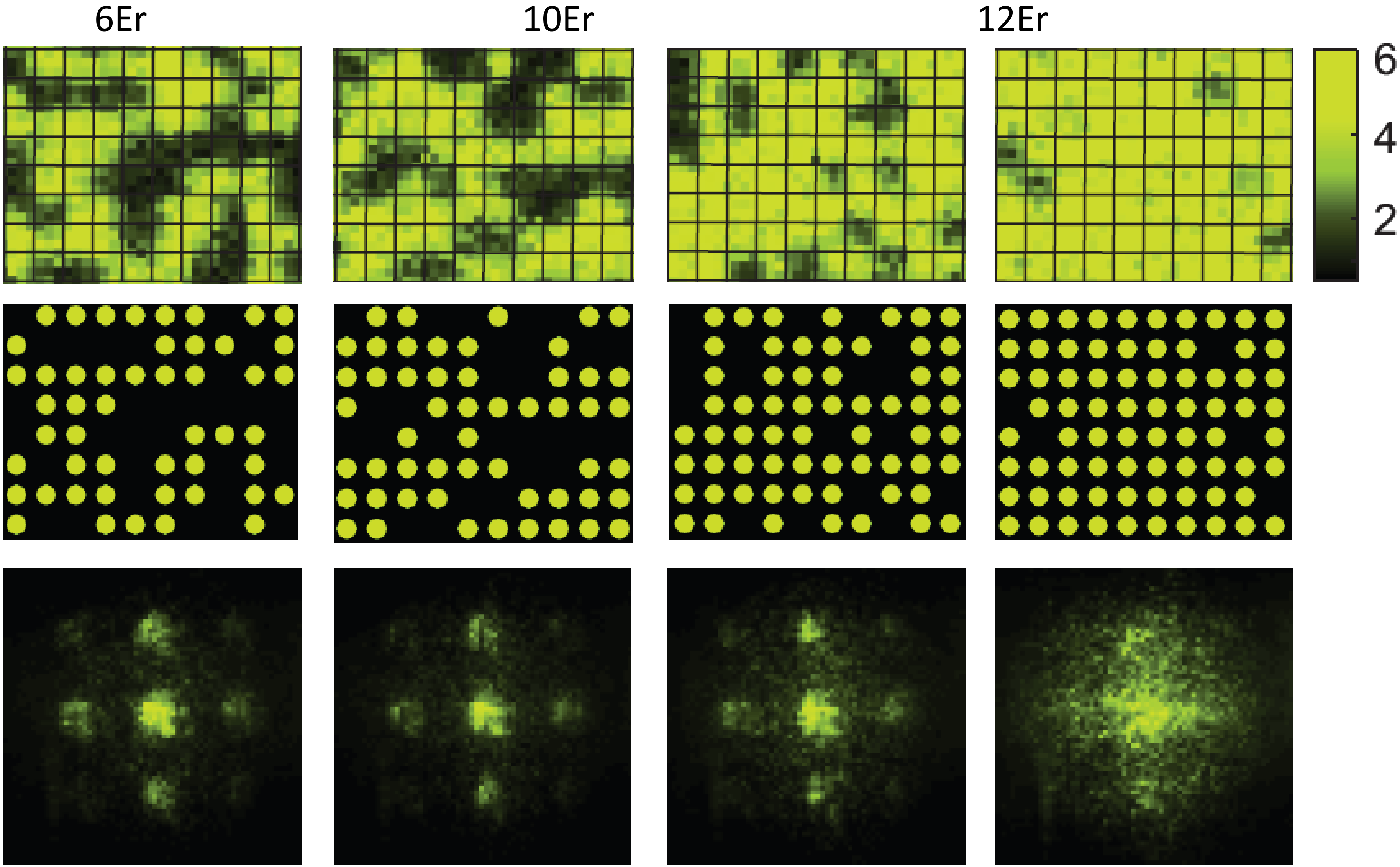

W. Bakr *et al.*, **Science** 329, 547-550 (2010)

Shell structure in a harmonic trap

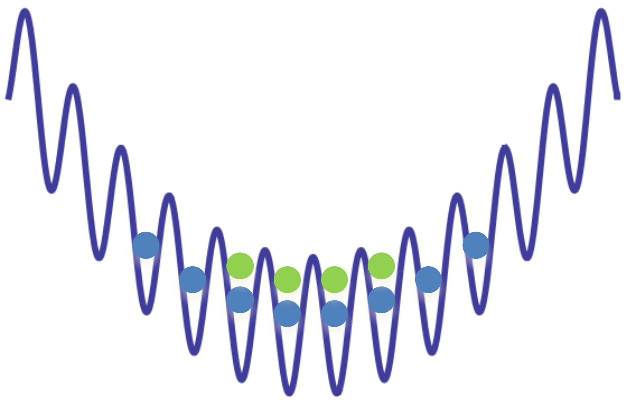

Shell structure with MI
of 3 – 2 – 1 atoms/site

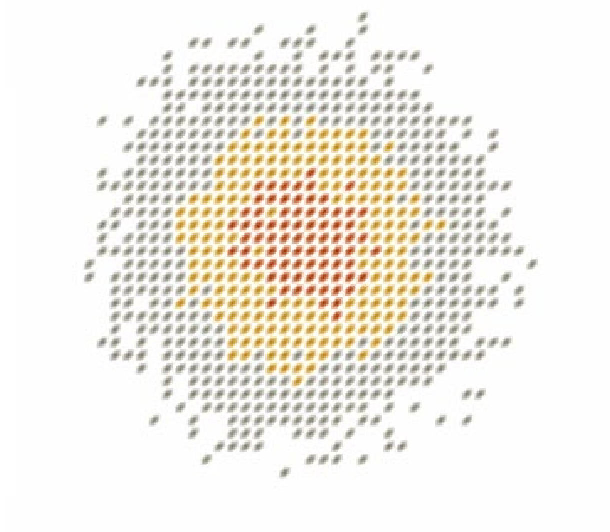

Expected population
on lattice sites

Detection as
1 – 0 – 1 atoms/site

Odd/Even detection
(N mod 2)

Shells detected in density (Bloch, Ketterle, Chin)

Single site imaging of shell structure

W. Bakr *et al.*,
Science 329, 547 (2010)

Sherson *et al.*, Nature
467, 68 (2010)

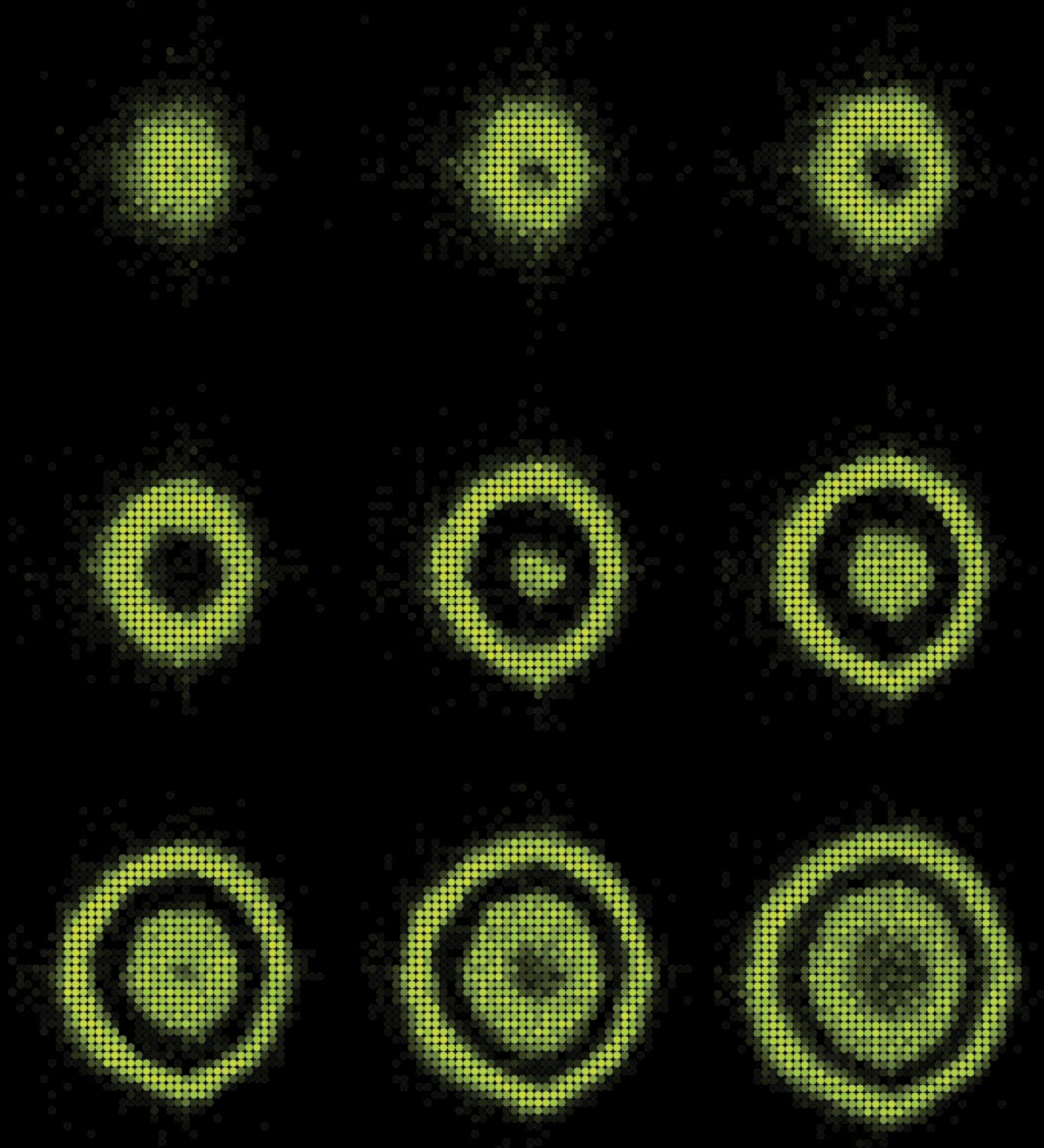

A sampling of experiments with bosonic microscopes (MPQ)

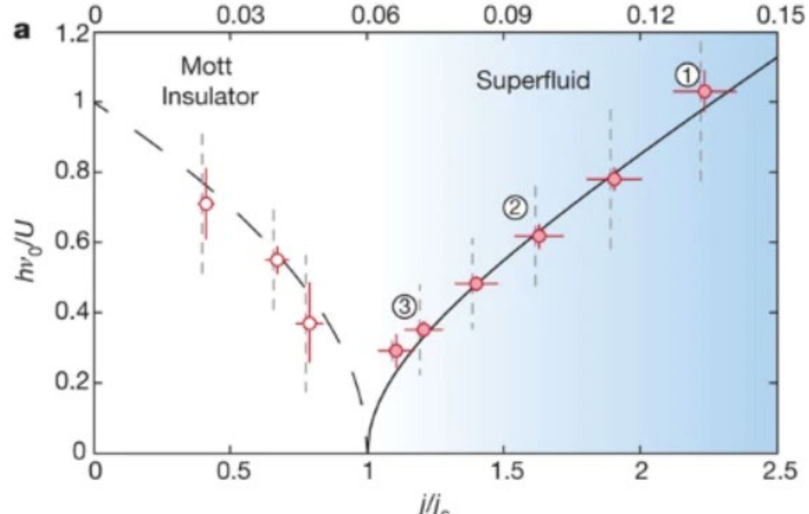

Observation of Higgs mode in SF-MI transition
Nature 487, 454 (2012)

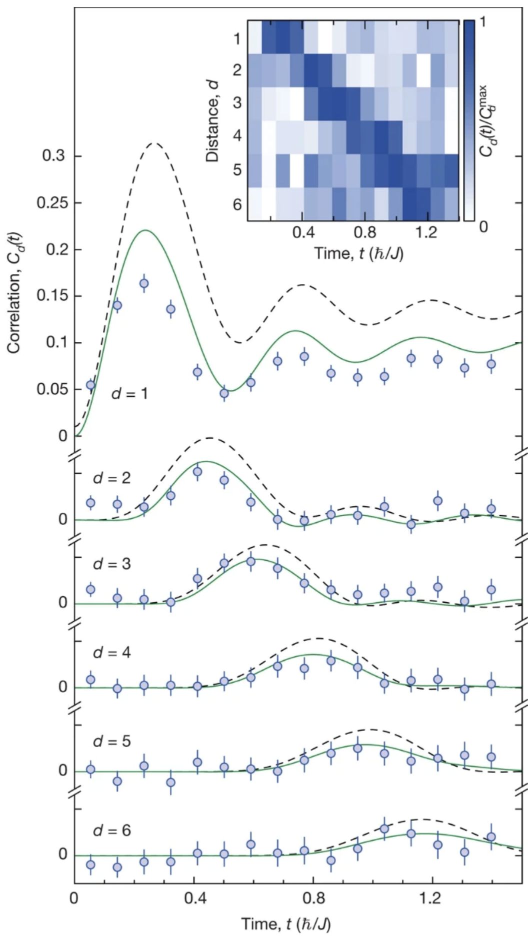

Light-cone spread of correlations
Nature 481, 484 (2012)

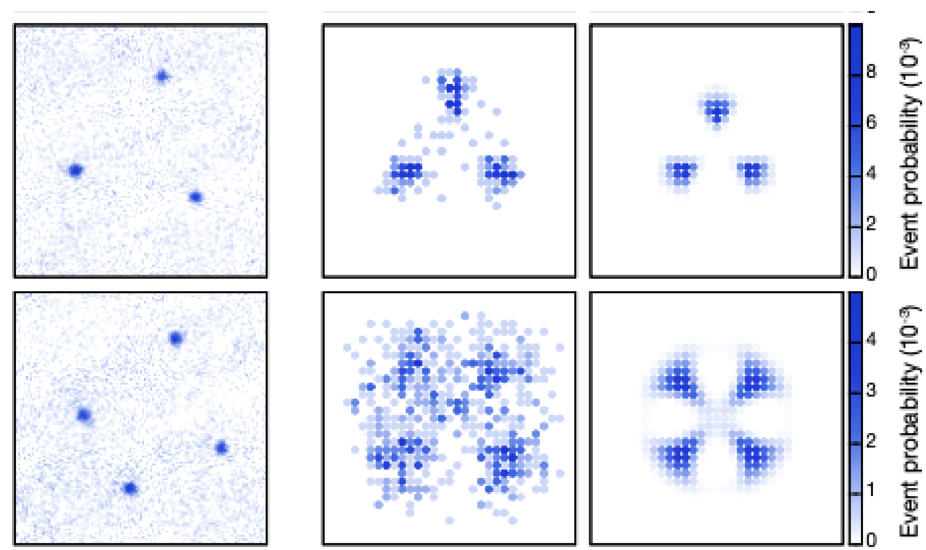

Imaging of Rydberg crystals
Nature 491, 87 (2012)

A sampling of experiments with bosonic microscopes (Harvard)

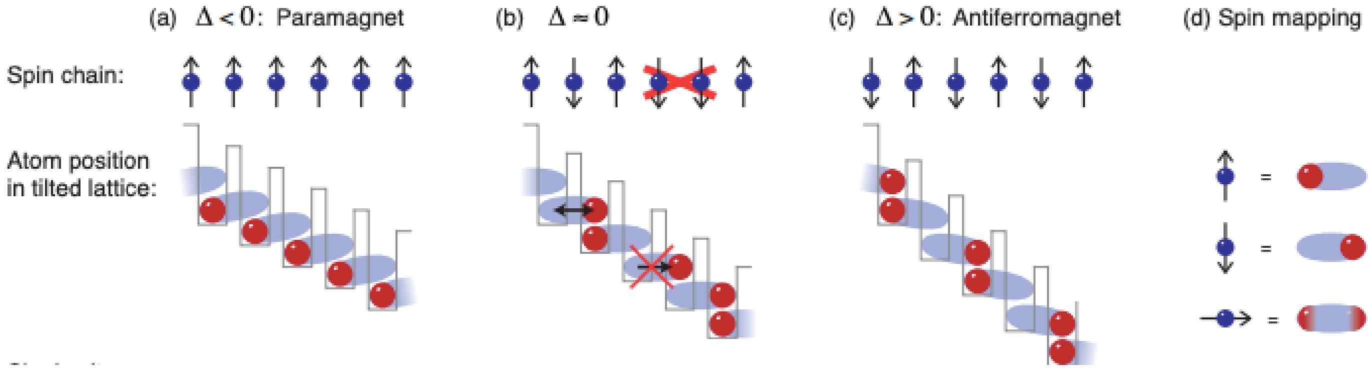

Quantum Ising AFs in tilted Bose-Hubbard model, Nature 472, 307 (2011)

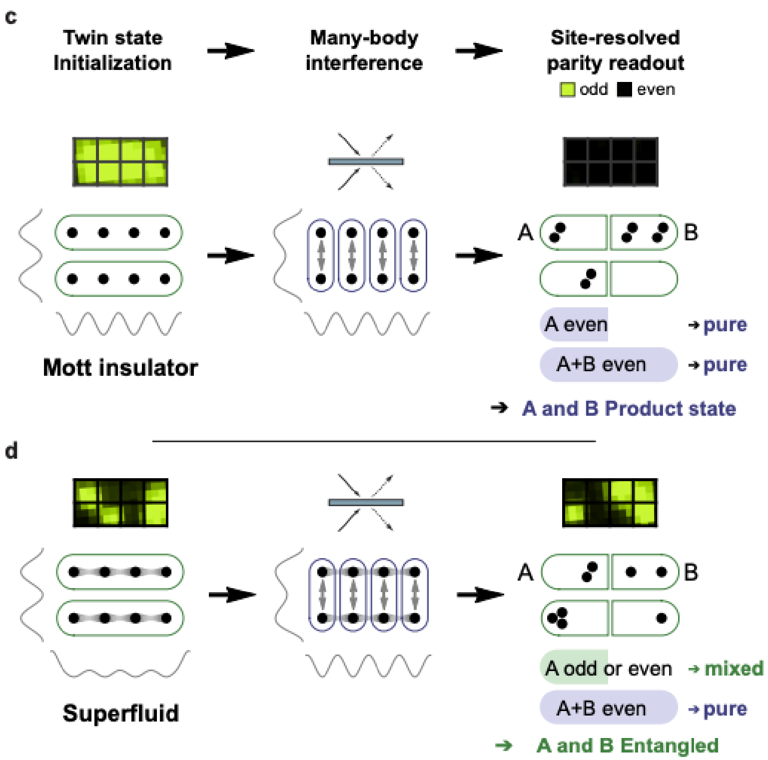

Measuring entanglement entropy
Nature 528, 77 (2015)

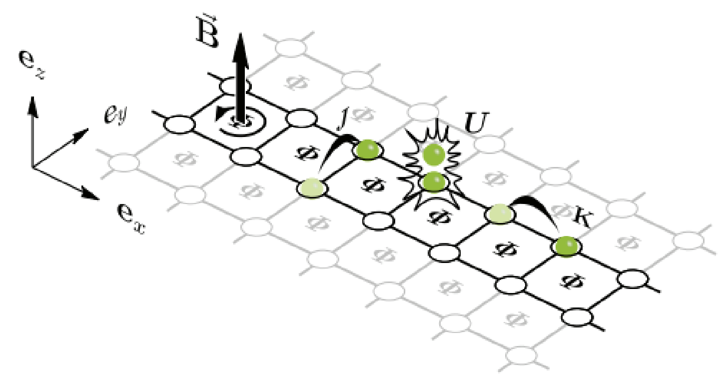

Microscopy of Harper-Hofstadter model
in few-body limit
Nature 546, 519 (2017)

The Fermi-Hubbard model

$$\mathcal{H} = -t \sum_{\langle ij \rangle, \sigma} \left(c^\dagger_{i,\sigma} c_{j,\sigma} + c^\dagger_{j,\sigma} c_{i,\sigma} \right) + U \sum_i n_{i,\uparrow} n_{i,\downarrow}$$

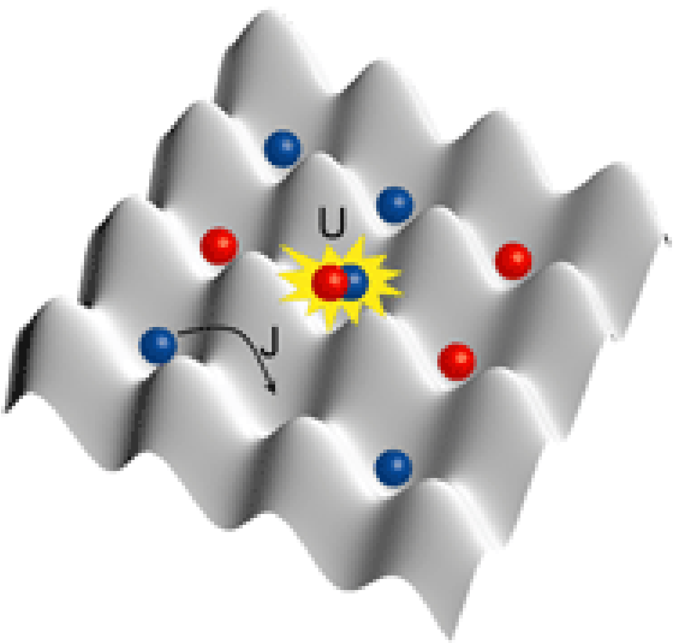

- Paradigm for studying strong-coupling physics in a lattice.
- With repulsive interactions, a possible minimal model for cuprate high-T_c superconductivity (P. Anderson)
- Realized naturally with cold atoms in optical lattices with fully tunable parameters (U/t, T/t, doping)

Realizing the Fermi-Hubbard model with cold atoms

Lithium-6: 3p + 3n + 3e = 9 (odd).

L = 0 in ground state (S-state), S = ½, I = 1.

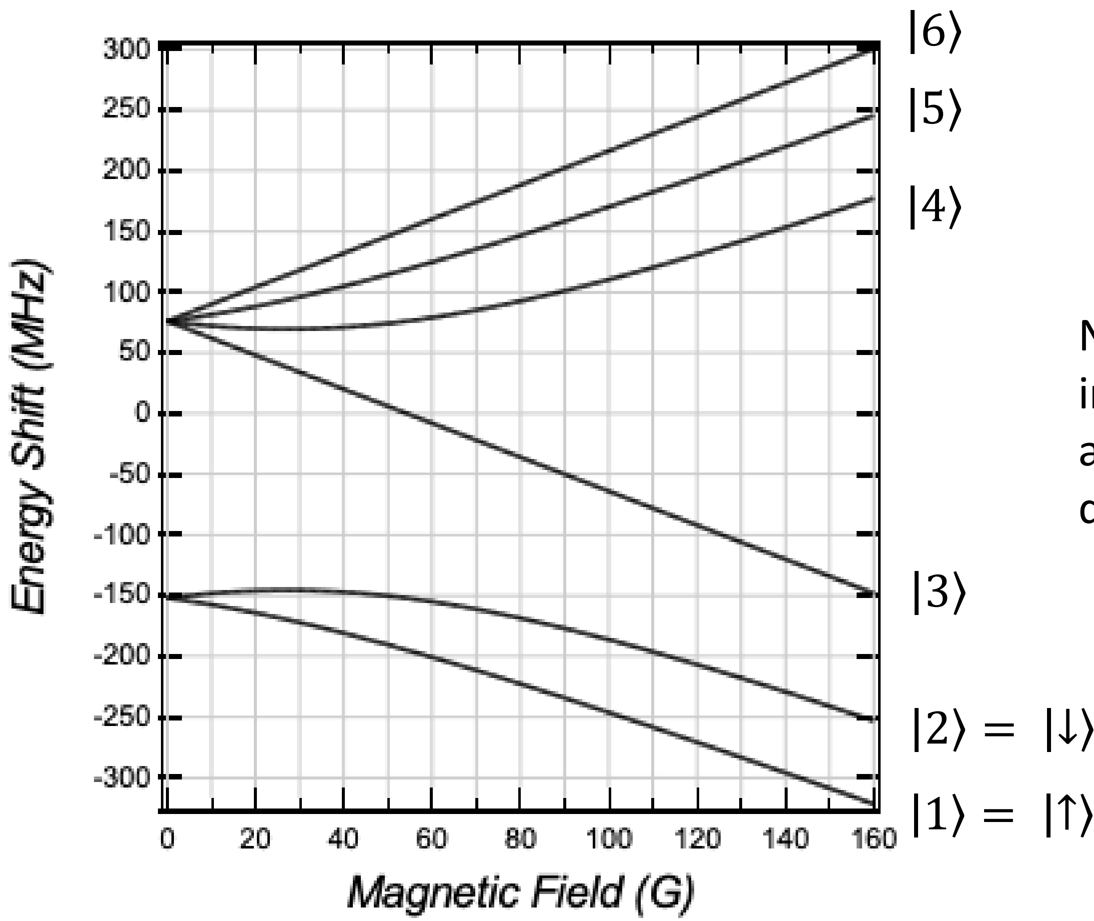

No spin-changing collisions, so initial populations $N_\uparrow$ and $N_\downarrow$ are preserved throughout quantum simulation.

Deriving the Fermi-Hubbard model: tunneling term

$$\hat{H} = \sum_{\sigma=\uparrow,\downarrow} \int \mathrm{d}\boldsymbol{r}\, \hat{\Psi}^\dagger_\sigma(\boldsymbol{r}) \left[\frac{-\hbar^2 \boldsymbol{\nabla}^2}{2m} + V(\boldsymbol{r})\right] \hat{\Psi}_\sigma(\boldsymbol{r}) + g \int \mathrm{d}\boldsymbol{r}\, \hat{\Psi}^\dagger_\uparrow(\boldsymbol{r}) \hat{\Psi}^\dagger_\downarrow(\boldsymbol{r}) \hat{\Psi}_\downarrow(\boldsymbol{r}) \hat{\Psi}_\uparrow(\boldsymbol{r})$$

$$\hat{\Psi}_\sigma(\boldsymbol{r}) = \sum_j w_j(\boldsymbol{r}) \hat{c}_{j,\sigma}$$

Wannier states: superpositions of Bloch states localized on lattice sites.

$$\hat{H}_1 = -\sum_{j,\ell,\sigma} t_{j,\ell}\, \hat{c}^\dagger_{j,\sigma} \hat{c}_{\ell,\sigma}$$

$$t_{j,\ell} = -\int \mathrm{d}\boldsymbol{r}\, w^*_j(\boldsymbol{r}) \left[-\hbar^2 \boldsymbol{\nabla}^2/2m + V(\boldsymbol{r})\right] w_\ell(\boldsymbol{r})$$

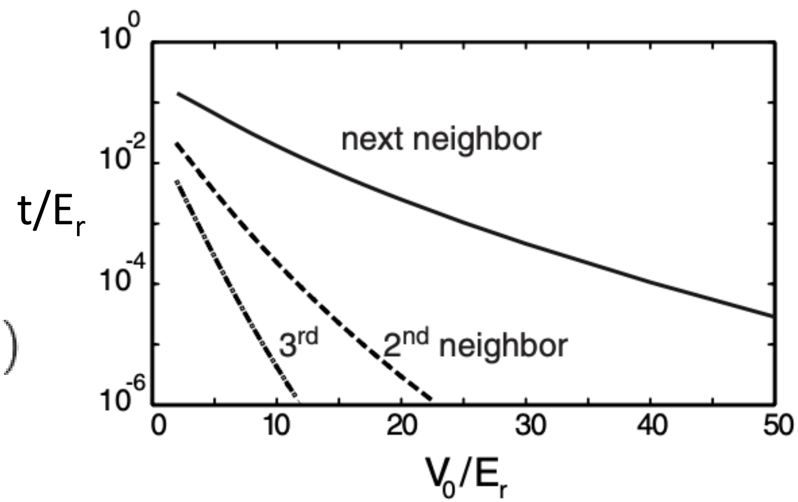

Tunneling tunable with laser intensity: $\frac{t}{E_\mathrm{r}} \simeq \frac{4}{\sqrt{\pi}} \left(\frac{V_0}{E_\mathrm{r}}\right)^{3/4} \exp\left(-2\sqrt{V_0/E_\mathrm{r}}\right)$

Deriving the Fermi-Hubbard model: interactions

$$\hat{H} = \sum_{\sigma=\uparrow,\downarrow} \int \mathrm{d}\boldsymbol{r}\, \hat{\Psi}_\sigma^\dagger(\boldsymbol{r}) \left[\frac{-\hbar^2\boldsymbol{\nabla}^2}{2m} + V(\boldsymbol{r})\right] \hat{\Psi}_\sigma(\boldsymbol{r}) + g \int \mathrm{d}\boldsymbol{r}\, \hat{\Psi}_\uparrow^\dagger(\boldsymbol{r}) \hat{\Psi}_\downarrow^\dagger(\boldsymbol{r}) \hat{\Psi}_\downarrow(\boldsymbol{r}) \hat{\Psi}_\uparrow(\boldsymbol{r})$$

Van der Waals interactions with short atomic radius scale cutoff.

Only s-wave scattering at low temperature

-> Model as contact interaction characterized by scattering length a_s

$$g = 4\pi\hbar^2 a_s/m$$

S-wave symmetric -> Only opposite spin fermions scatter.

$$U = g \int \mathrm{d}\boldsymbol{r}\, |w_j(\boldsymbol{r})|^4$$

(off-site interactions negligible)

Entering the strong correlation regime

U/t tunable over orders of magnitude with lattice depth or Feshbach resonance.

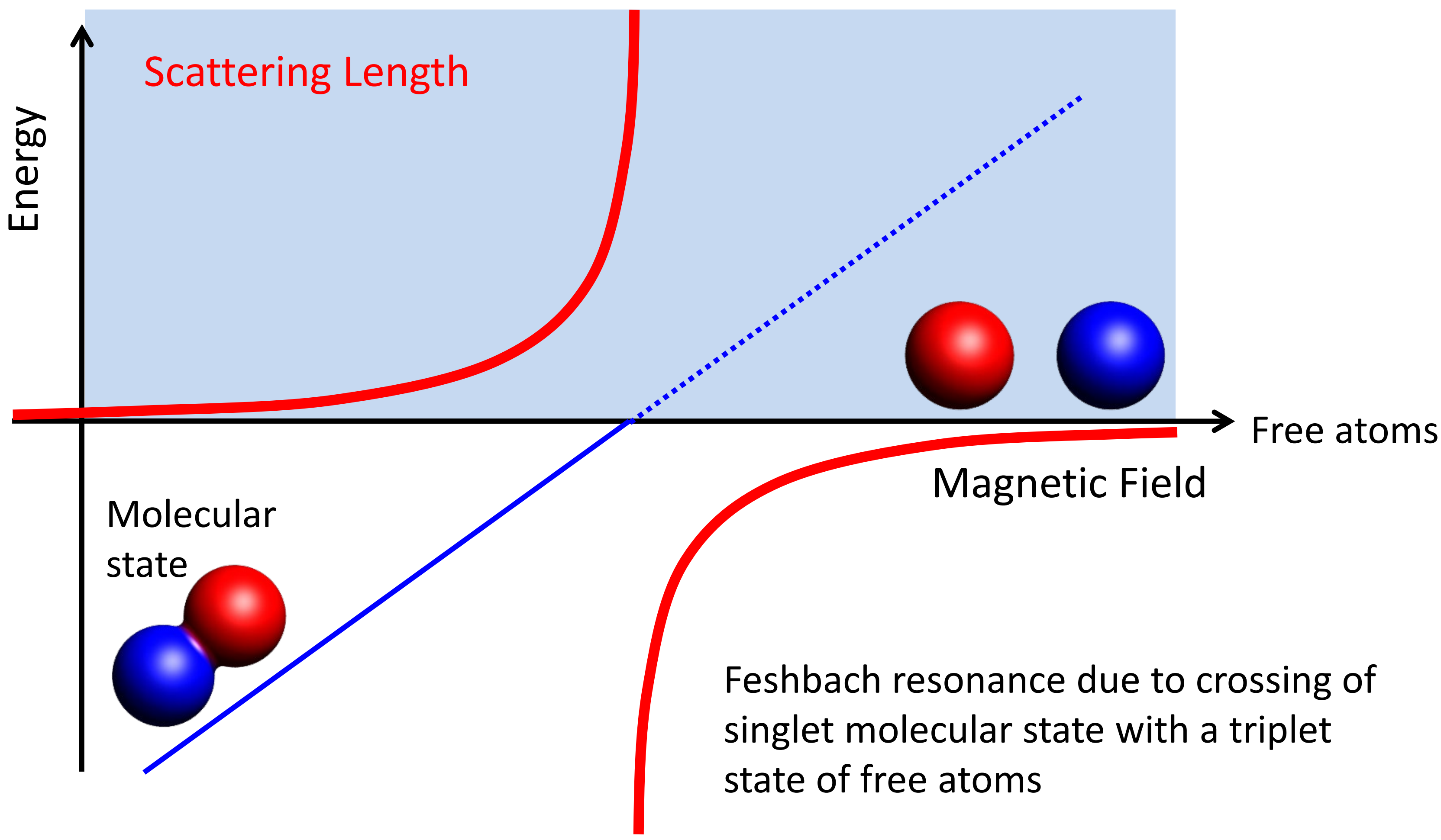

Feshbach resonance due to crossing of singlet molecular state with a triplet state of free atoms

Cuprate phase diagram

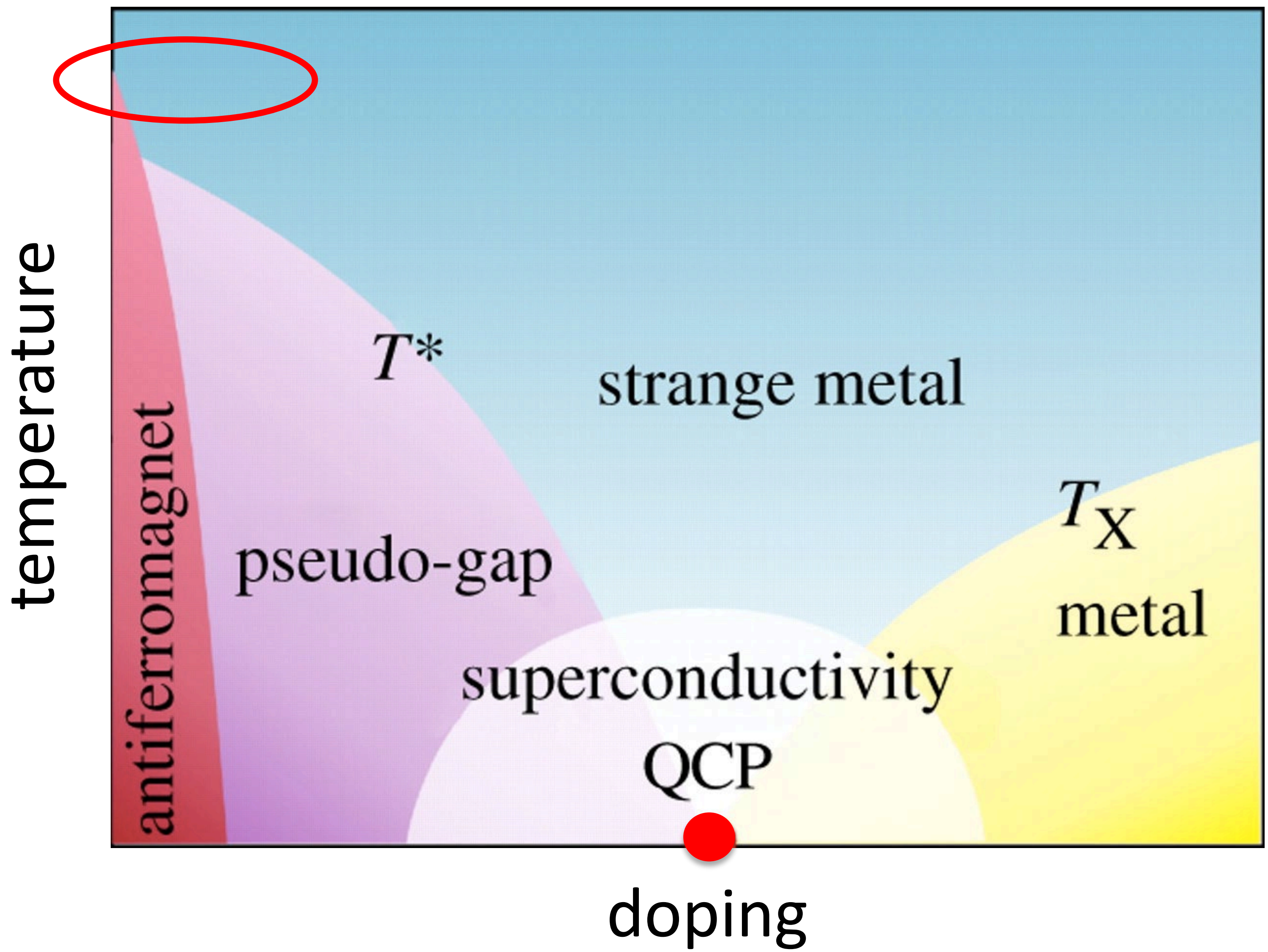

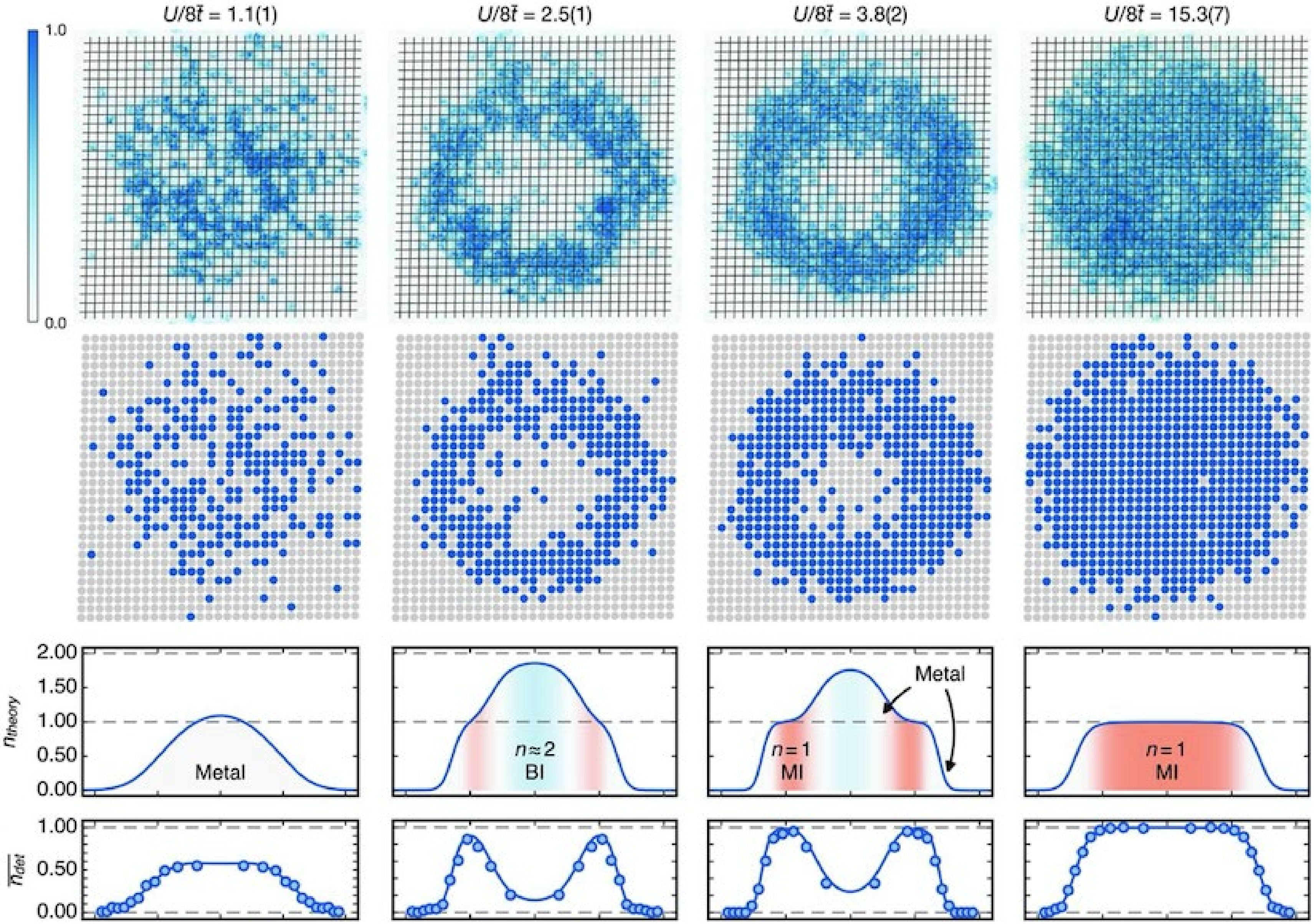

Microscopy of fermionic Mott insulators:
Greif ... Greiner, Science 351, 953 (2016)
Cheuk … Zwierlein, PRL 116, 235301 (2016)

Previous work without microscopes:
Jördens … Esslinger, Nature 455, 204 (2008)
Schneider … Bloch, Science 322, 1520 (2008)

“Charge” correlations in doped systems

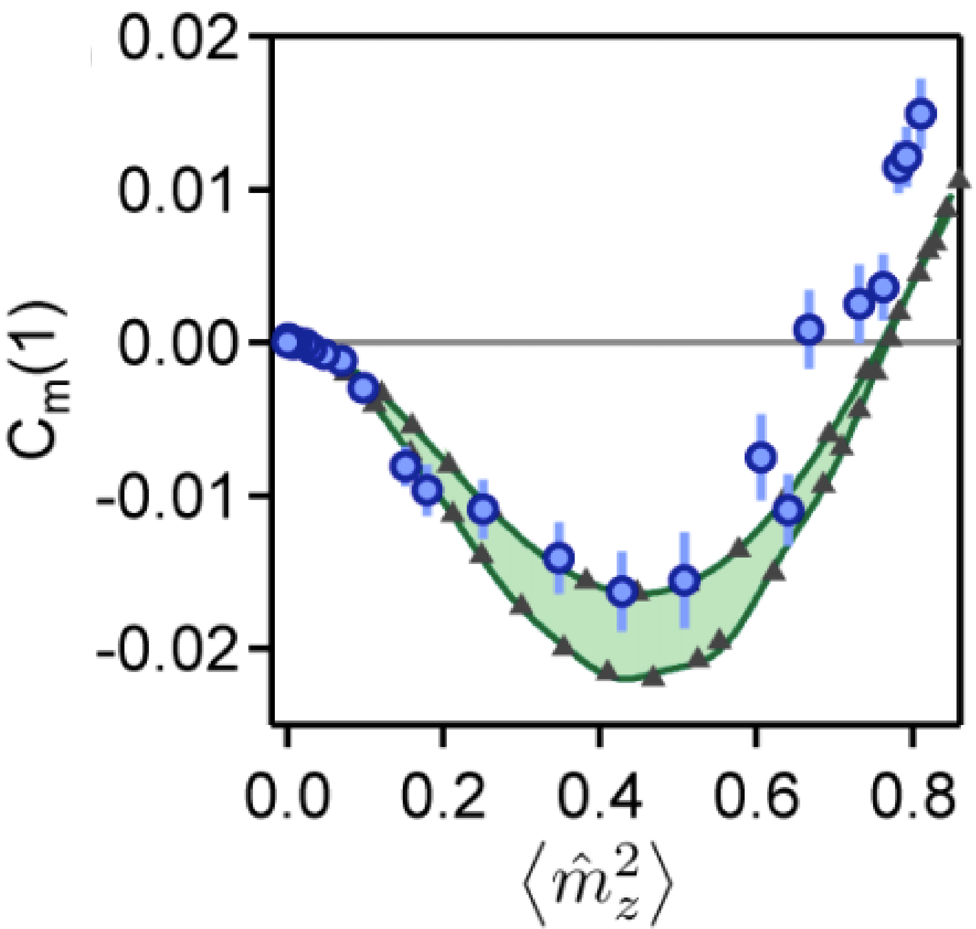

$$\hat{m}_{z,i}^2 = (\hat{n}_{\uparrow,i} - \hat{n}_{\downarrow,i})^2$$

“Moment”: 1 if site is singly occupied, 0 otherwise.

Nearest-neighbor moment correlations:

Positive in Mott insulator due to doublon-hole fluctuations.

Negative in metal due to Pauli hole + repulsive interactions.

Cheuk … Zwierlein, Science 353, 1260 (2016)

Antiferromagnetic spin correlations

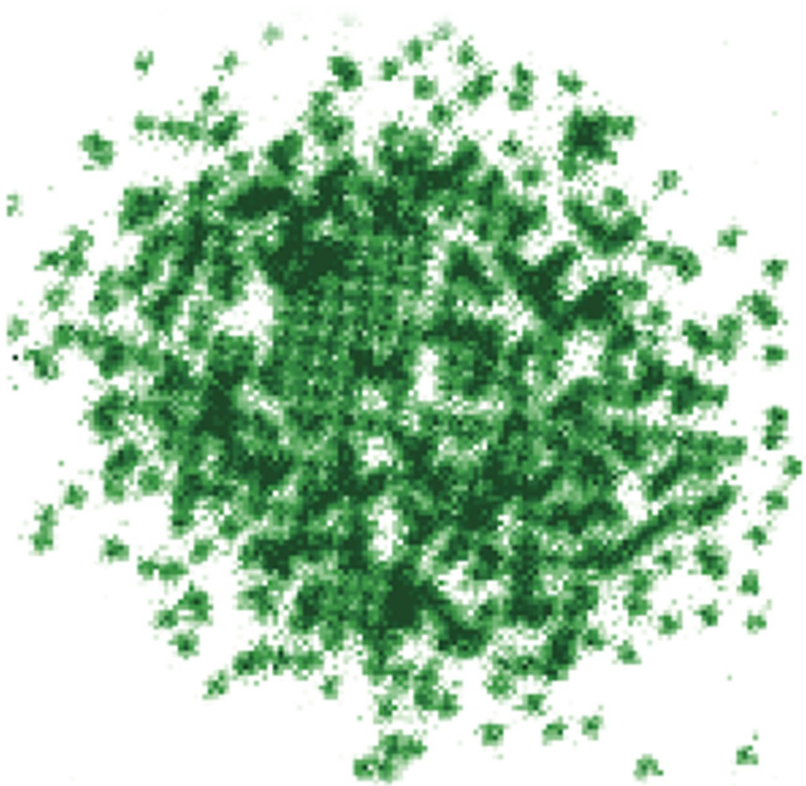

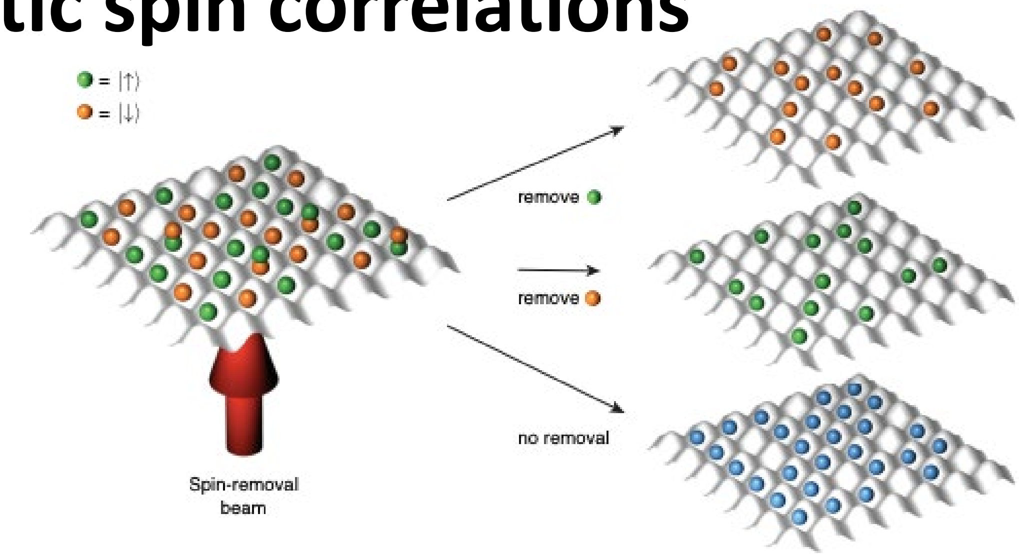

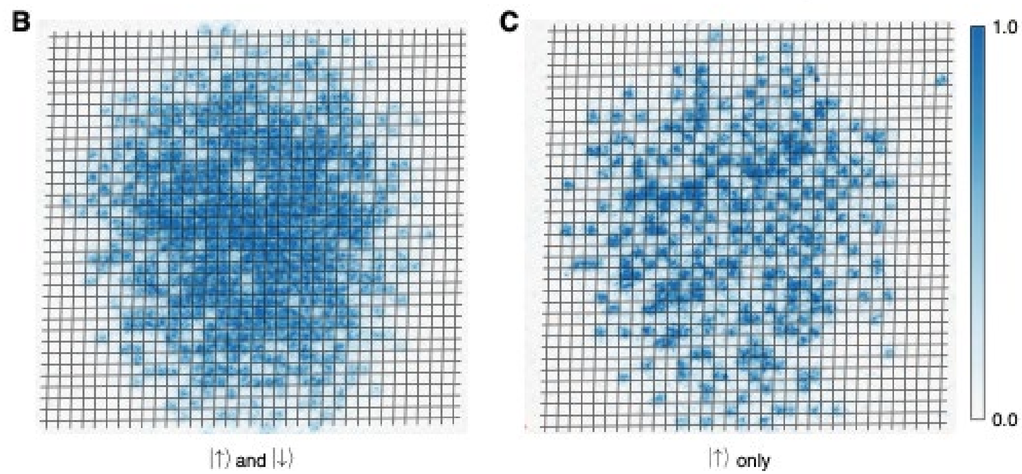

Detection of AFMs with microscopes:
Parsons … Greiner, Science 353, 1253 (2016)
Boll … Bloch, Gross, Science 353, 1257 (2016)
Cheuk … Zwierlein, Science 353, 1260 (2016)
Brown … Bakr, Science 357, 1385 (2017)

Previous work without microscopes:
Greif … Esslinger, Science 340, 1307 (2013)
Hart … Hulet, Nature 519, 211 (2015)
Drewes … Köhl, PRL 118, 170401 (2017)

Potential engineering with DMDs

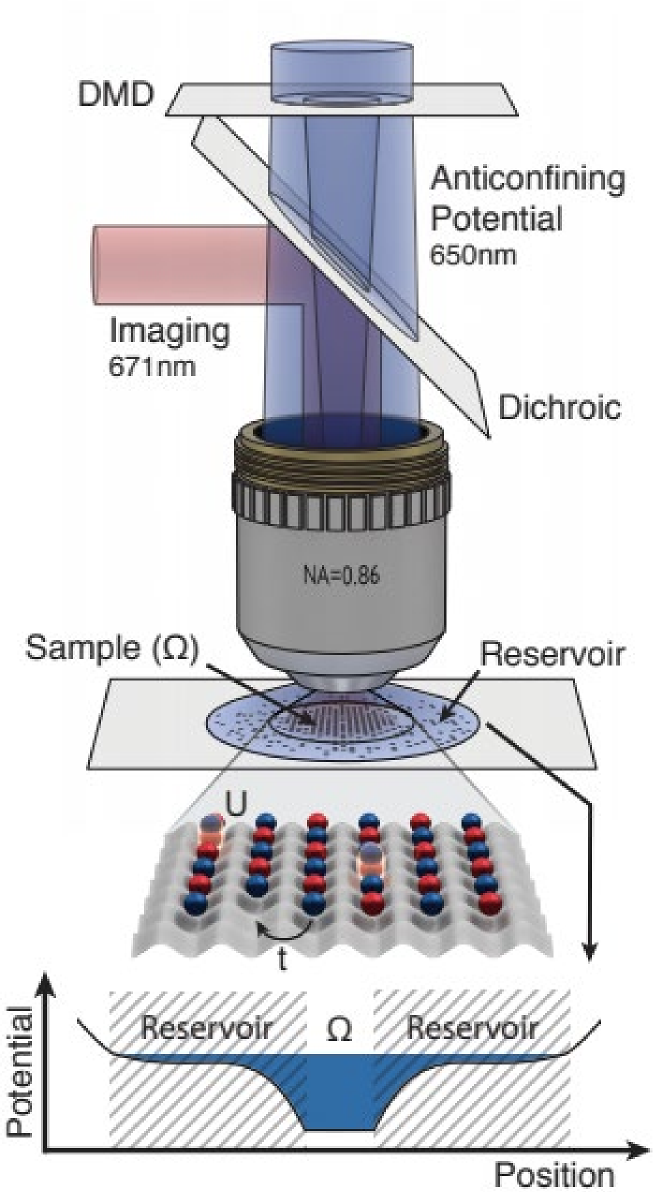

We work with fixed entropy systems (can still talk about temperature for local observables in the ETH sense).

Charge gap in Mott insulator expels entropy to low-density metallic regions.

Spatial light modulators (digital micromirror devices) can be used to shape potential landscape:

1. Enhance entropy redistribution.
2. Study systems at fixed doping.

Greiner group

Antiferromagnetic correlations at half-filling

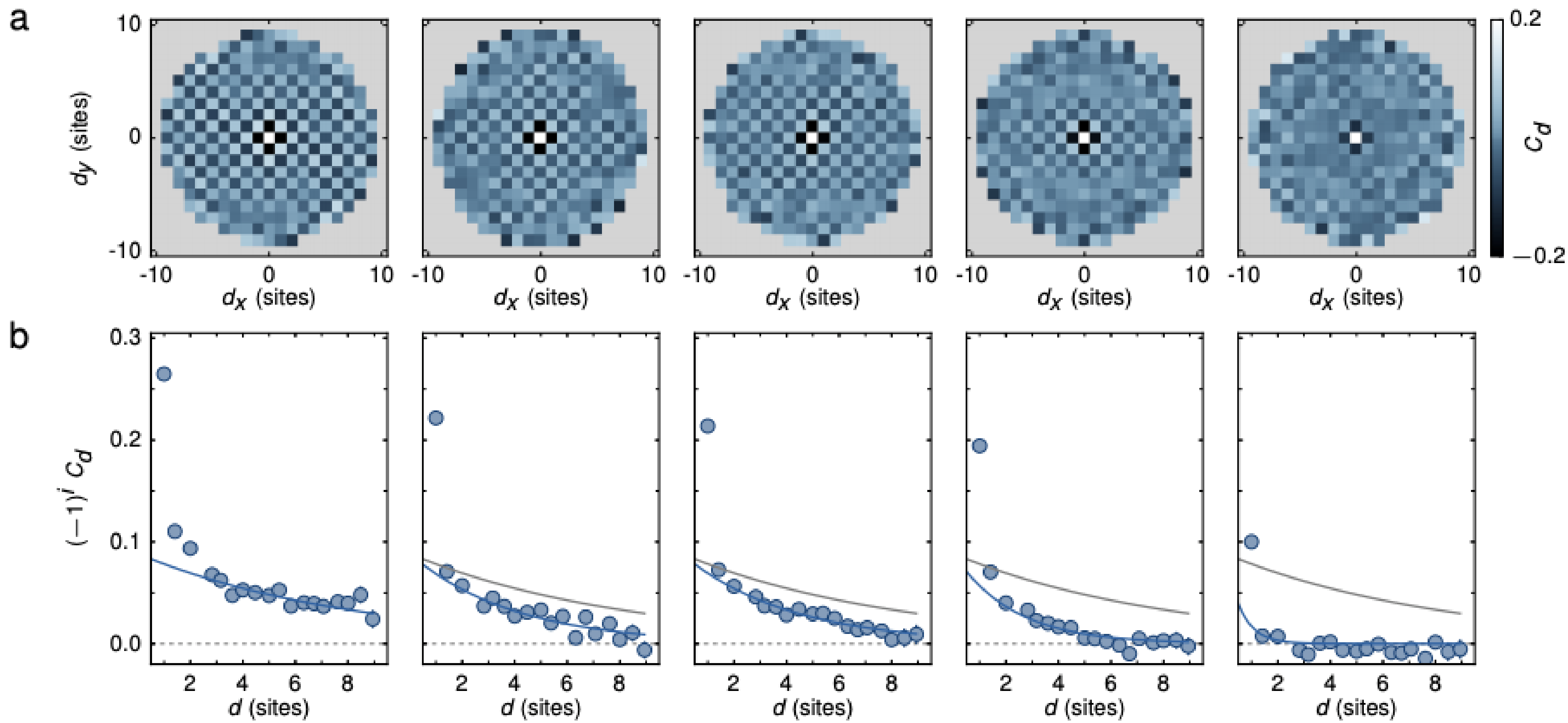

$$C_{\boldsymbol{d}} = \frac{1}{\mathcal{N}_{\boldsymbol{d}}} \frac{1}{S^2} \sum_{\substack{\boldsymbol{r},\boldsymbol{s}\in\Omega \\ \boldsymbol{d}=\boldsymbol{r}-\boldsymbol{s}}} \langle \hat{S}^z_{\boldsymbol{r}} \hat{S}^z_{\boldsymbol{s}} \rangle - \langle \hat{S}^z_{\boldsymbol{r}} \rangle \langle \hat{S}^z_{\boldsymbol{s}} \rangle$$

Usually do thermometry by comparison of one correlator (e.g. nearest neighbor spin correlator) to Quantum Monte Carlo calculations.

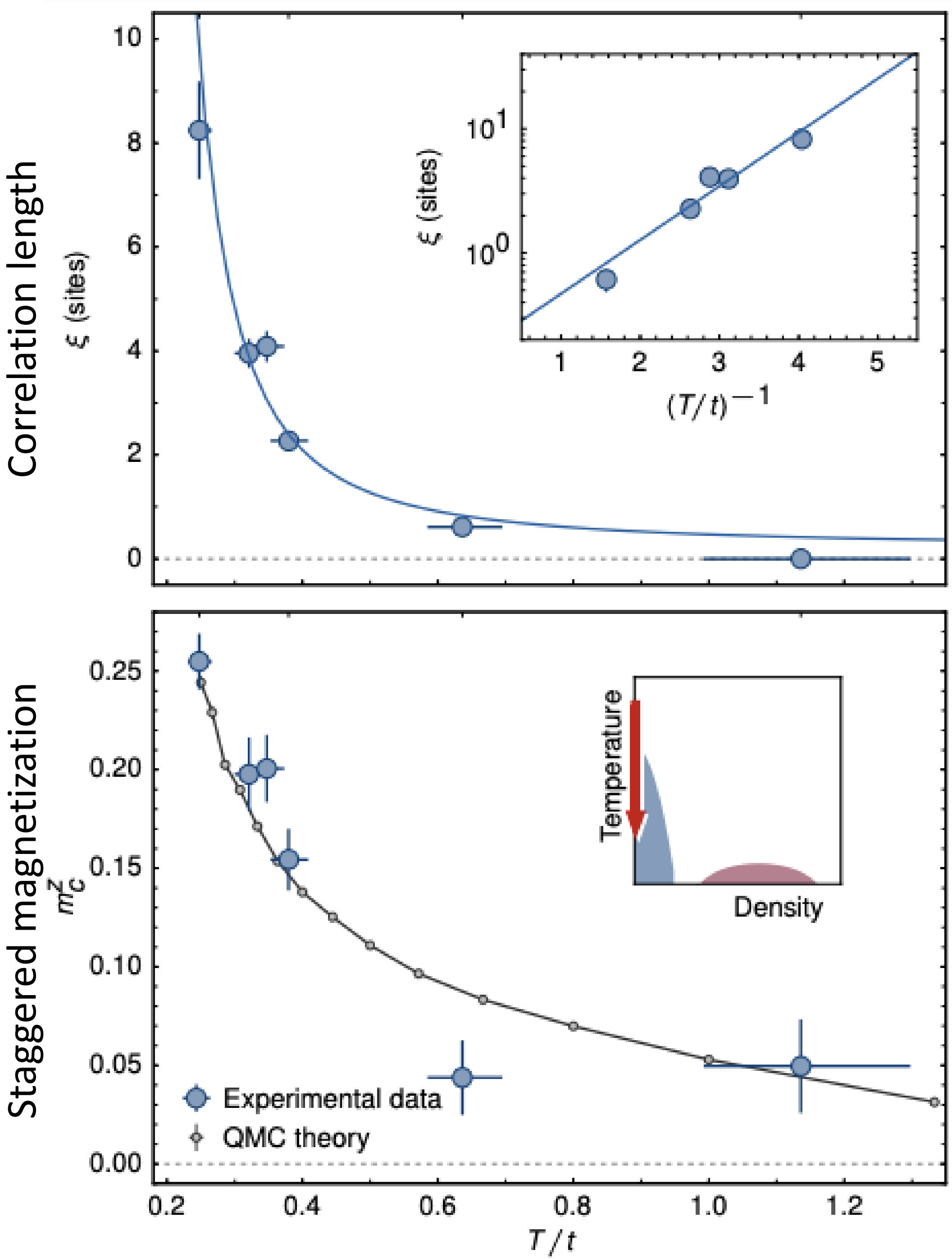

Long-range antiferromagnets (i.e. correlation length approaching system size) Mazurenko … Greiner, Nature 545, 462 (2017)

Lowest temperatures achieved: *T/t* ~ 0.25 (around 0.3-0.4 kB per particle)

$$m^z = \sqrt{\langle (\hat{m^z})^2 \rangle} = \sqrt{\left\langle \left(\frac{1}{N} \sum_i (-1)^i \frac{1}{S} \hat{S}_i^z \right)^2 \right\rangle}$$

Doping quickly destroys antiferromagnetic correlations

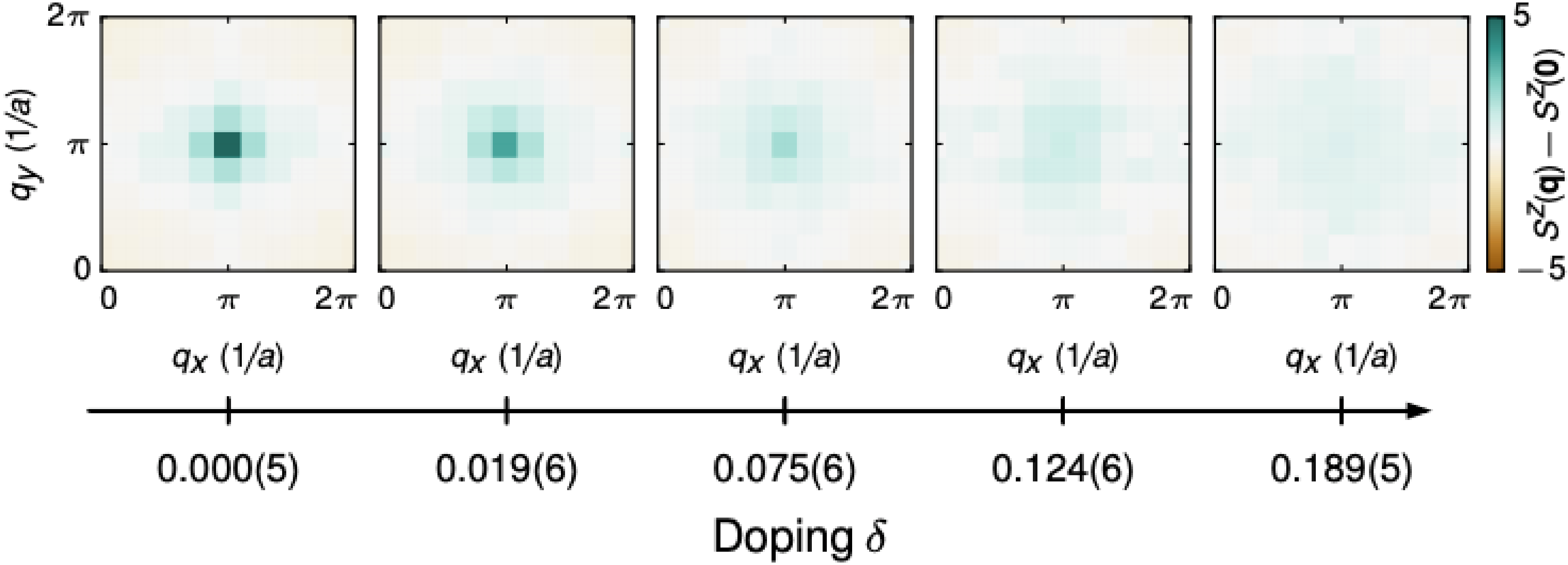

Spin structure factor (the sort of quantity measured in the solid state e.g. with neutron scattering) vanishes quickly with doping.

Reaching lower entropies?

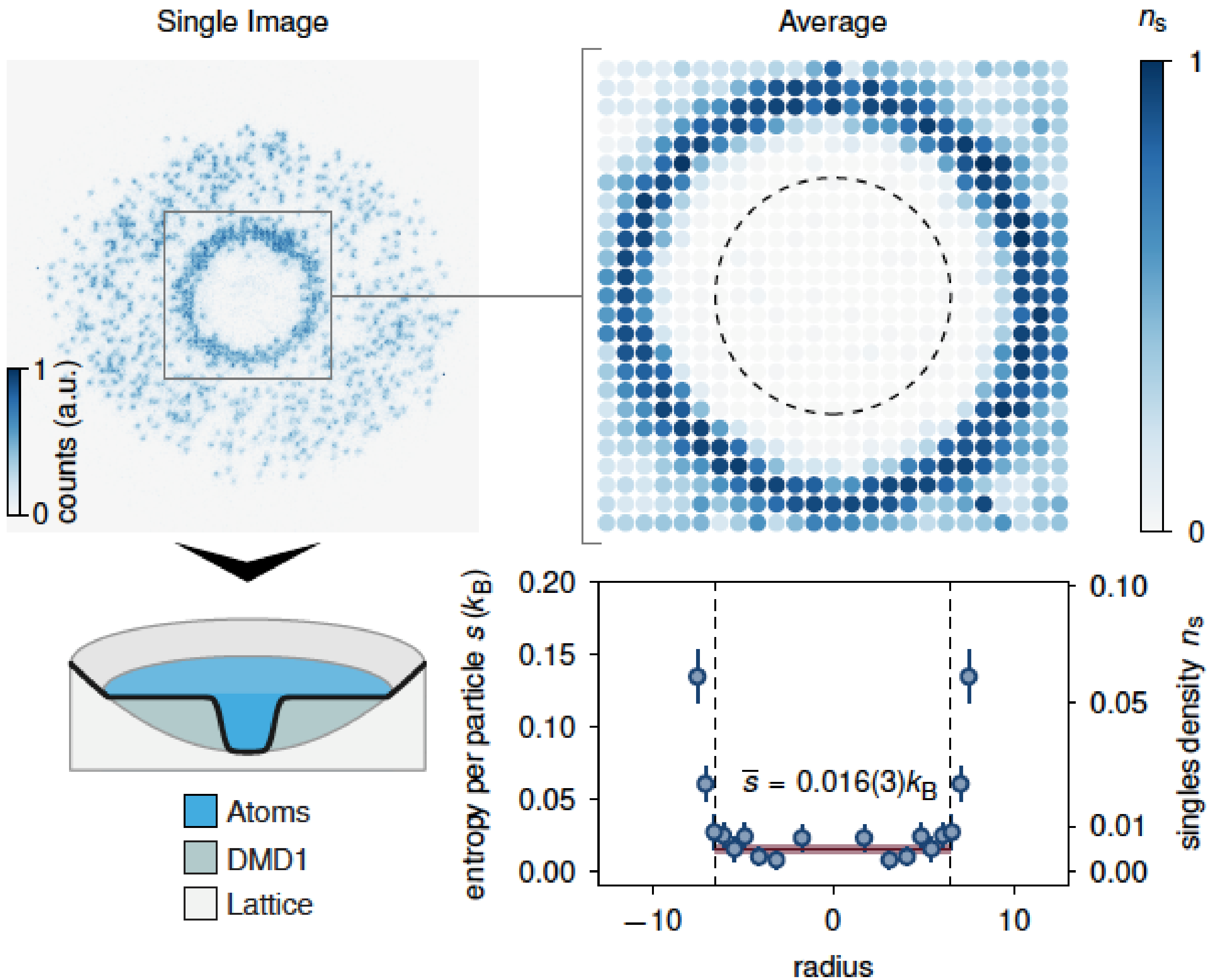

Greiner group

Spin imbalance in a Hubbard system

Condensed matter system:
Spin imbalance by applied magnetic field (Zeeman effect)

Cold atoms:

- Spin-imbalance by evaporation in spin-dependent potential.
- No spin-relaxation.

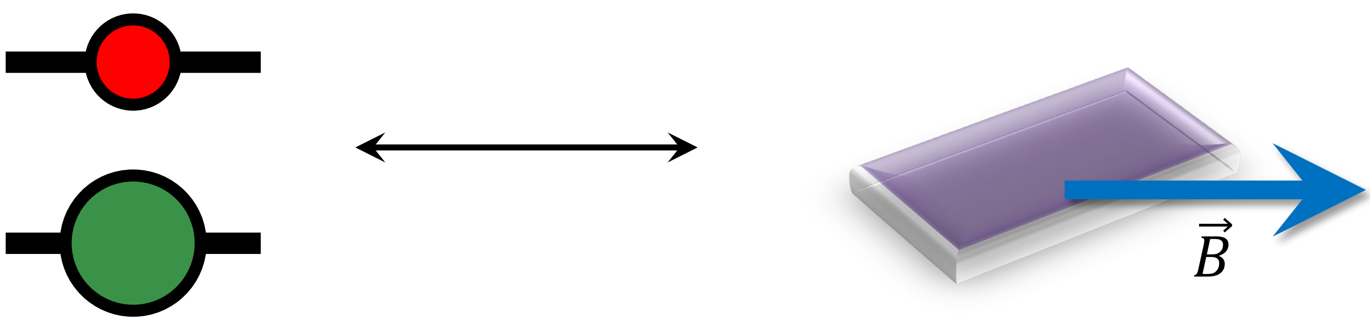

Spin-polarization Zeeman field

Spin imbalance at half-filling

Heisenberg model in an effective field

$$\mathcal{H} = J \sum_{\langle ij \rangle} \mathbf{S}_i \cdot \mathbf{S}_j - 2h \sum_i S_i^z \qquad h = (\mu_\uparrow - \mu_\downarrow)/2$$

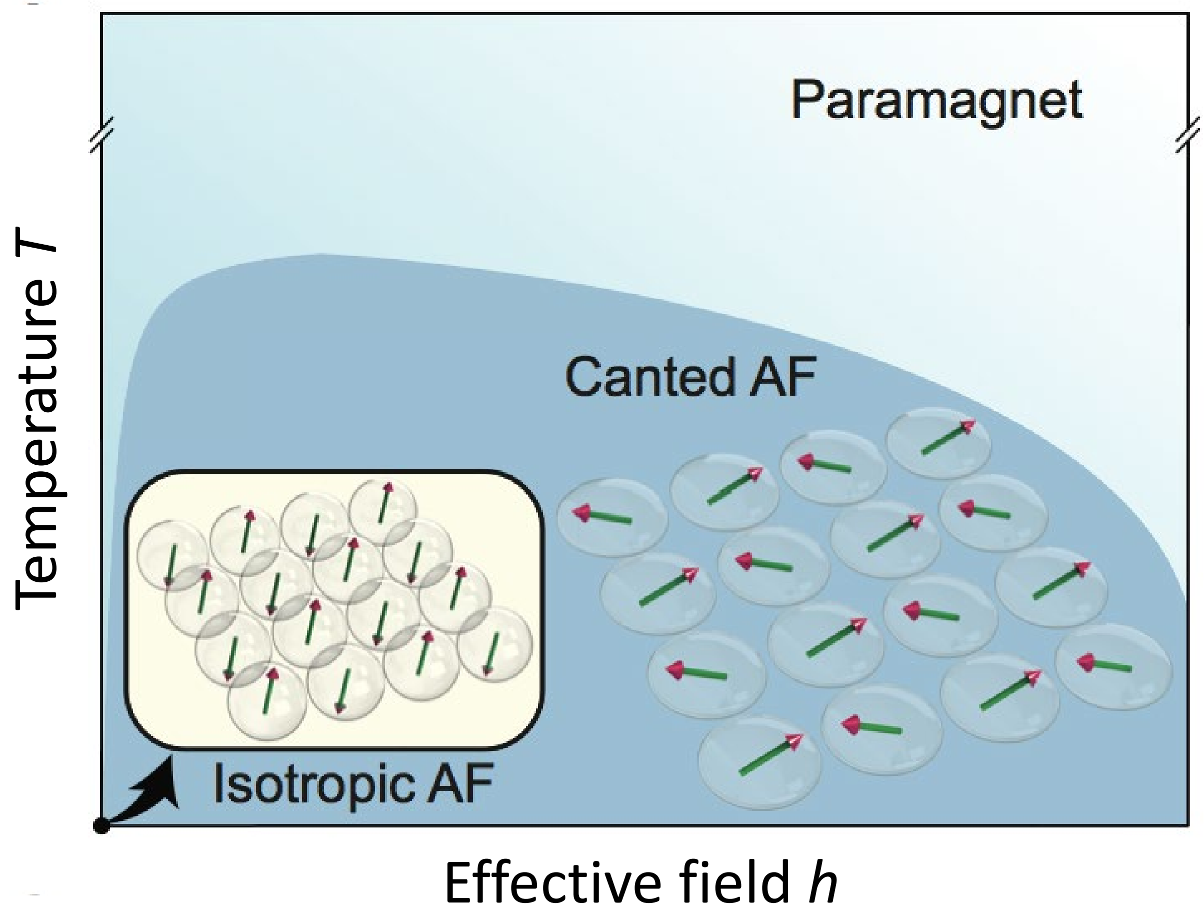

$h = 0$:
SU(2) symmetric AFM
Exponentially decaying correlations, diverging correlation length at $T = 0$

$|h| > 0$:
BKT-transition to canted AFM

AFM correlations build up preferably in XY plane.

Canted antiferromagnetic correlations

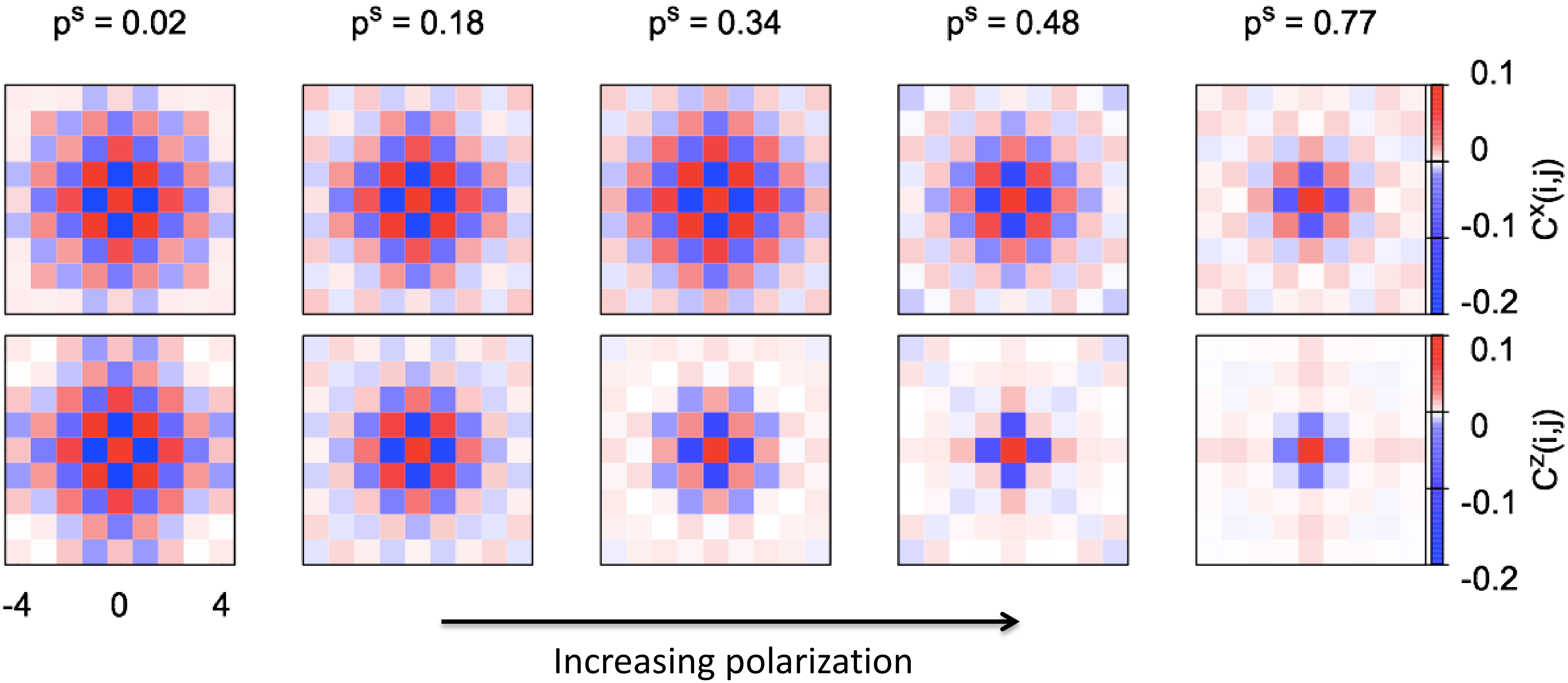

Brown … Bakr, Science 357, 1385 (2017)

Unpolarized gas: isotropic spin correlations

Polarized gas: AFM correlations preferred in the plane

Mapping between the attractive and repulsive Hubbard models

$$\mathcal{H} = -t \sum_{\langle \mathbf{r}\mathbf{r}' \rangle, \sigma} \left(c^\dagger_{\mathbf{r},\sigma} c_{\mathbf{r}',\sigma} + c^\dagger_{\mathbf{r}',\sigma} c_{\mathbf{r},\sigma} \right) + U \sum_{\mathbf{r}} n_{\mathbf{r},\uparrow} n_{\mathbf{r},\downarrow}$$

$$- \mu \sum_{\mathbf{r},\sigma} n_{\mathbf{r},\sigma} - h \sum_{\mathbf{r}} (n_{\mathbf{r},\uparrow} - n_{\mathbf{r},\downarrow})$$

Use the partial particle hole transformation:

$$c_{i\downarrow} = c_{i_x i_y \downarrow} \longleftrightarrow (-1)^{i_x + i_y} \; c^\dagger_{i\downarrow}$$

$$c_{i\uparrow} \longleftrightarrow c_{i\uparrow}.$$

Hamiltonian takes the same form but:

1. Interaction flips sign.
2. Chemical potential and effective field swap roles.

Mapping between the models

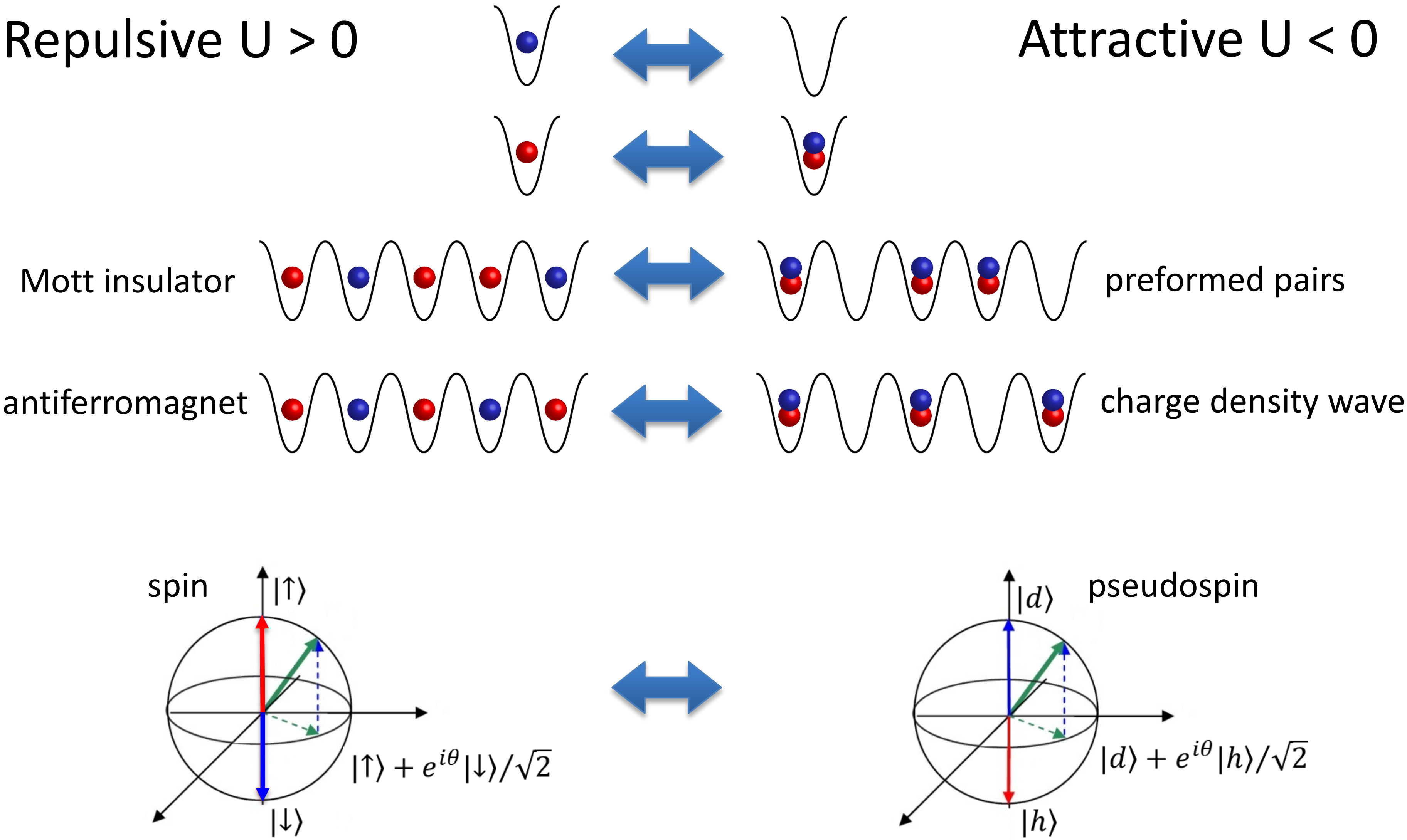

Phys. Rev. A **79**, 033620 (2009)

Fermi-Hubbard phase diagram at half-filling

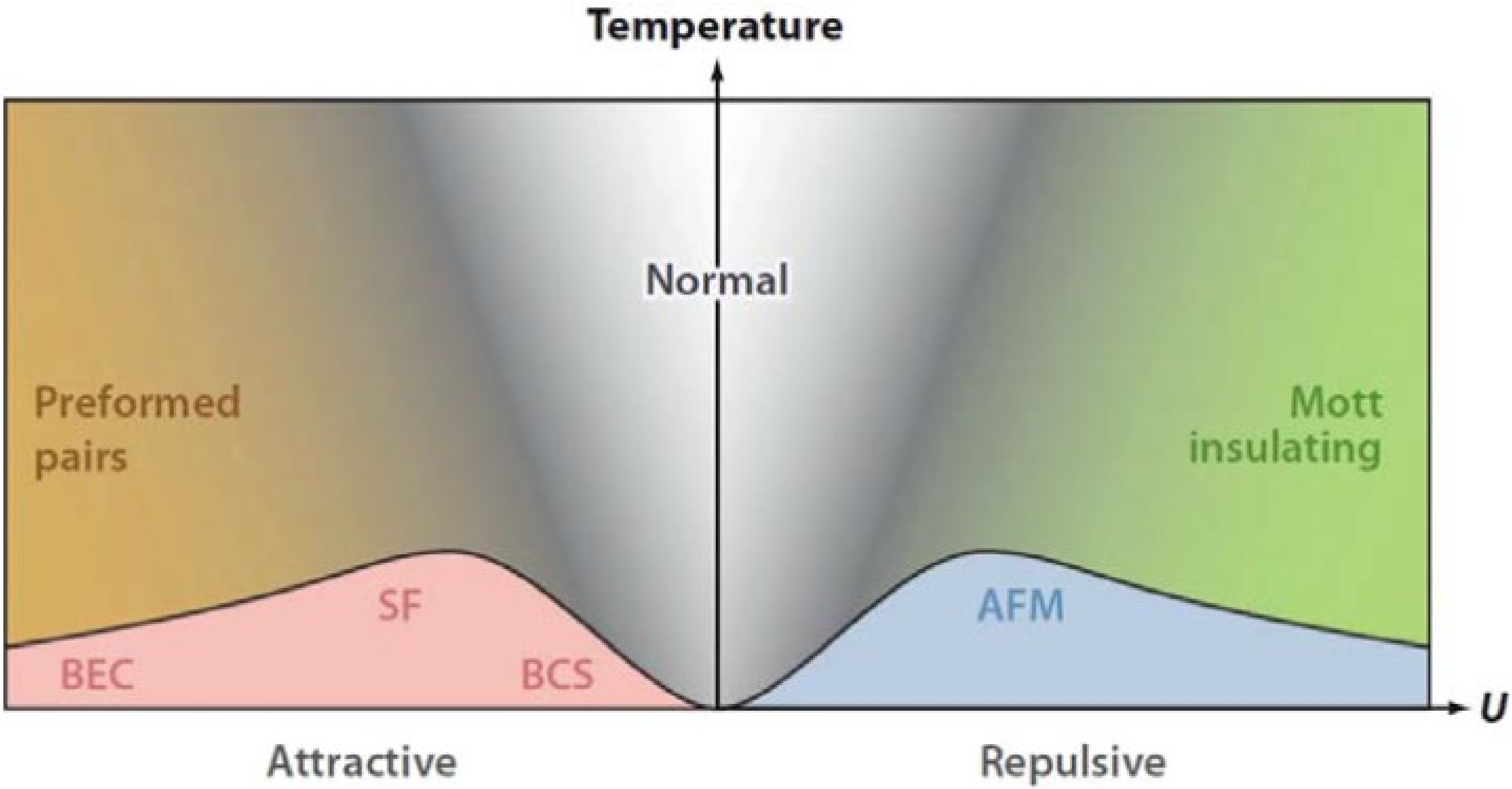

T. Esslinger

SU(2)xSU(2) symmetry of Hubbard model at half-filling

SU(2) spin symmetry in absence of effective field

$$S_{\mathbf{r}}^{-} = c_{\mathbf{r},\downarrow}^{\dagger} c_{\mathbf{r},\uparrow}$$

$$S_{\mathbf{r}}^{+} = (S_{\mathbf{r}}^{-})^{\dagger} = c_{\mathbf{r},\uparrow}^{\dagger} c_{\mathbf{r},\downarrow}$$

$$S_{\mathbf{r}}^{z} = \frac{1}{2}(c_{\mathbf{r},\uparrow}^{\dagger} c_{\mathbf{r},\uparrow} - c_{\mathbf{r},\downarrow}^{\dagger} c_{\mathbf{r},\downarrow}) = \frac{1}{2}(n_{\mathbf{r},\uparrow} - n_{\mathbf{r},\downarrow})$$

$$[S_{\mathbf{r}}^{z}, S_{\mathbf{r}}^{\pm}] = \pm S_{\mathbf{r}}^{\pm}, \quad [S_{\mathbf{r}}^{+}, S_{\mathbf{r}}^{-}] = 2S_{\mathbf{r}}^{z}$$

$$S^{z} = \sum_{r} S_{\mathbf{r}}^{z}$$

$$S^{\pm} = \sum_{r} S_{\mathbf{r}}^{\pm}$$

$$[\mathcal{H}, S^{\pm}] = [\mathcal{H}, S^{z}] = 0$$

SU(2) pseudospin symmetry at half-filling

$$\eta_{\mathbf{r}}^{-} = (-1)^{r_x + r_y} c_{\mathbf{r},\uparrow} c_{\mathbf{r},\downarrow}$$

$$\eta_{\mathbf{r}}^{+} = (\eta_{\mathbf{r}}^{-})^{\dagger}$$

$$\eta_{\mathbf{r}}^{z} = \frac{1}{2}(n_{\mathbf{r}} - 1)$$

$$[\eta_{\mathbf{r}}^{z}, \eta_{\mathbf{r}}^{\pm}] = \pm\eta_{\mathbf{r}}^{\pm} \quad [\eta_{\mathbf{r}}^{+}, \eta_{\mathbf{r}}^{-}] = 2\eta_{\mathbf{r}}^{z}$$

$$\eta^{z} = \sum_{r} \eta_{\mathbf{r}}^{z}$$

$$\eta^{\pm} = \sum_{r} \eta_{\mathbf{r}}^{\pm}$$

$$[\mathcal{H}, \eta^{\pm}] = \pm(U - 2\mu)\eta^{\pm}, \quad [\mathcal{H}, \eta^{z}] = 0$$

$$\Delta_{\mathbf{r}}^{x} = c_{\mathbf{r},\uparrow} c_{\mathbf{r},\downarrow} + c_{\mathbf{r},\downarrow}^{\dagger} c_{\mathbf{r},\uparrow}^{\dagger}$$

Spin-balanced attractive Hubbard model

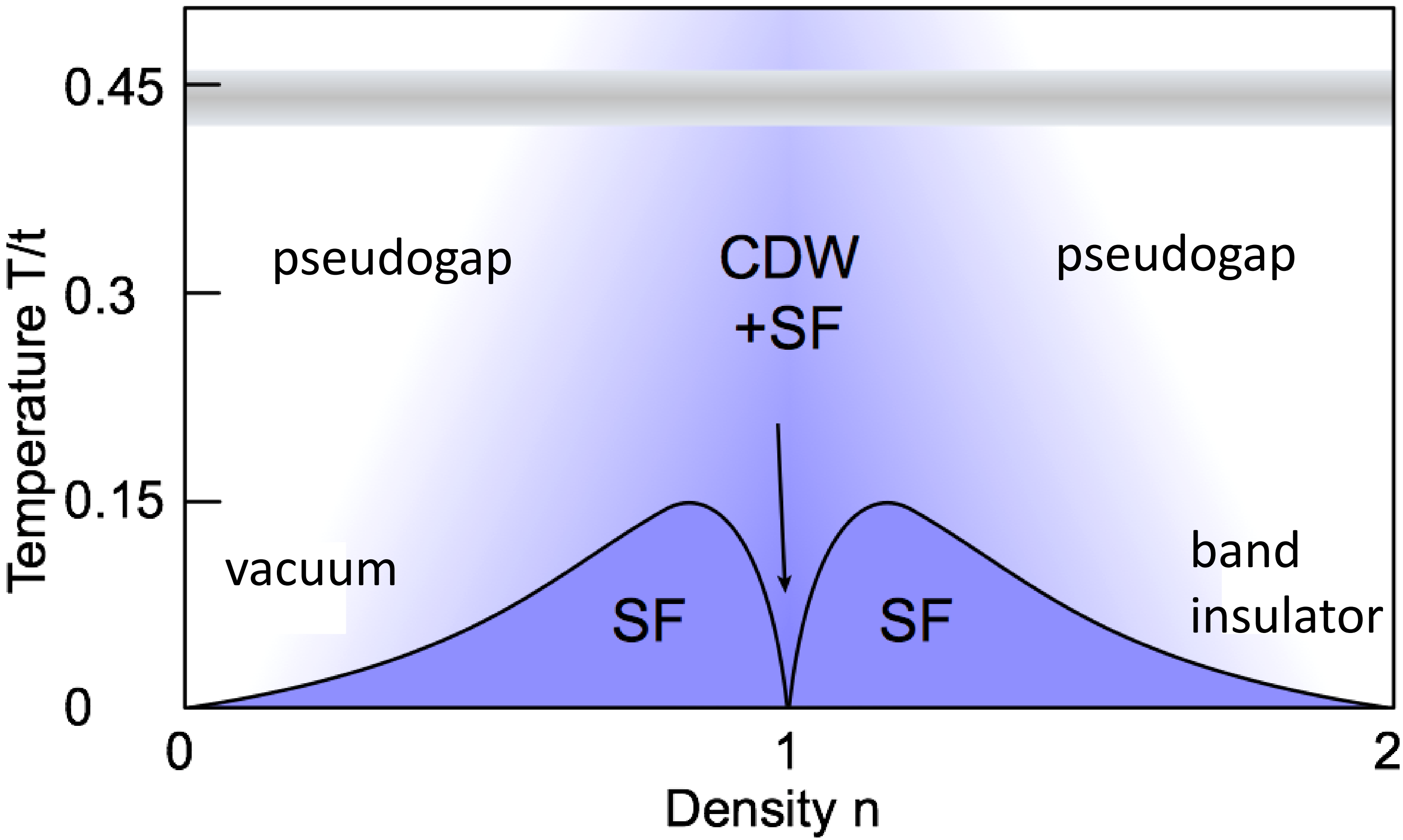

Preformed pairs: U

Superfluidity: $4t^2/U$

Site-resolved doublon detection

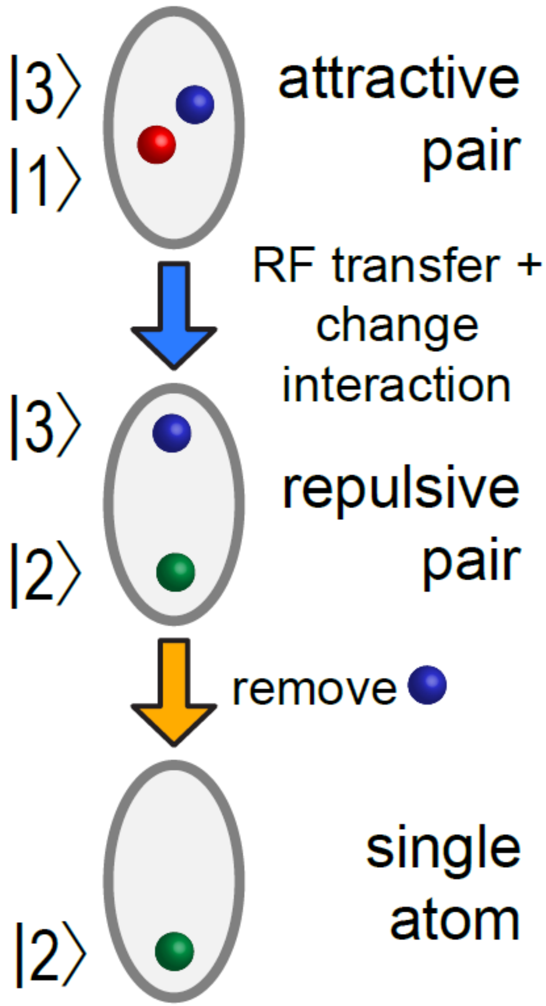

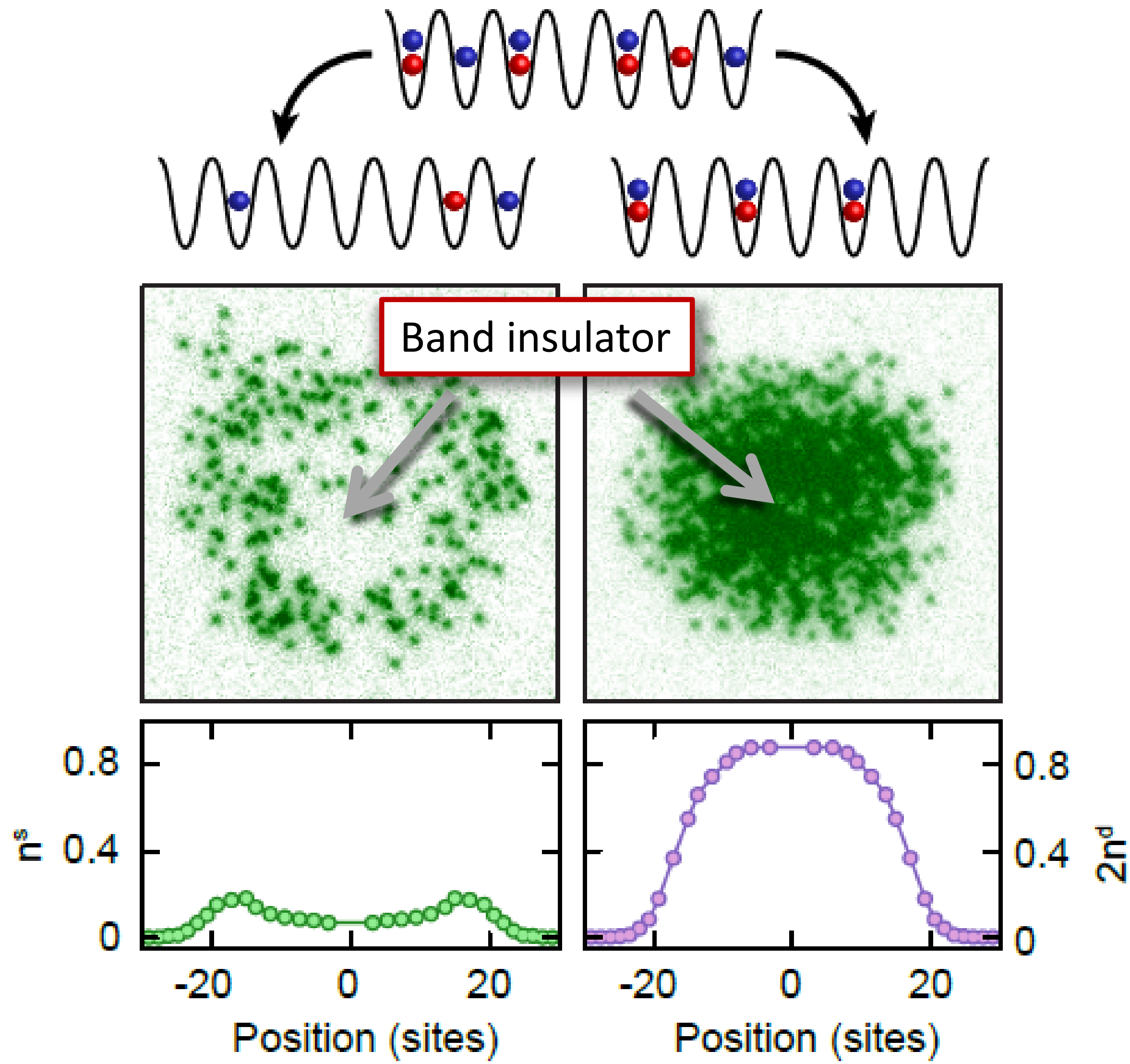

90 % fidelity

Correlator symmetry

Attractive Hubbard

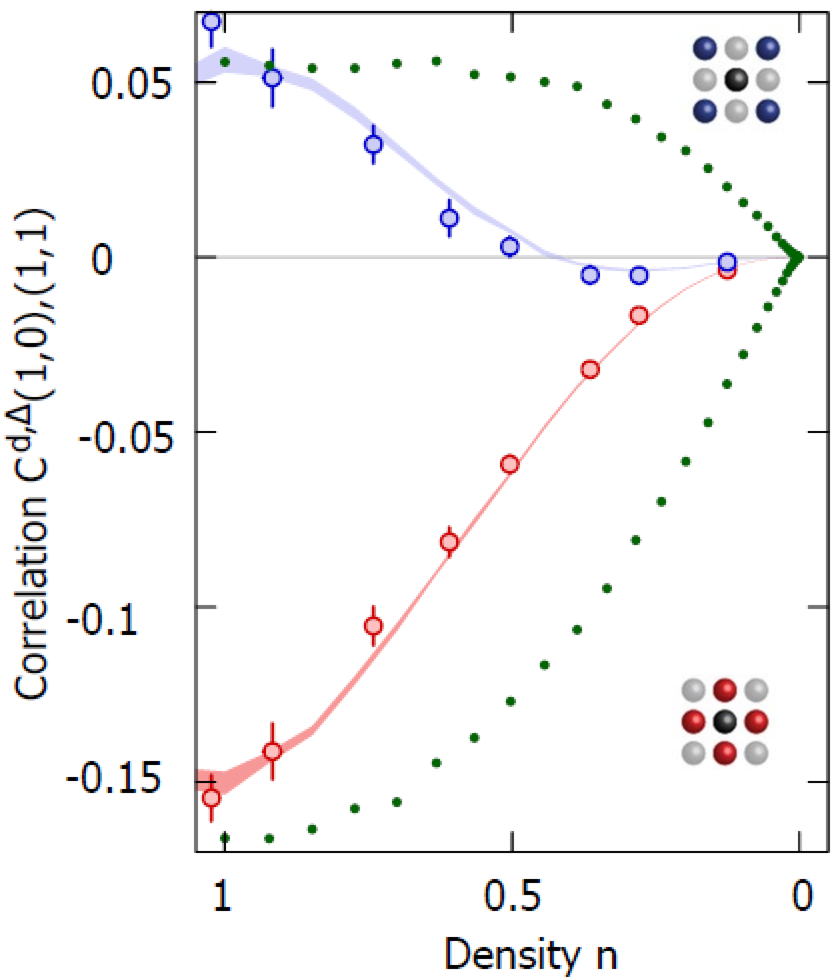

Repulsive Hubbard

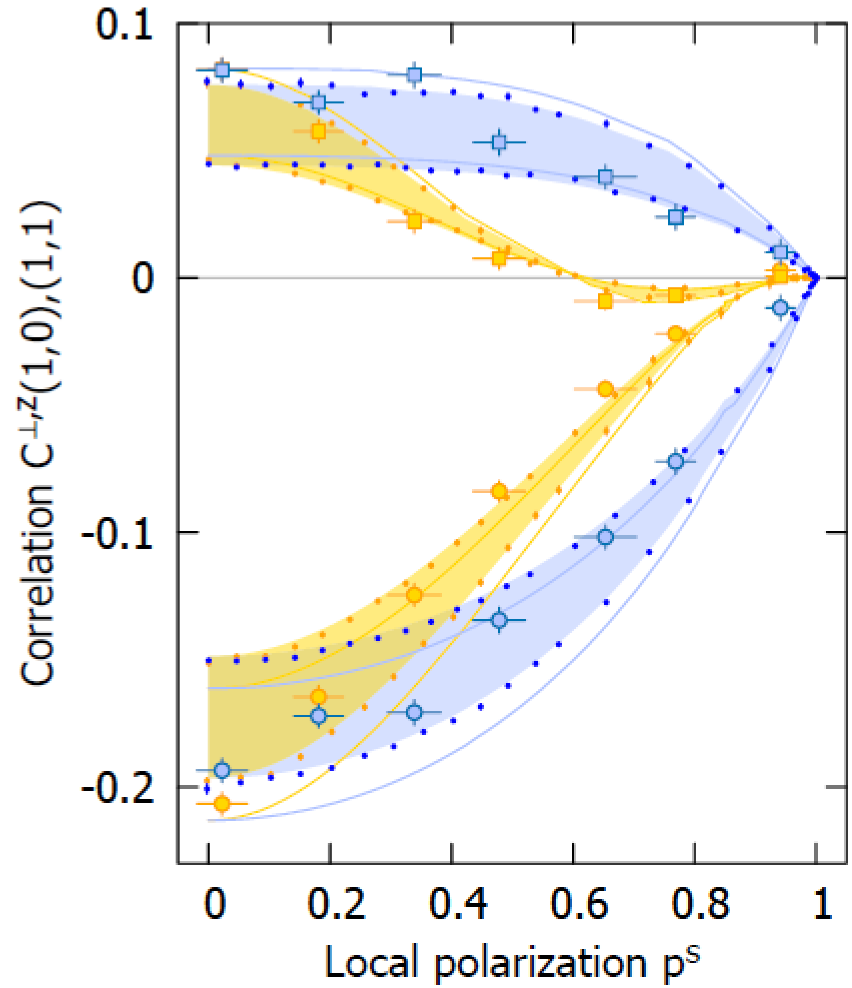


QUESTIONS

Quantum gas microscopy (Lecture II)
Conventional probes: Transport & ARPES

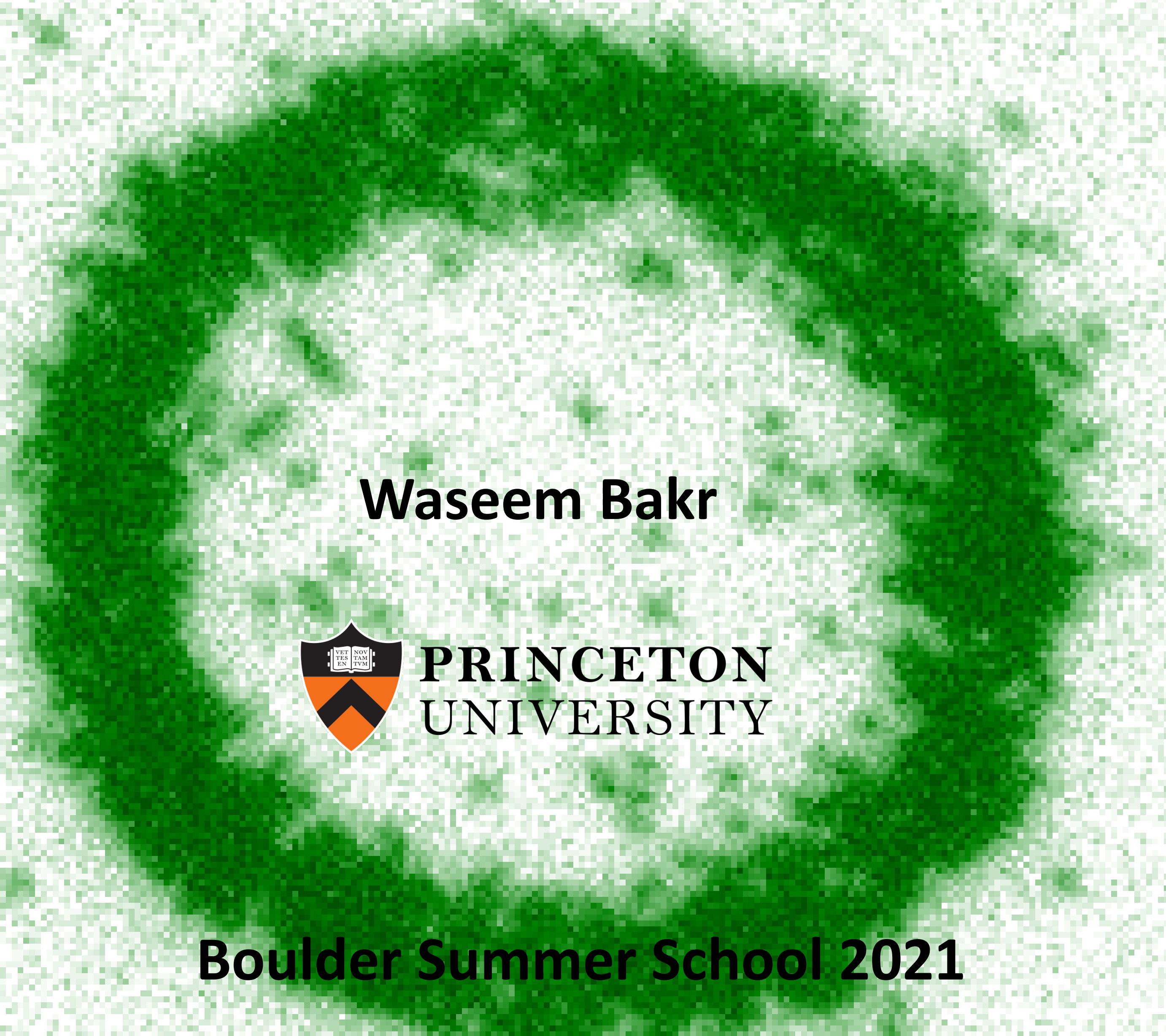

Waseem Bakr

PRINCETON UNIVERSITY

Boulder Summer School 2021

Developing tools to probe the pseudogap

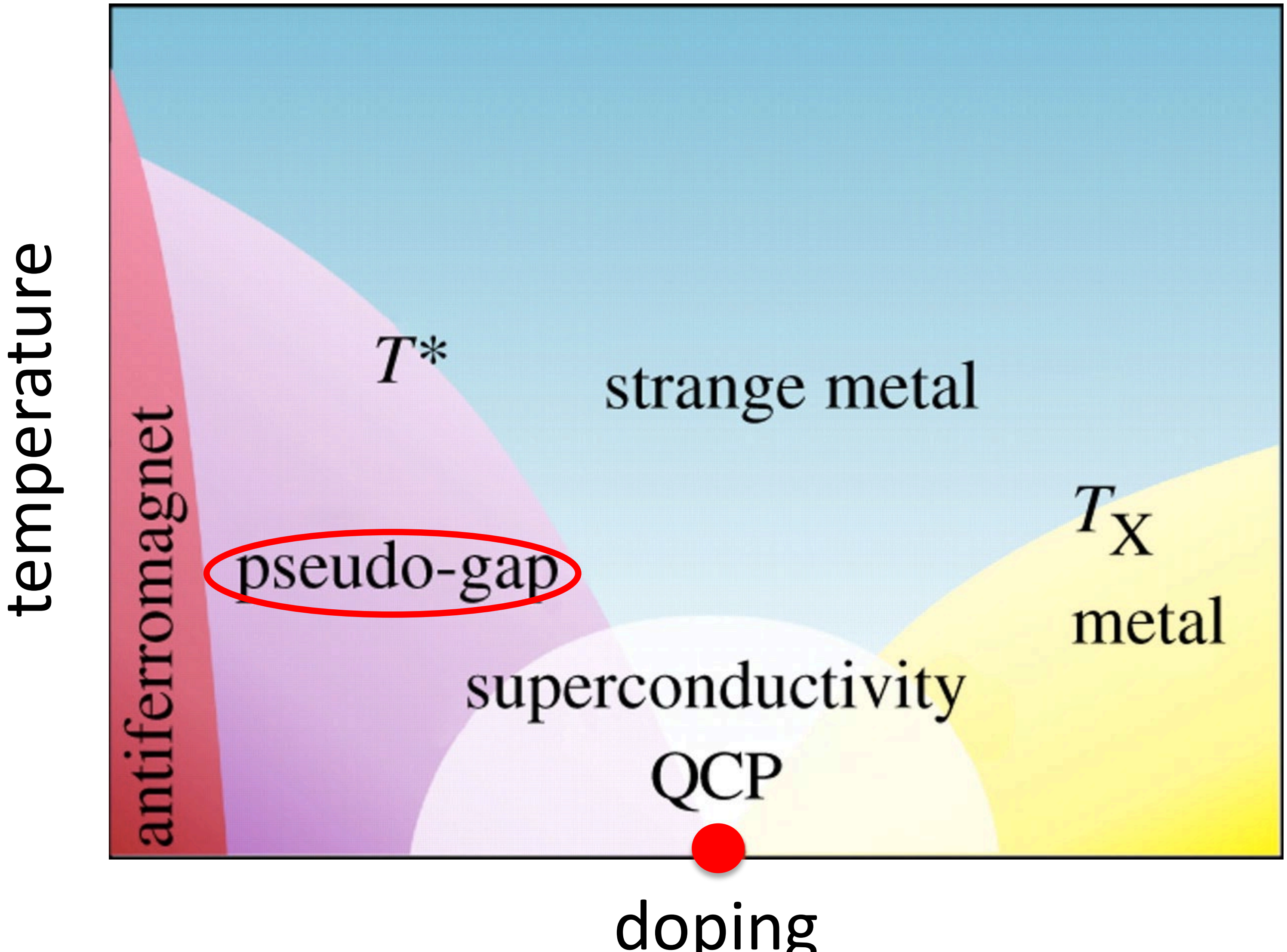

Photoemission spectroscopy

- Using a photon, excite a particle from an interacting system
- Measure the energy and momentum of the ejected particle
- Single-particle excitations of a many-body system

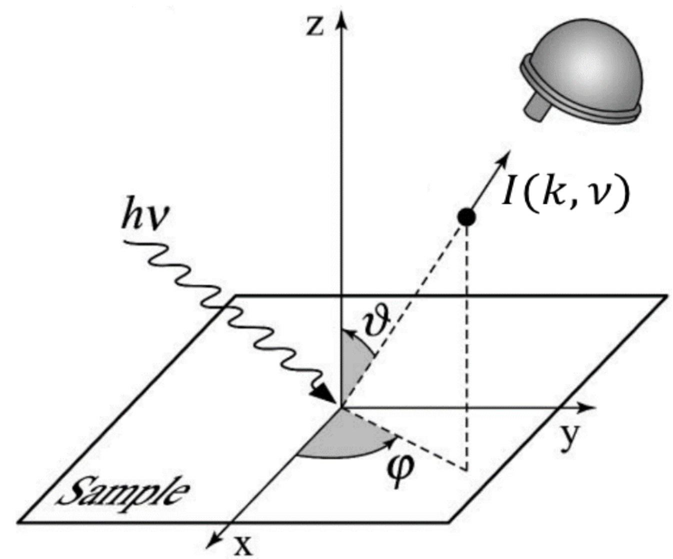

Rev. Mod. Phys. **75**, 473 (2003)

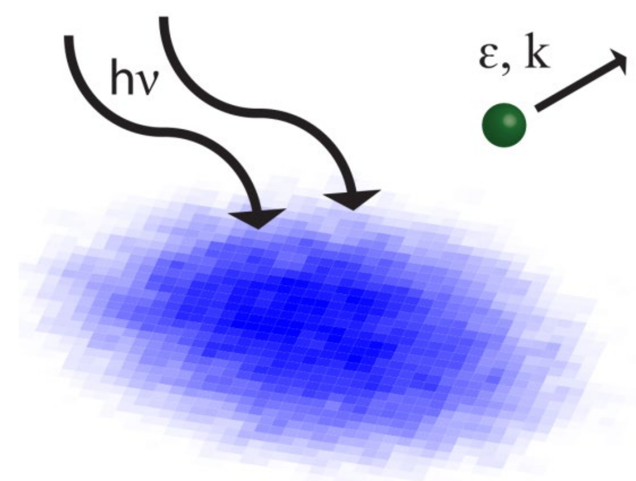

What does ARPES measure?

- How does an excitation propagate in a many-body system?
- Momentum resolved density of states
- ARPES particle current gives access to *emission*

$$G^R(k,t) = -i\theta(t)\left\langle \underbrace{c_k(t)c_k^\dagger(0)}_{\text{Remove hole (injection)}} + \overbrace{c_k^\dagger(0)c_k(t)}^{\text{Remove particle (emission)}} \right\rangle$$

$$A(k,\omega) = \underbrace{-\frac{1}{\pi}\mathrm{Im}\{G^R(k,\omega)\}}_{\text{Emission + injection}}$$

$$A^-(k,\omega) = \underbrace{A(k,\omega)f(\omega)}_{\text{Emission only}}$$

ARPES with a QGM

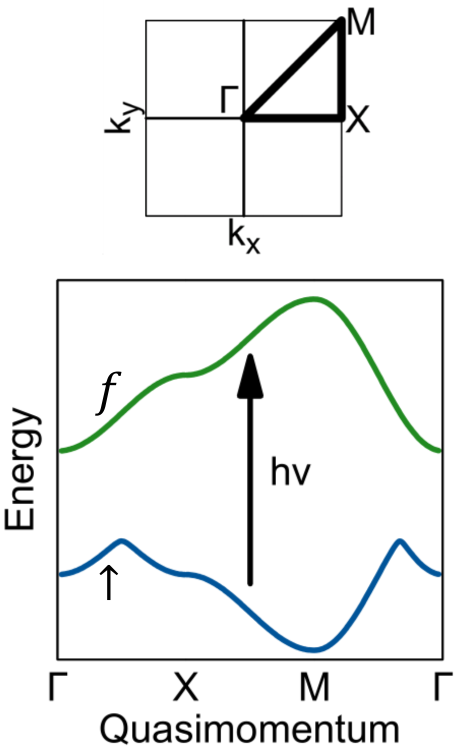

$$\mathcal{H} = \underbrace{\mathcal{H}_o}_{\text{Hubbard system}} - \Omega \sum_k \left(\underbrace{c^\dagger_{k\,f} c_{k\uparrow} + c^\dagger_{k\uparrow} c_{k\,f}}_{\text{rf probe}}\right)$$

- Radiofrequency photon transfers to non-interacting state but preserves momentum

ARPES with a QGM

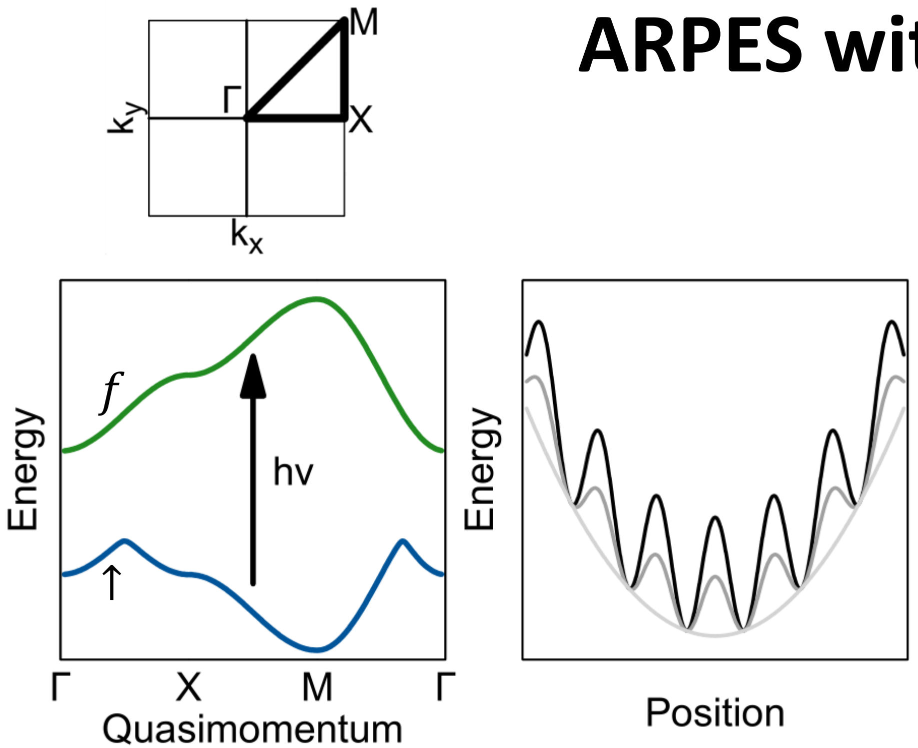

- Radiofrequency photon transfers to non-interacting state but preserves momentum
- Band mapping transforms quasimomentum to real momentum

ARPES with a QGM

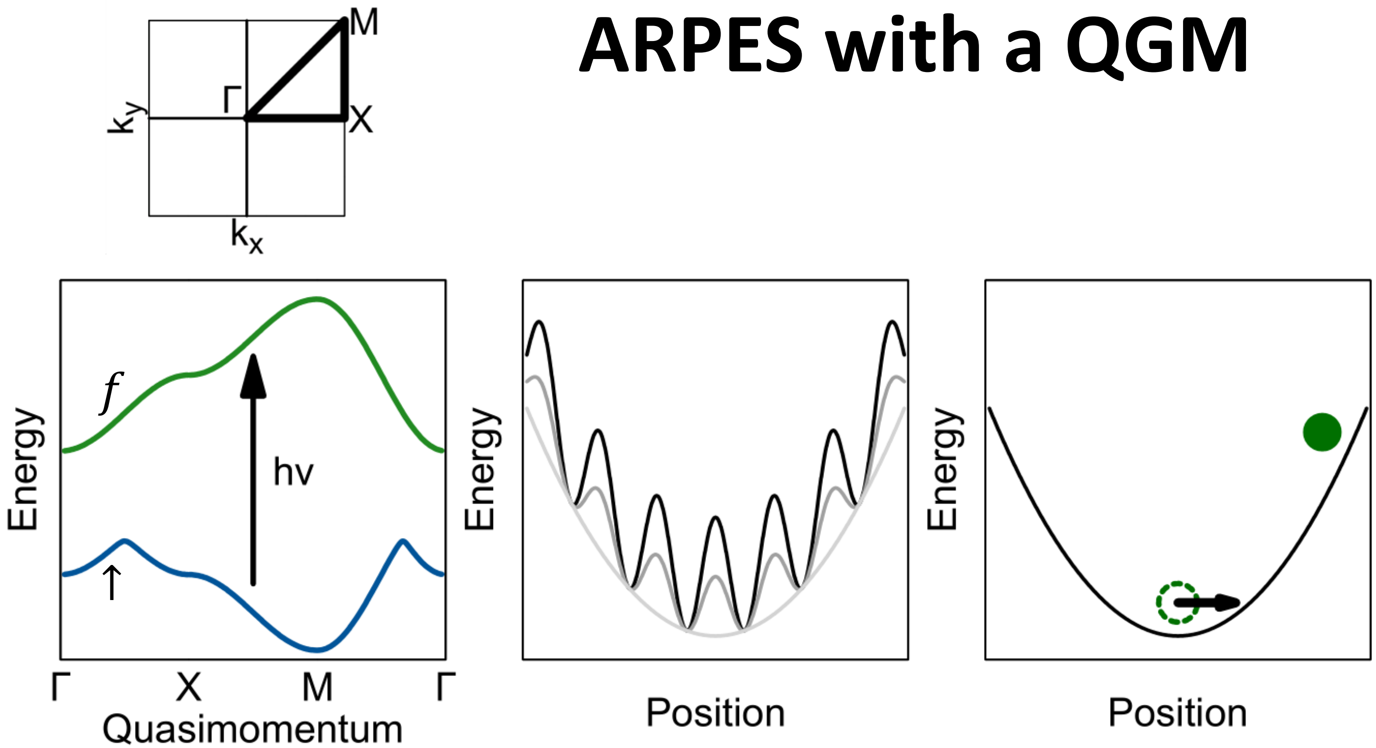

- Radiofrequency photon transfers to non-interacting state but preserves momentum
- Band mapping transforms quasimomentum to real momentum
- $^{T}/_{4}$ expansion in harmonic trap maps momentum space to real space (similar to time-of-flight measurement)

ARPES with a QGM

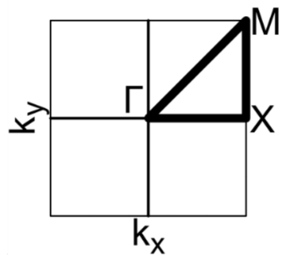

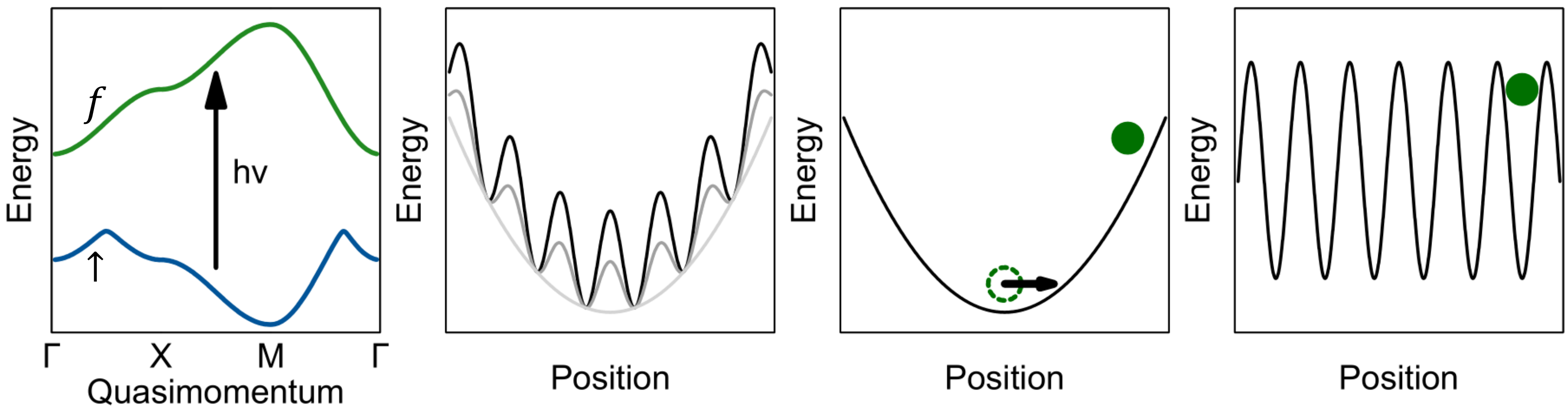

- Radiofrequency photon transfers to non-interacting state but preserves momentum
- Band mapping transforms quasimomentum to real momentum
- $T/_4$ expansion in harmonic trap maps momentum space to real space (similar to time-of-flight measurement)
- Freeze atoms in deep lattice and detect

ARPES data: increasing interaction strength

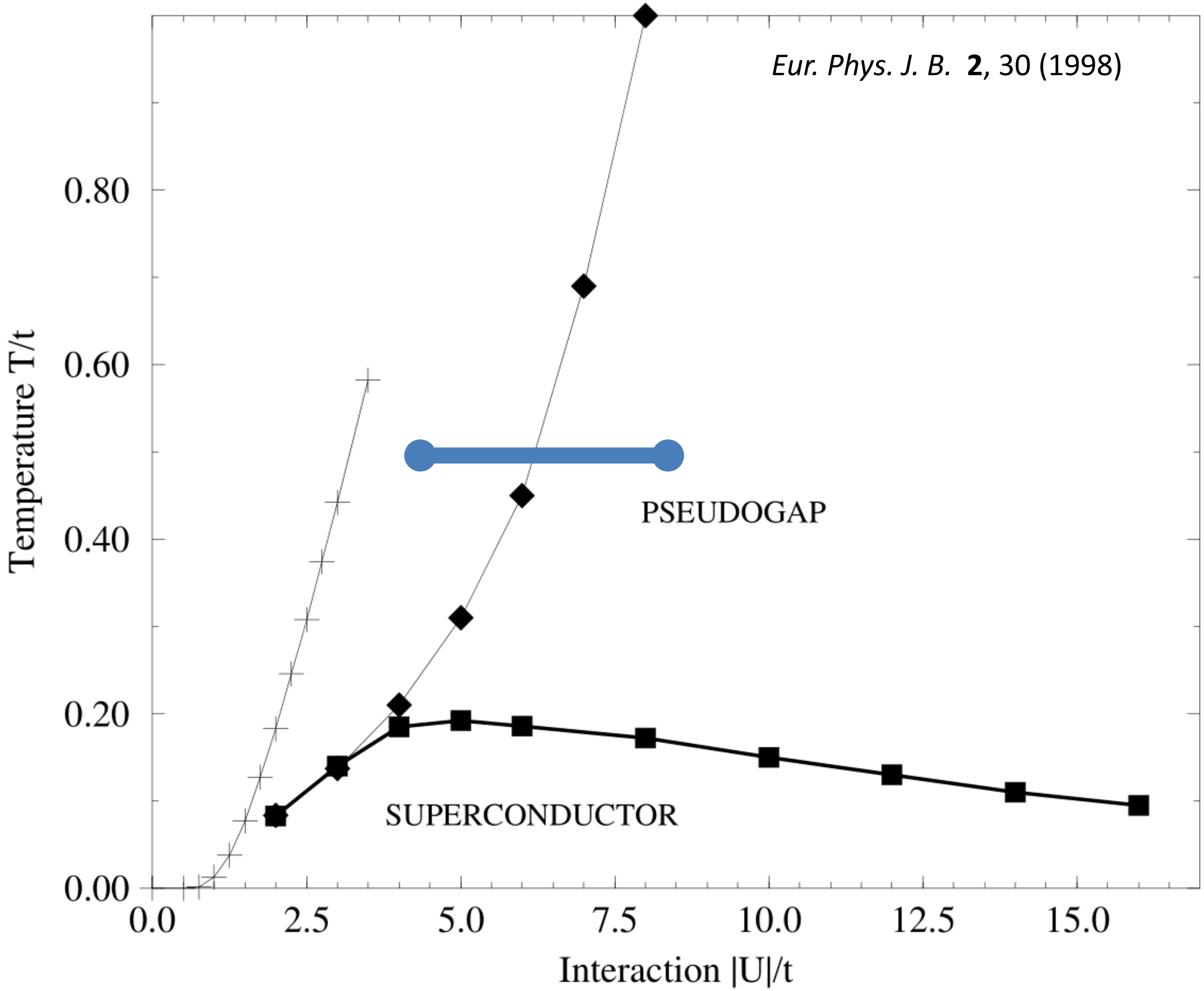

Opening of pseudogap across BCS-BEC crossover

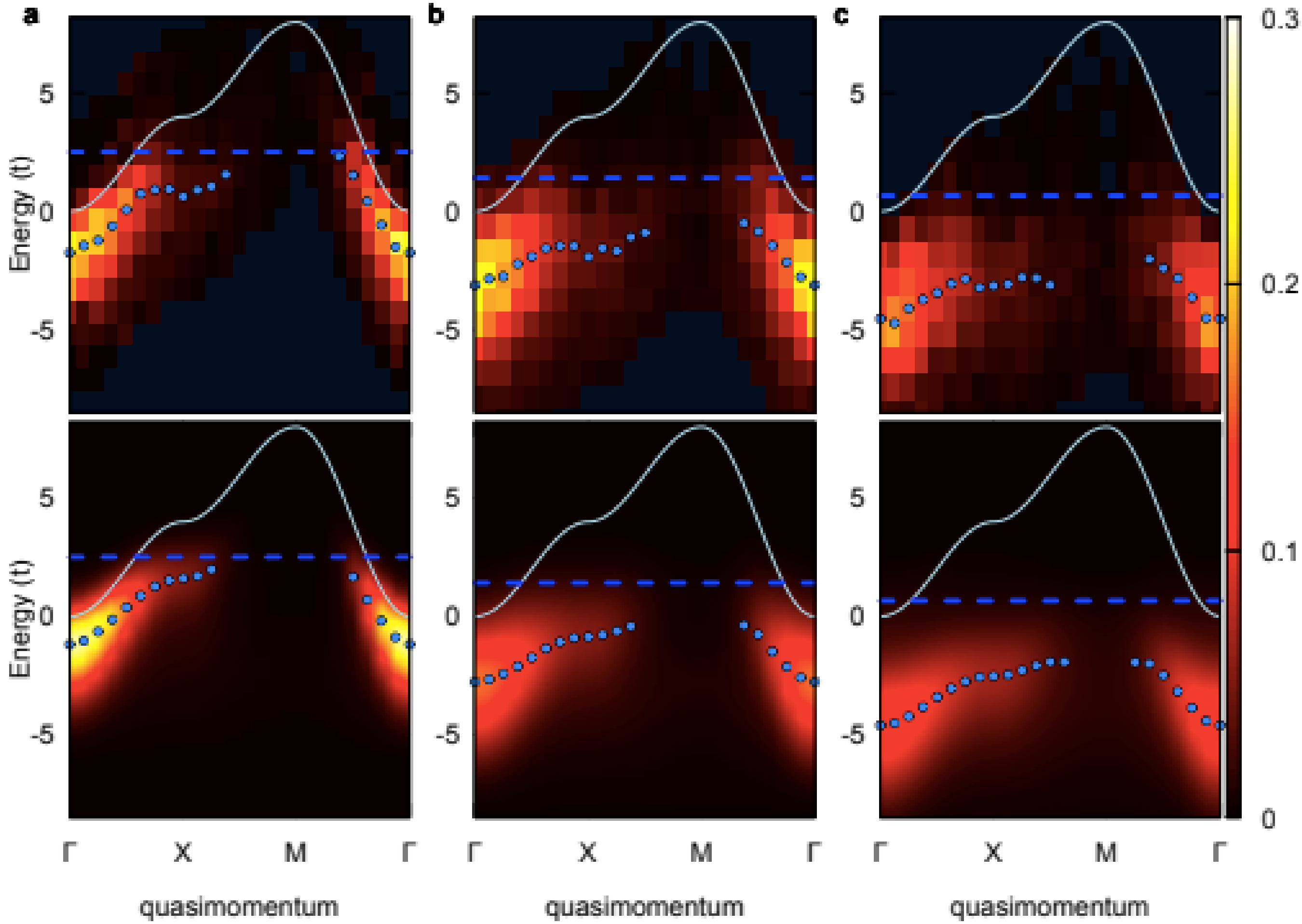

Brown … Bakr, Nature Phys. 16, 26 (2020)

ARPES: outlook for +U model

Pseudogap and Fermi-Surface Topology in the Two-Dimensional Hubbard Model

Wei Wu, Mathias S. Scheurer, Shubhayu Chatterjee, Subir Sachdev, Antoine Georges, and Michel Ferrero
Phys. Rev. X **8**, 021048 – Published 22 May 2018

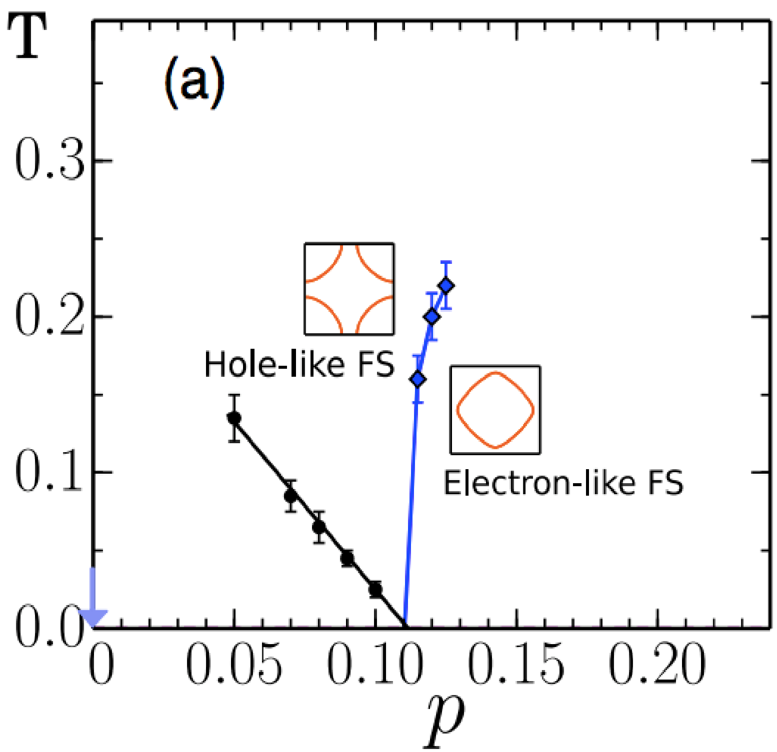

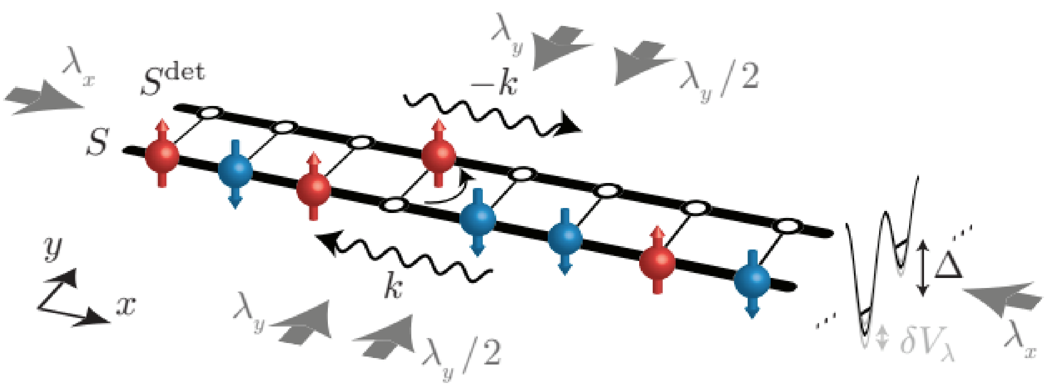

Bohrdt … Grusdt, Phys. Rev. B 97, 125117 (2018)


QUESTIONS

Cuprate phase diagram

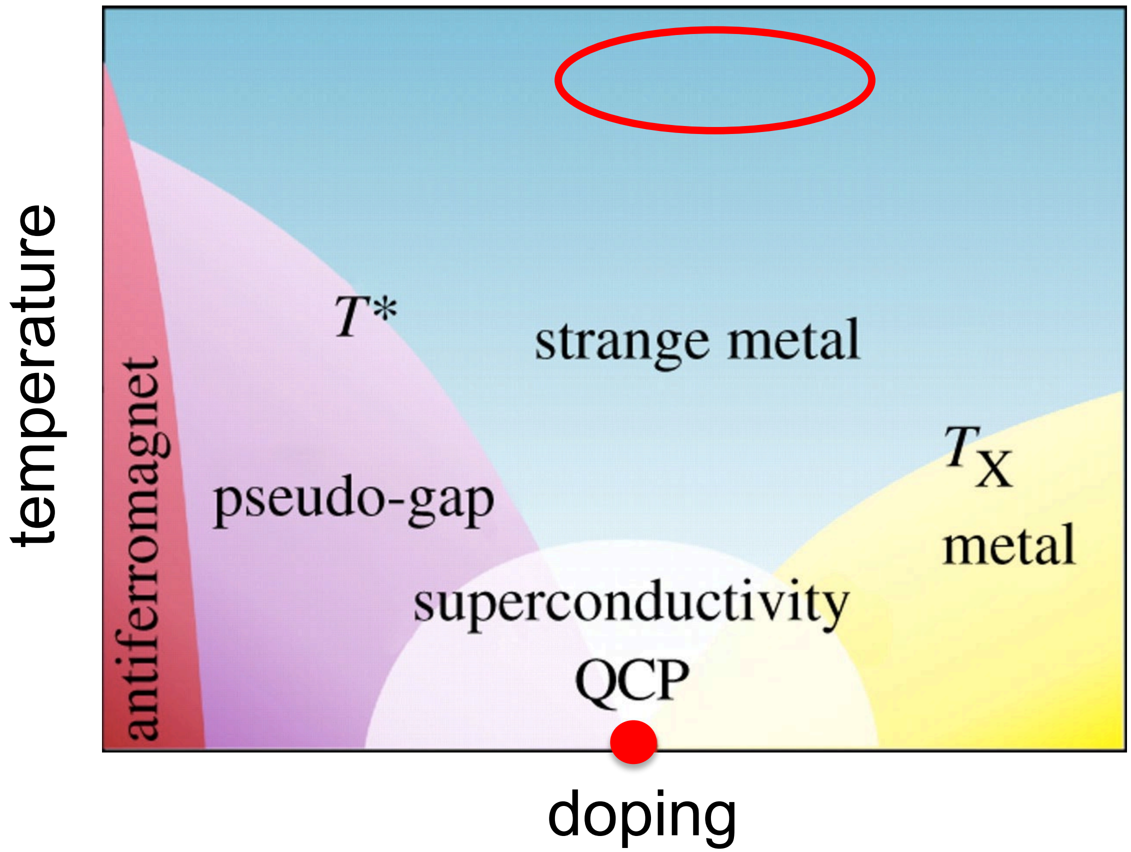

Conventional
(weakly interacting)

$$\Gamma = \frac{\langle v \rangle}{l}$$

$$\frac{1}{\rho} = \frac{ne^2}{m^* \Gamma}$$

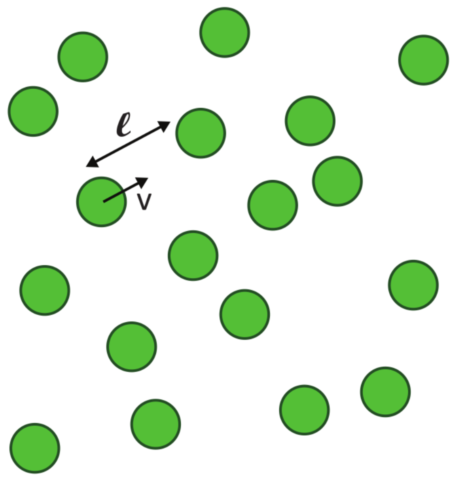

- Charge, spin, energy transported by quasiparticles
- Mean free path must be larger than lattice spacing. Mott-Ioffe-Regel (MIR) limit
- $\rho \sim T^2$, Fermi-liquid

Unconventional
(strongly correlated)

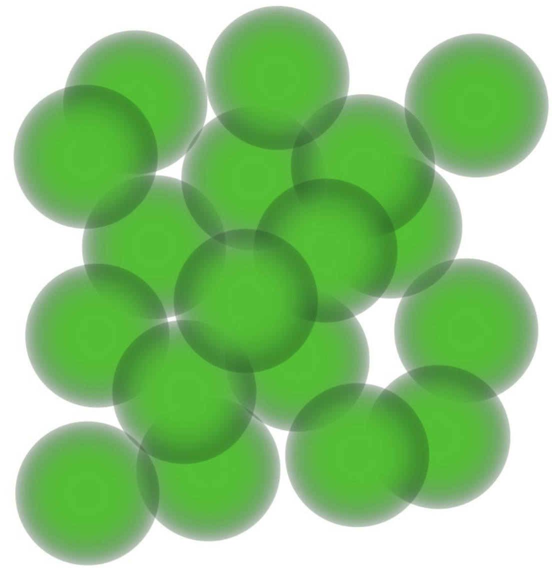

- Strong enough interactions destroy quasiparticles
- Momentum relaxation rate no longer gives resistivity
- “Bad metals” violate MIR limit and commonly show $\rho \sim T$

Bad metallic transport in a cold atom Fermi-Hubbard system

Bakr group, Brown *et. al.*, Science **363**, 379 (2019)

Measurement Protocol

- Load atoms in combined optical lattice + repulsive potential with sinusoidal modulation
- Turn off modulation, take fluorescence images at different times
- Macroscopic (ρ) transport connected to microscopic (D) through Nernst-Einstein relation:

$$^{1}/_{\rho} = \left(\frac{\partial n}{\partial \mu}\right)\bigg|_{T} D$$

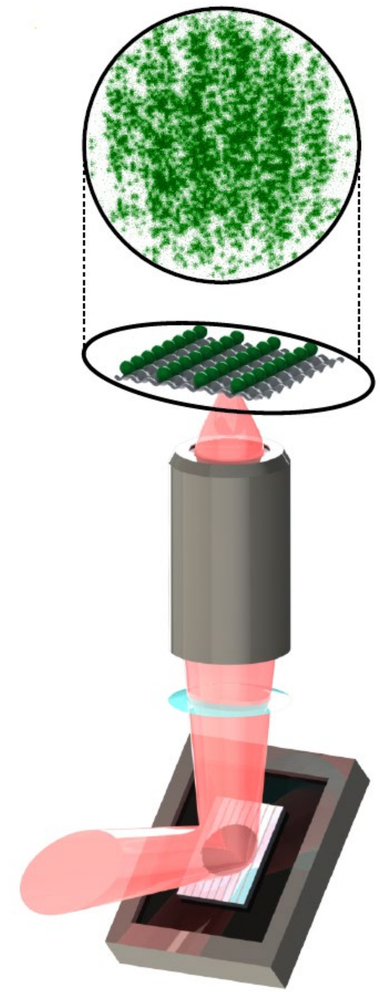

Measurement Protocol

- Load atoms in combined optical lattice + repulsive potential with sinusoidal modulation
- Turn off modulation, take fluorescence images at different times
- Macroscopic (ρ) transport connected to microscopic (D) through Nernst-Einstein relation:

$$^{1}/_{\rho} = \left(\frac{\partial n}{\partial \mu}\right)\bigg|_{T} D$$

Brown *et. al.*, Science **363**, 379 (2019)

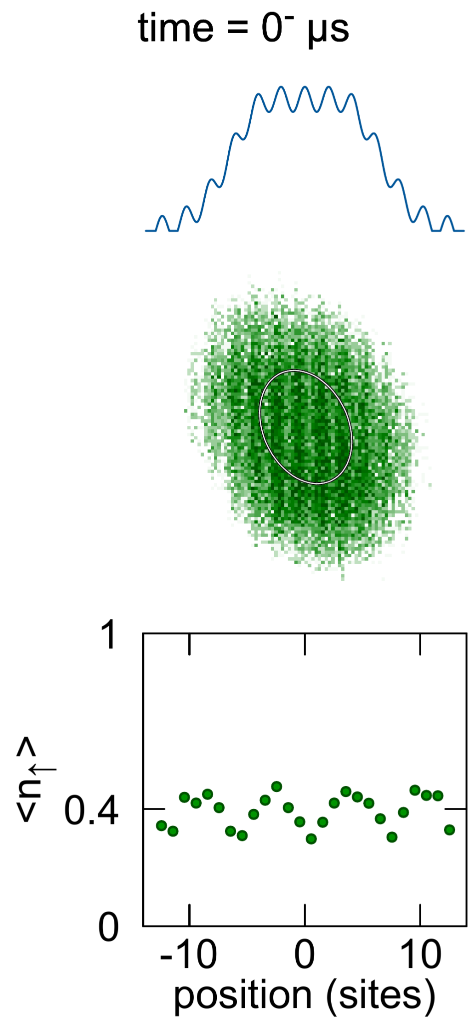

Measurement Protocol

- Load atoms in combined optical lattice + repulsive potential with sinusoidal modulation
- Turn off modulation, take fluorescence images at different times
- Macroscopic (ρ) transport connected to microscopic (D) through Nernst-Einstein relation:

$$1/\rho = \left(\frac{\partial n}{\partial \mu}\right)\bigg|_T D$$

Brown *et. al.*, Science **363**, 379 (2019)

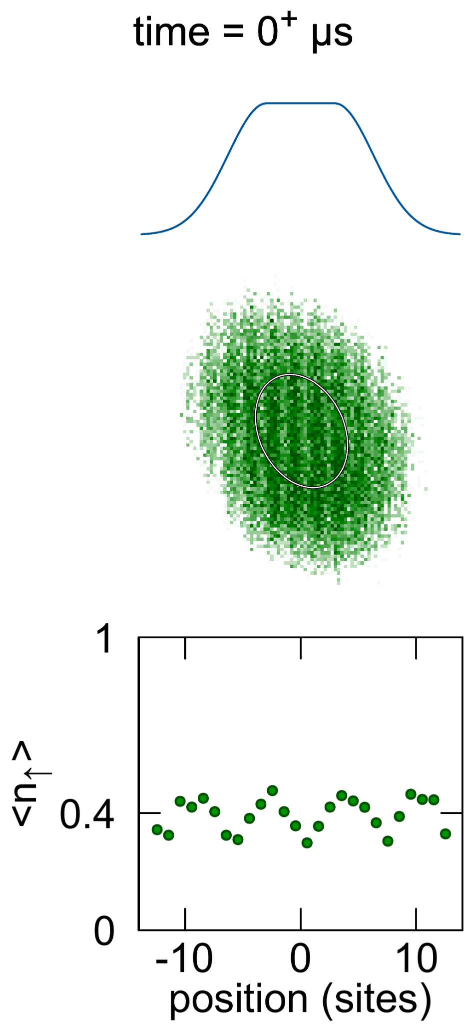

Measurement Protocol

- Load atoms in combined optical lattice + repulsive potential with sinusoidal modulation
- Turn off modulation, take fluorescence images at different times
- Macroscopic (ρ) transport connected to microscopic (D) through Nernst-Einstein relation:

$$1/\rho = \left(\frac{\partial n}{\partial \mu}\right)\Bigg|_T D$$

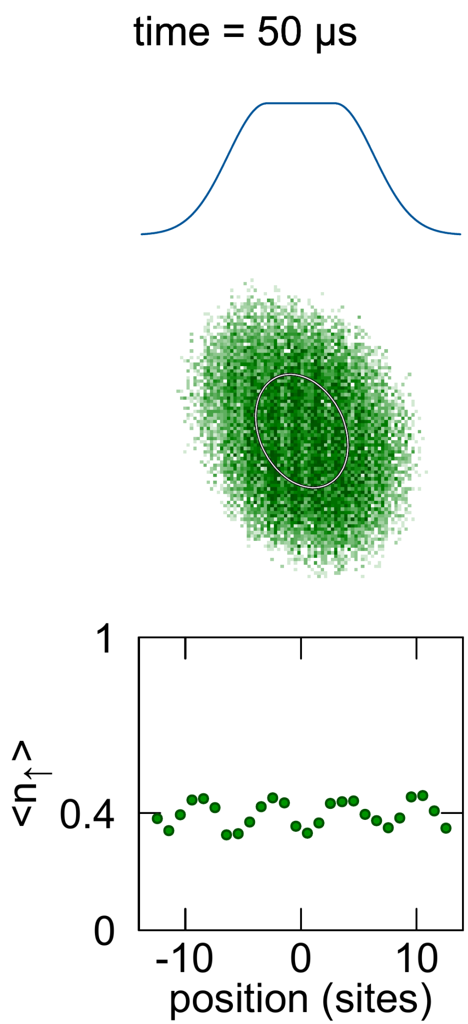

Brown *et. al.*, Science **363**, 379 (2019)

Measurement Protocol

- Load atoms in combined optical lattice + repulsive potential with sinusoidal modulation
- Turn off modulation, take fluorescence images at different times
- Macroscopic (ρ) transport connected to microscopic (D) through Nernst-Einstein relation:

$$1/\rho = \left(\frac{\partial n}{\partial \mu}\right)\bigg|_T D$$

Brown *et. al.,* Science **363**, 379 (2019)

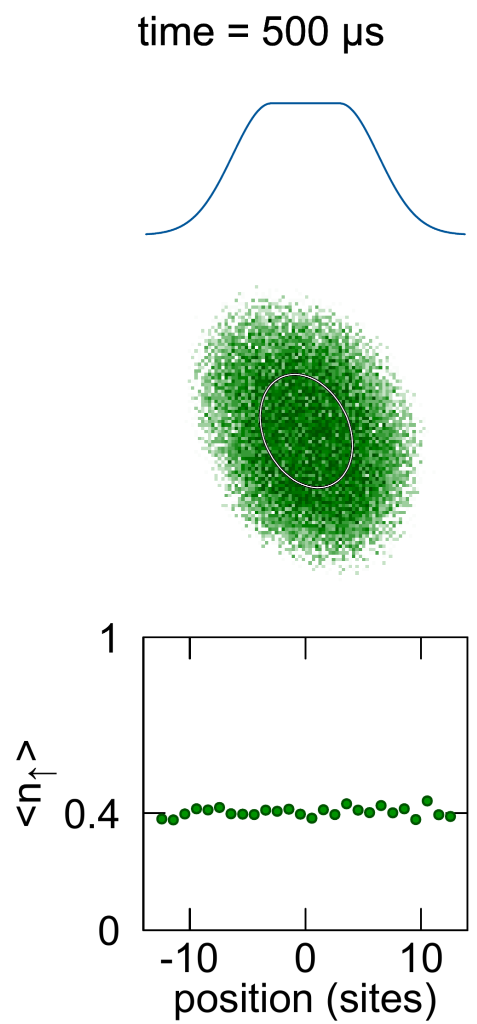

Decaying density modulation

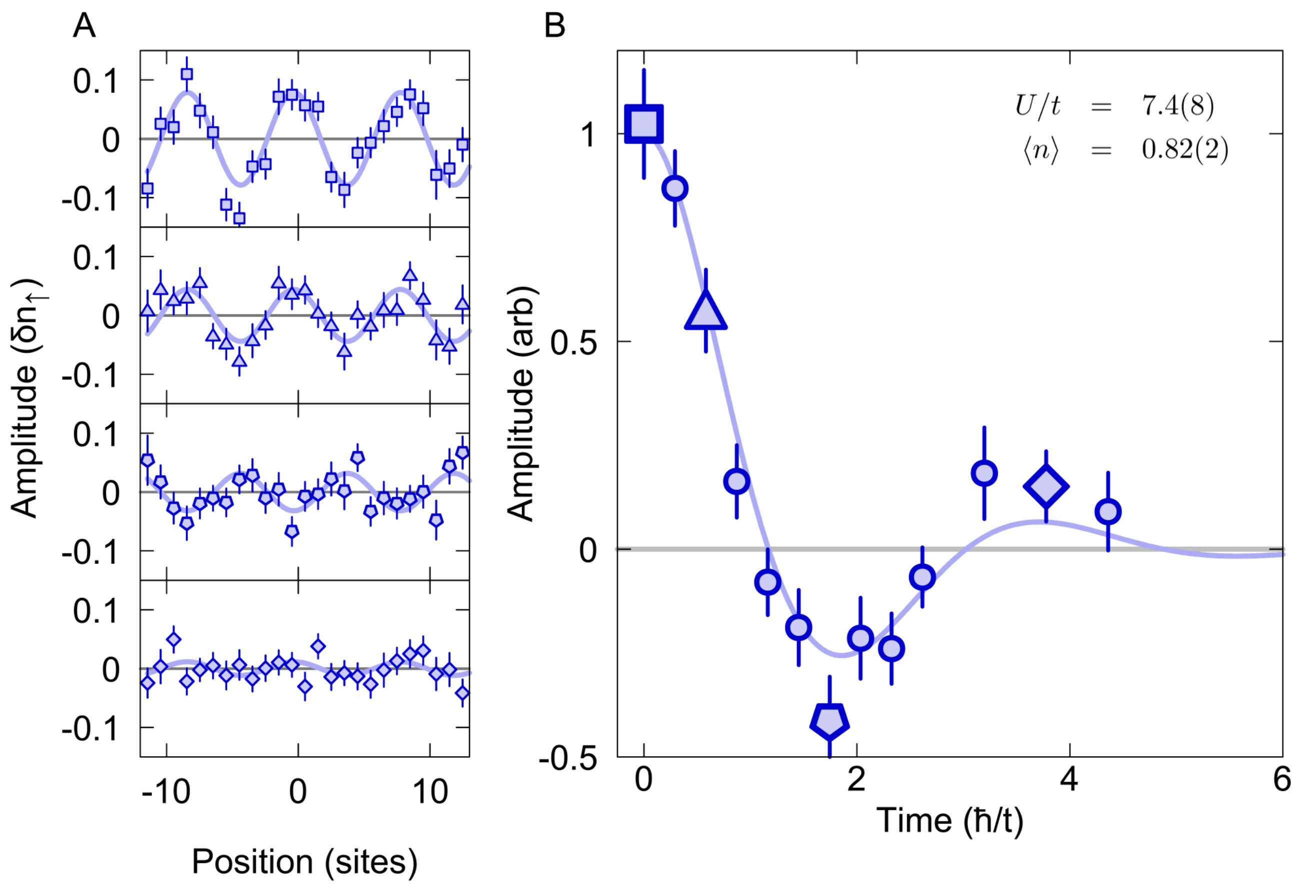

Decaying density modulation

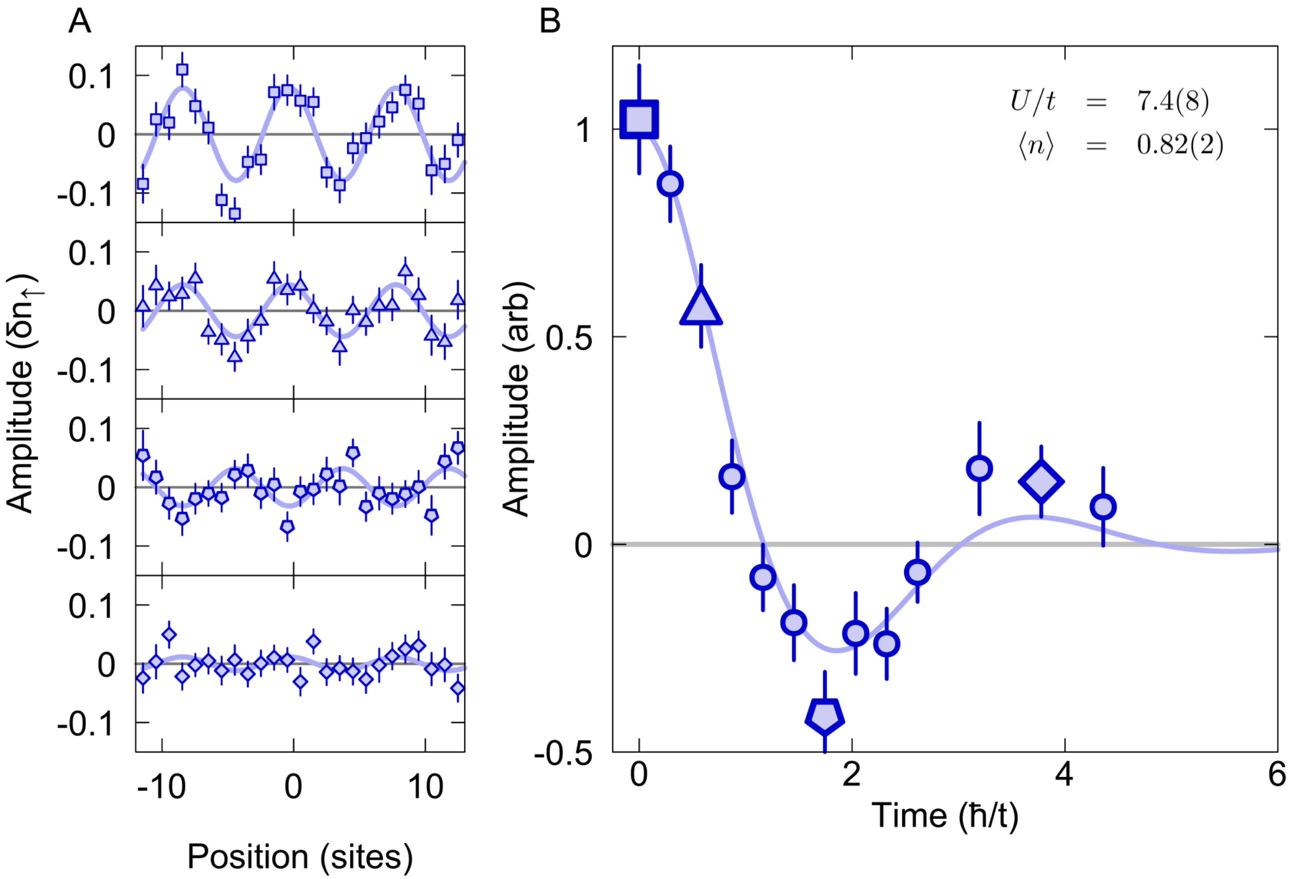

Decaying density modulation

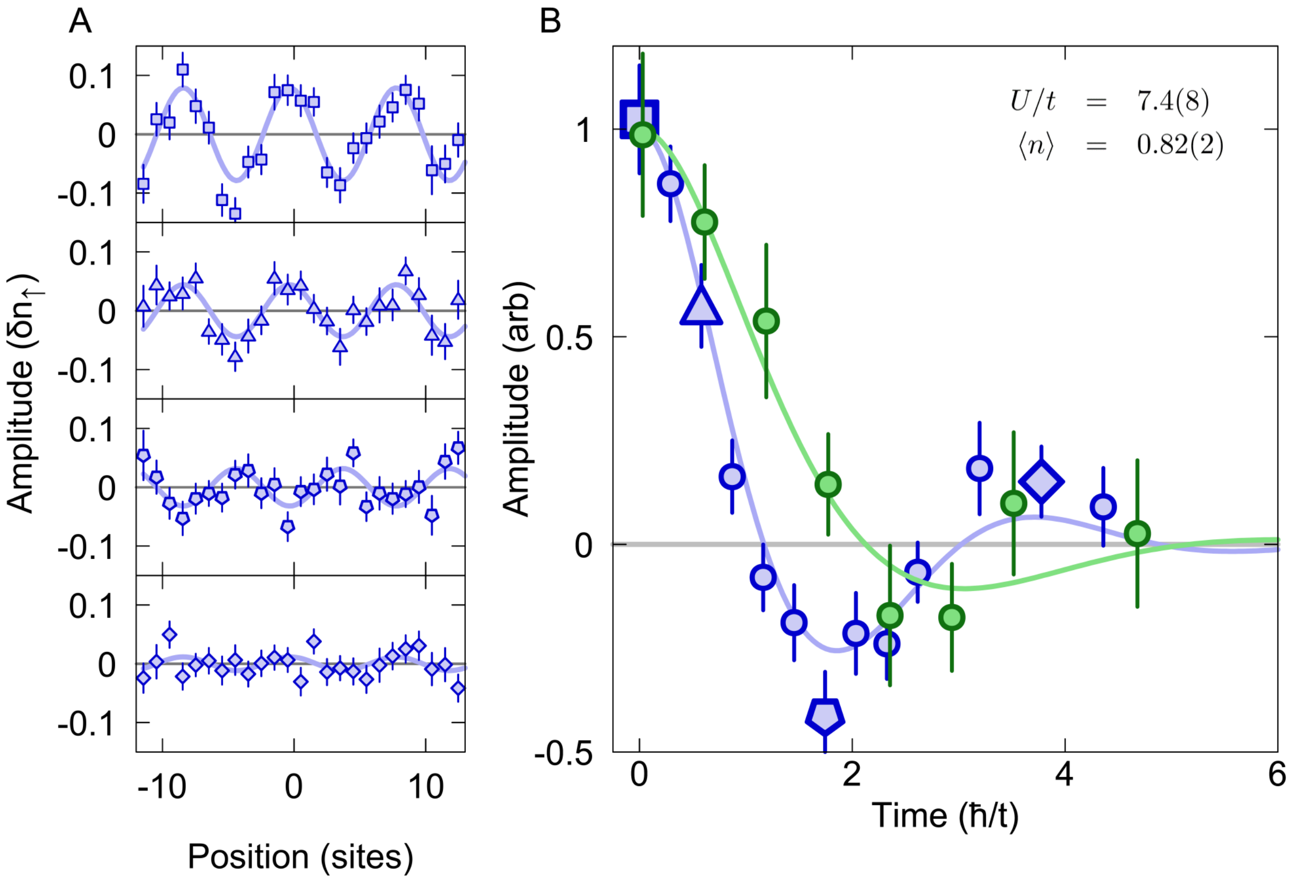

Decaying density modulation

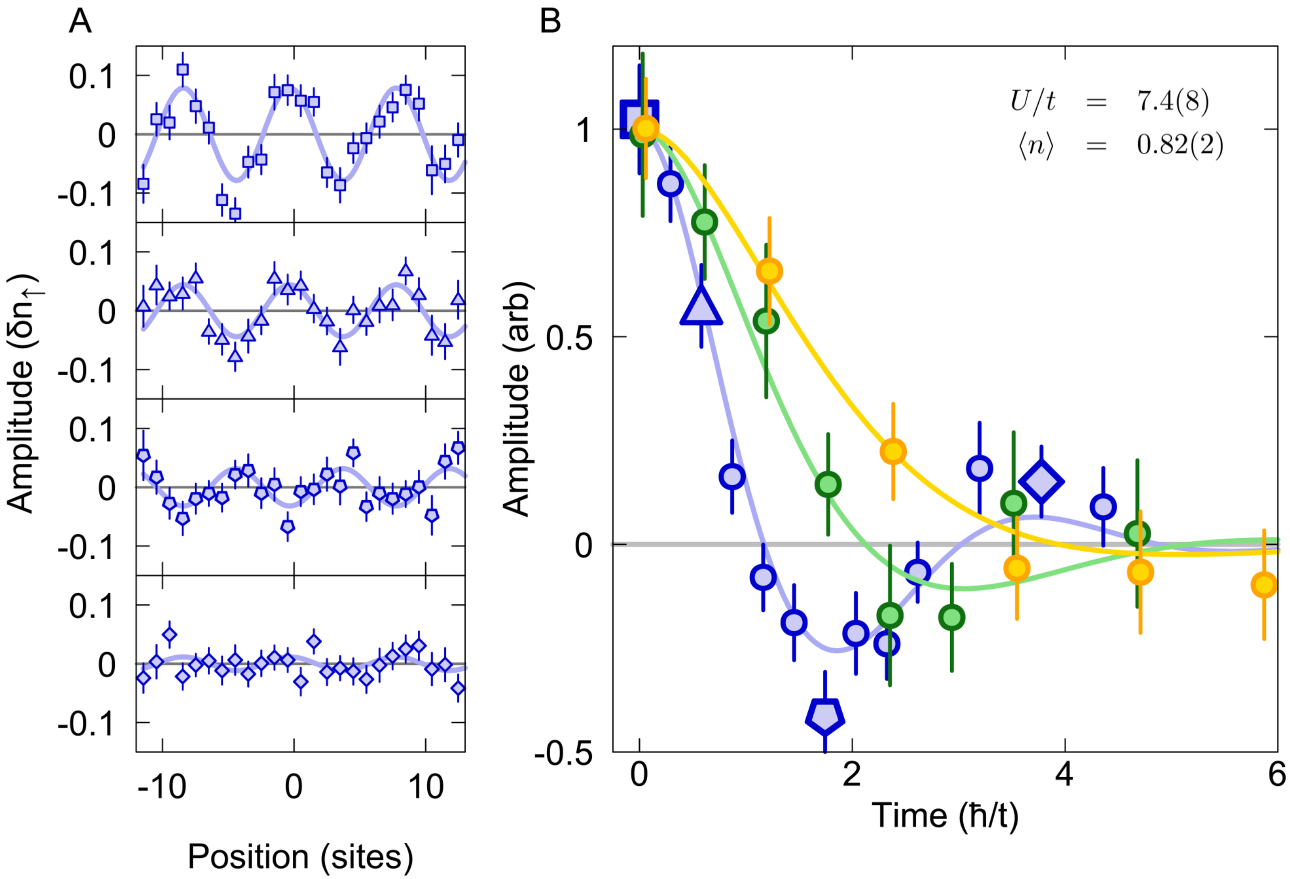

Decaying density modulation

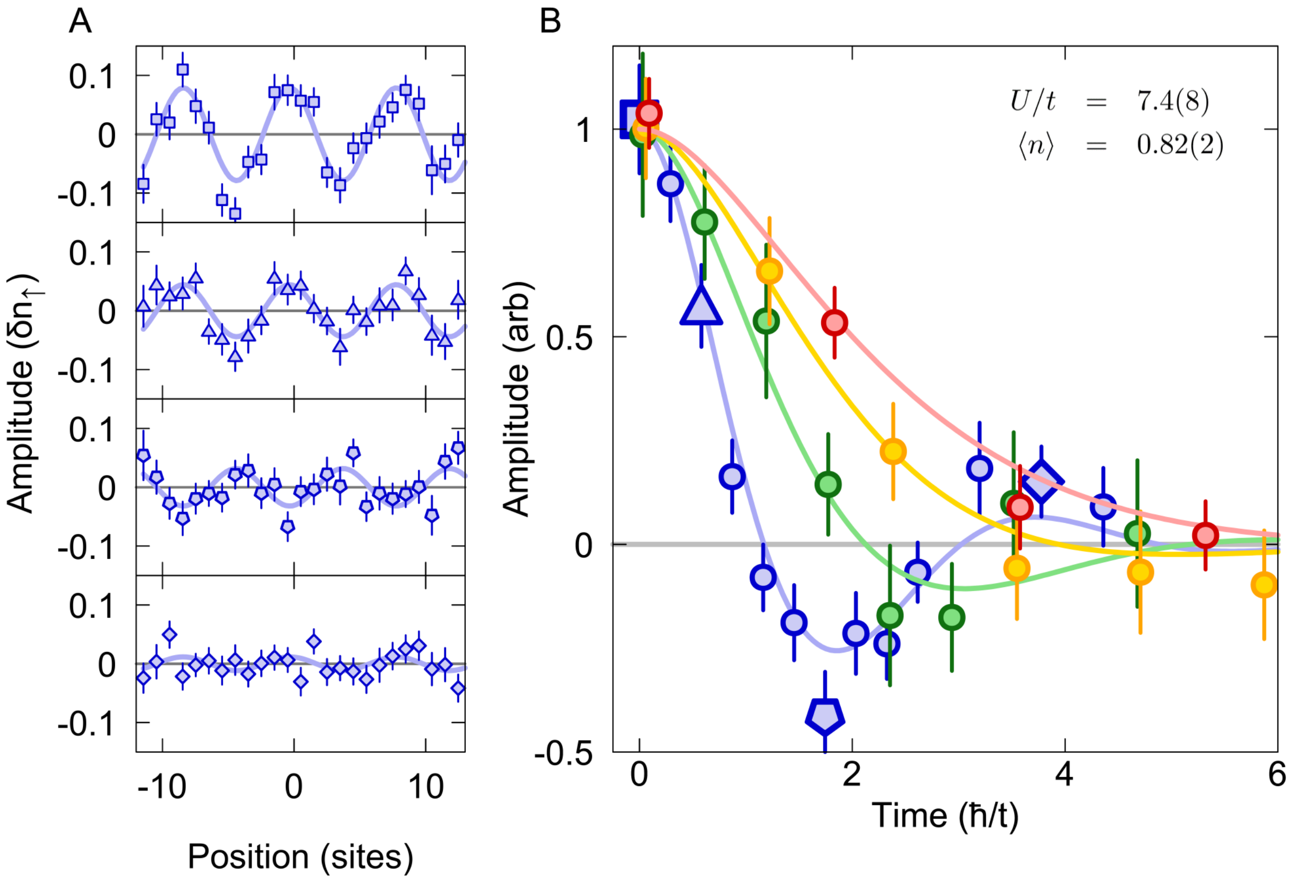

Hydrodynamic Model

- Diffusion (Fick's Law) neglects finite time to establish current
- D, diffusion constant
- Γ, current relaxation rate
- Crossover from diffusive mode to sound mode

$$\overbrace{\partial_t n(\mathbf{r},t) = -\nabla\cdot\mathbf{J}(\mathbf{r},t)}^{\text{“charge” conservation}}$$

$$\partial_t \mathbf{J}(\mathbf{r},t) = -\Gamma\left(\underbrace{D\nabla n(\mathbf{r},t) + \mathbf{J}(\mathbf{r},t)}_{\text{Fick's Law}}\right)$$

$$\boxed{\partial_t^2 n + \Gamma\partial_t n + \Gamma D k^2 n = 0}$$

P.T. Brown, D. Mitra, E. Guardado-Sanchez, R. Nourafkan, A. Reymbaut, C.D. Hebert, S. Bergeron, A-M.S. Tremblay, J. Kokalj, D.A. Huse, P. Schauss, and W.S. Bakr. Science **363**, 379 (2019)

Hydrodynamic Parameters

- *Simultaneous* fit of all wavelength data for each temperature
- Low temperature, Pauli blocking closes scattering channels
- D does not violate MIR derived bound.
- Model less sensitive to Γ in overdamped limit.

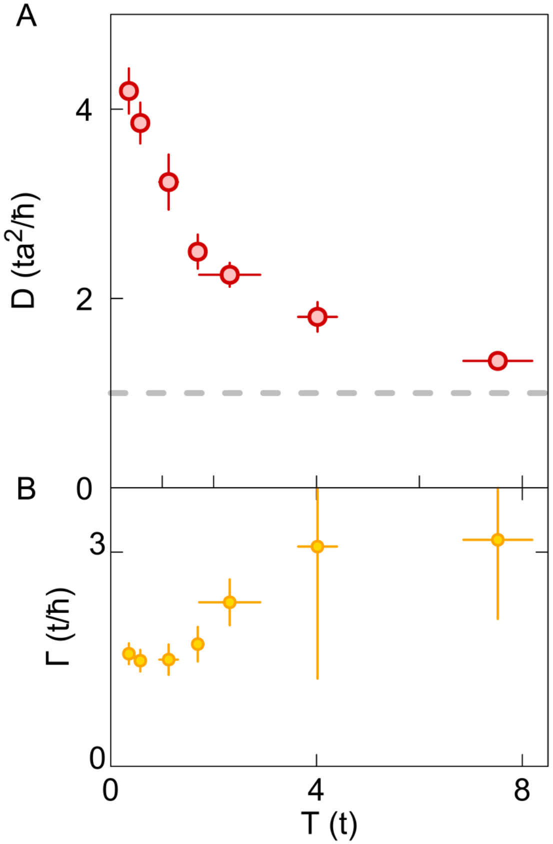

$$D \approx \frac{\langle v \rangle l}{2} > \frac{ta^2}{\hbar}$$

P.T. Brown, D. Mitra, E. Guardado-Sanchez, R. Nourafkan, A. Reymbaut, C.D. Hebert, S. Bergeron, A-M.S. Tremblay, J. Kokalj, D.A. Huse, P. Schauss, and W.S. Bakr. Science **363**, 379 (2019)

Compressibility

- Images of both spin states versus chemical potential
- Temperature dependent in this range
- In high temperature limit of single band model:

$$\chi = n(1 - {}^{n}/_{2})/T$$

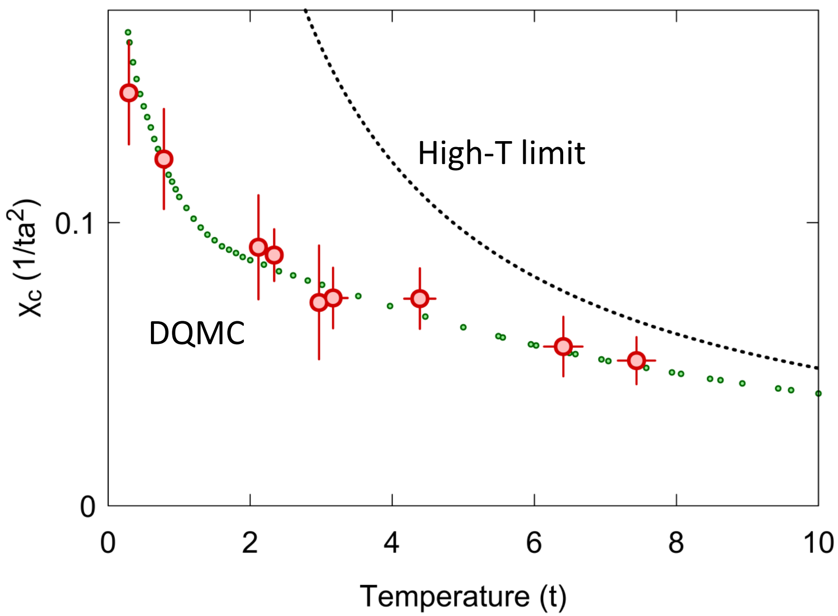

P.T. Brown, D. Mitra, E. Guardado-Sanchez, R. Nourafkan, A. Reymbaut, C.D. Hebert, S. Bergeron, A-M.S. Tremblay, J. Kokalj, D.A. Huse, P. Schauss, and W.S. Bakr. Science **363**, 379 (2019)

Resistivity Versus Temperature

- Resistivity from Nernst-Einstein $^1/_\rho = \left(\frac{\partial n}{\partial \mu}\right) D$
- Linear over this temperature range
- Exceeds resistivity bound inferred from MIR limit ("bad metal")

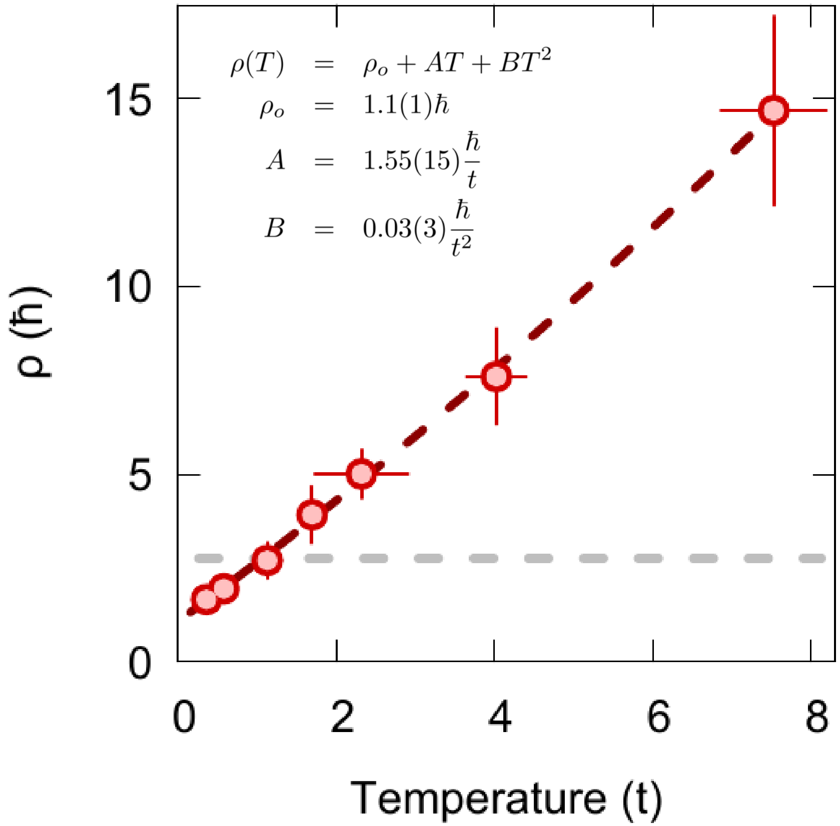

$$\rho_{\max} \approx \sqrt{\frac{2\pi}{n}}\hbar$$

P.T. Brown, D. Mitra, E. Guardado-Sanchez, R. Nourafkan, A. Reymbaut, C.D. Hebert, S. Bergeron, A-M.S. Tremblay, J. Kokalj, D.A. Huse, P. Schauss, and W.S. Bakr. Science **363**, 379 (2019)

Resistivity Versus Temperature

- Resistivity from Nernst-Einstein $^1/_\rho = \left(\frac{\partial n}{\partial \mu}\right) D$
- Linear over this temperature range
- Exceeds resistivity bound inferred from MIR limit ("bad metal")

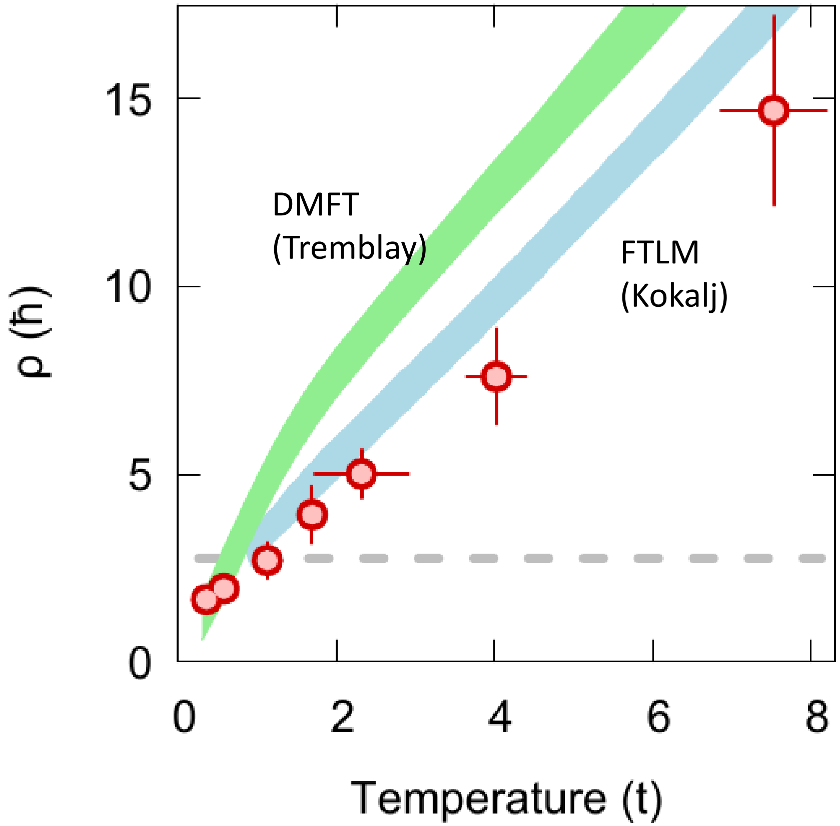

$$\rho_{\max} \approx \sqrt{\frac{2\pi}{n}}\hbar$$

P.T. Brown, D. Mitra, E. Guardado-Sanchez, R. Nourafkan, A. Reymbaut, C.D. Hebert, S. Bergeron, A-M.S. Tremblay, J. Kokalj, D.A. Huse, P. Schauss, and W.S. Bakr. Science **363**, 379 (2019)

MIT Experiment: Fermi-Hubbard Model in a Box

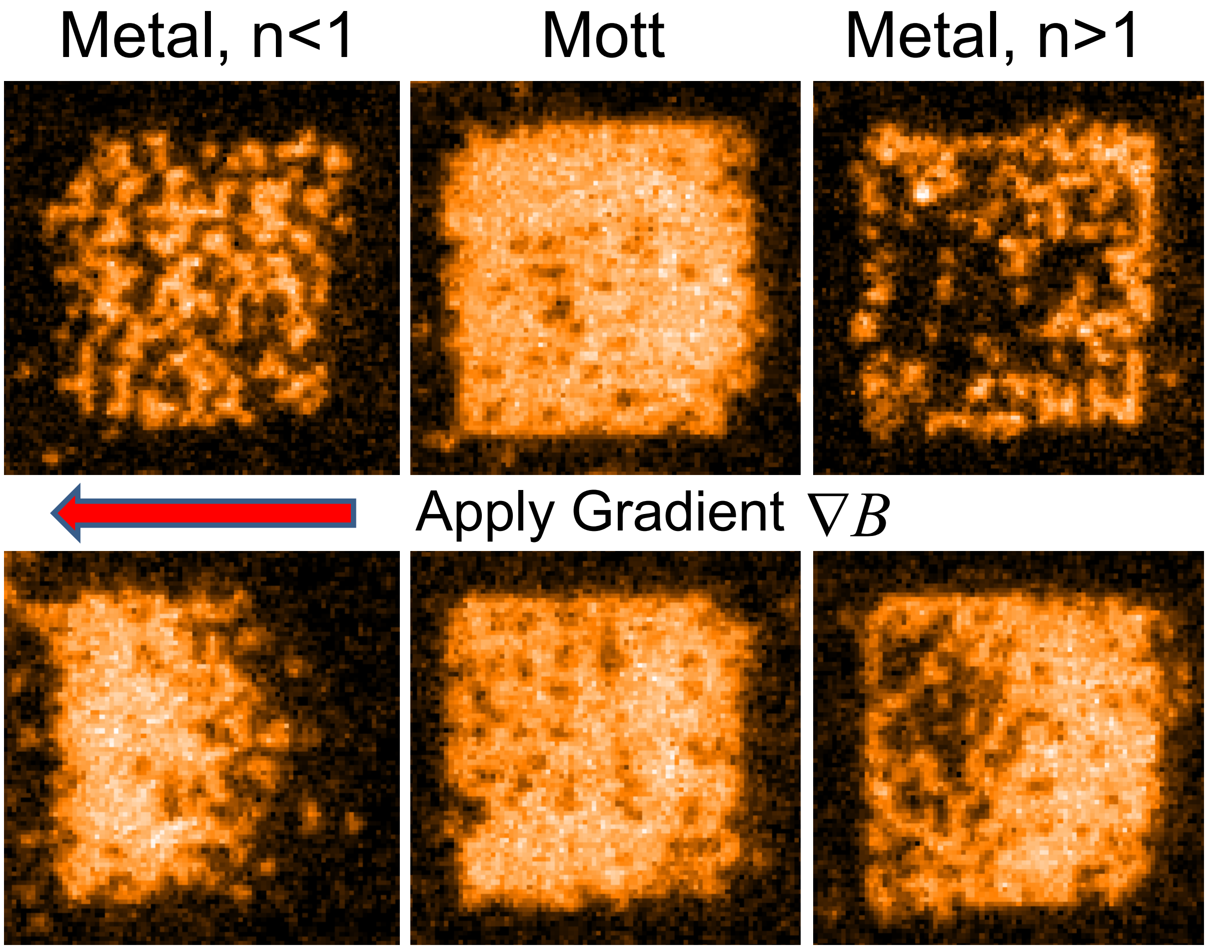

Courtesy M. Zwierlein

Spin Diffusivity in a Mott Insulator

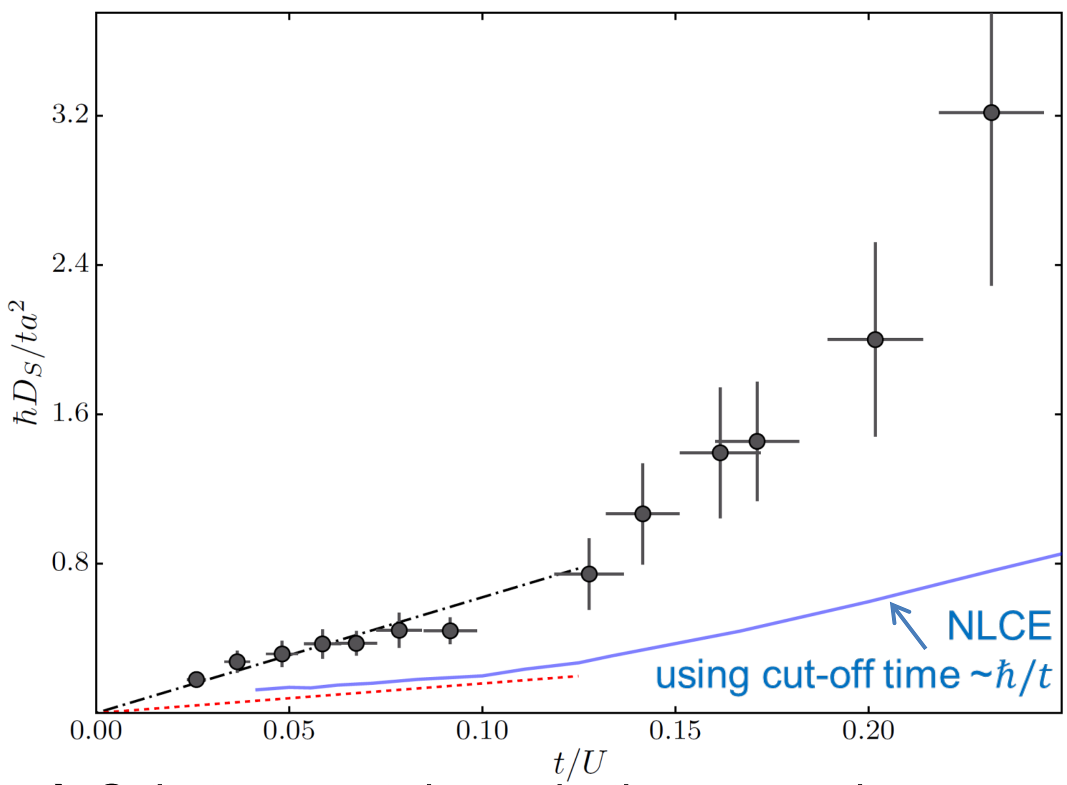

For further recent theory (in agreement with NLCE) see Ulaga et al., arXiv:2011.05750

→ Spin transport due to both superexchange and doublon-hole assisted tunneling

M. Nichols, L. Cheuk, M. Okan, T. Hartke, E. Mendez, T. Senthil, E. Khatami, H. Zhang, MWZ, Science 363, 383 (2019)


QUESTIONS

Quantum gas microscopy (Lecture III) Microscopy of doped systems, future directions

Waseem Bakr

PRINCETON UNIVERSITY

Boulder Summer School 2021

Heat Transport in a Fermi-Hubbard System

One more transport topic that I couldn't cover fully last time…

E. Guardado-Sanchez, A. Morningstar, B. M. Spar, P. T. Brown, D. A. Huse, and W. S. Bakr
Phys. Rev. X **10**, 011042 (2020)

- Displaced beam provides near uniform tilt potential at lattice axis.
- Hard walls constrain motion in direction orthogonal to gradient.

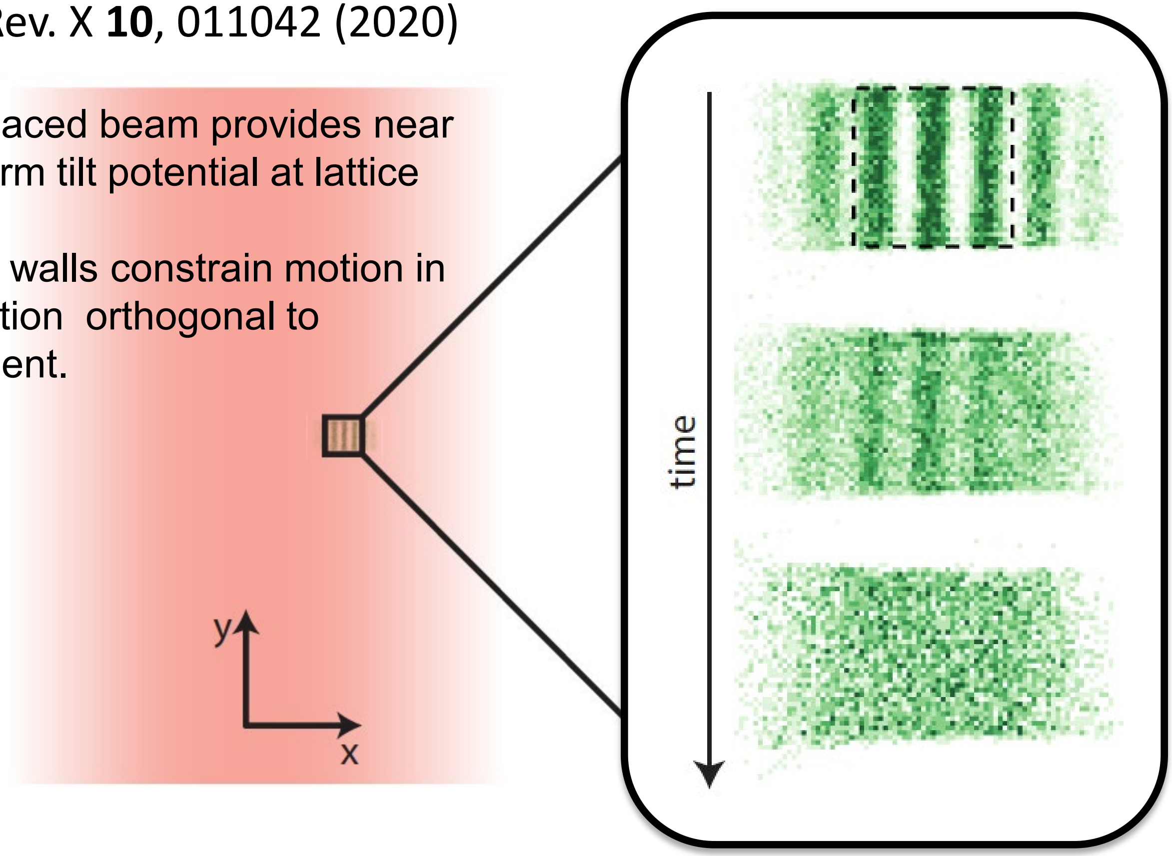

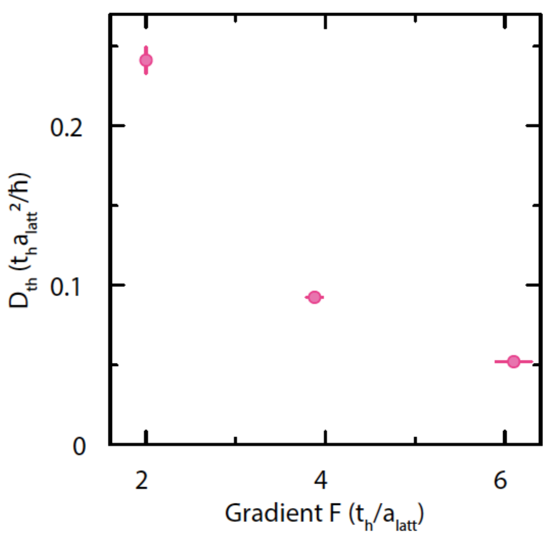

Thermalization in a 2D Hubbard system

Hopping orthogonal to the tilt enables thermalization

F/t = 0 ; U/t = 4

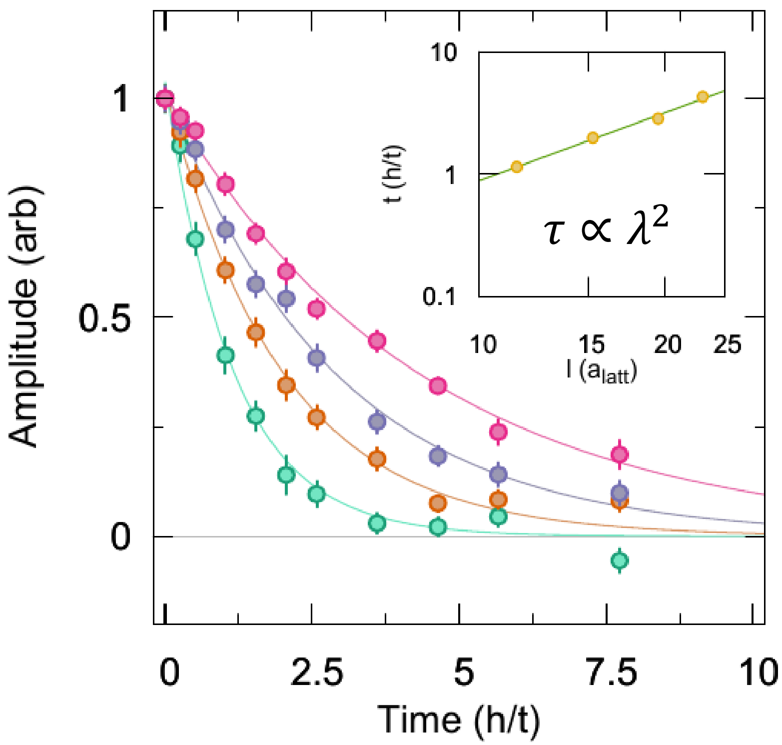

F/t = 2 ; U/t = 4

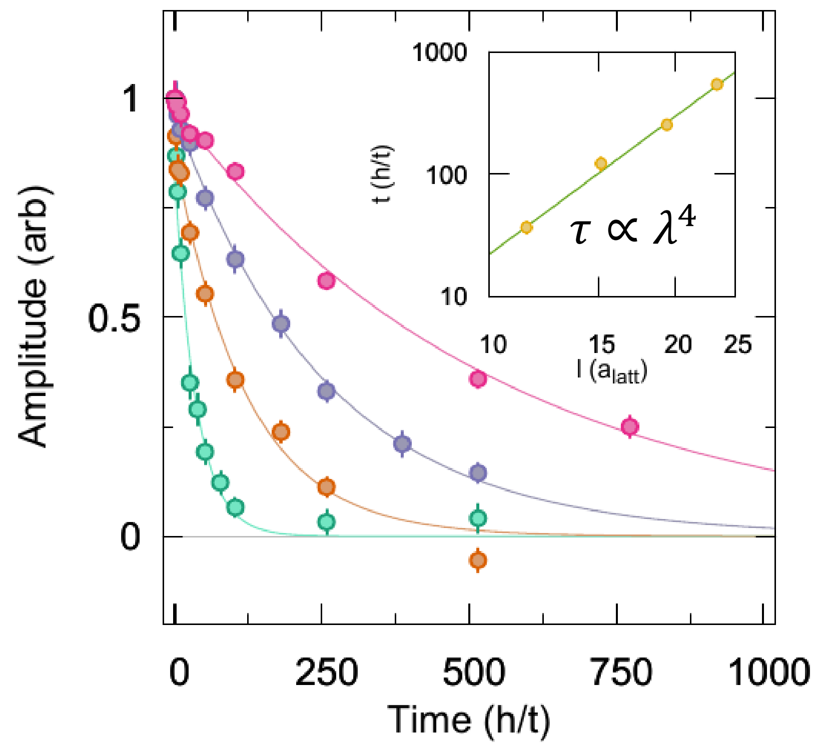

Modulation wavelengths in a_{latt}: 12 (green), 16 (orange), 20 (purple), and 24 (pink)

Crossover from diffusive to sub-diffusive transport

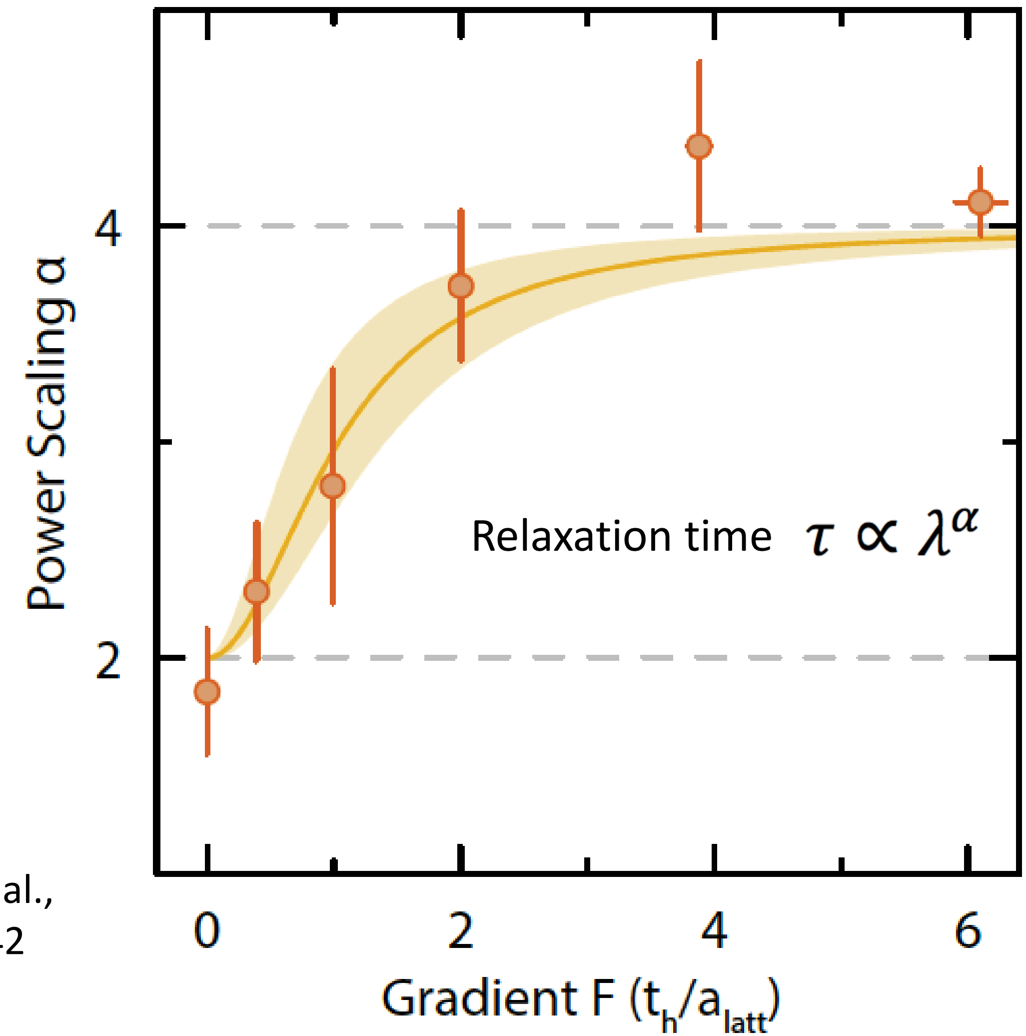

Guardado-Sanchez et al., Phys. Rev. X **10**, 011042 (2020)

Heating up to near infinite temperature

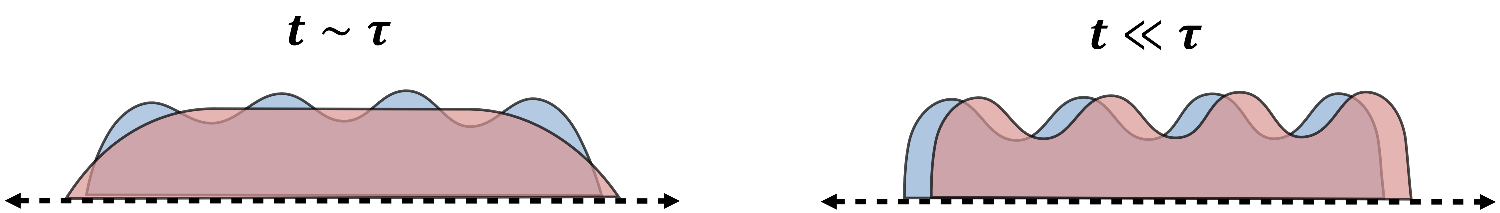

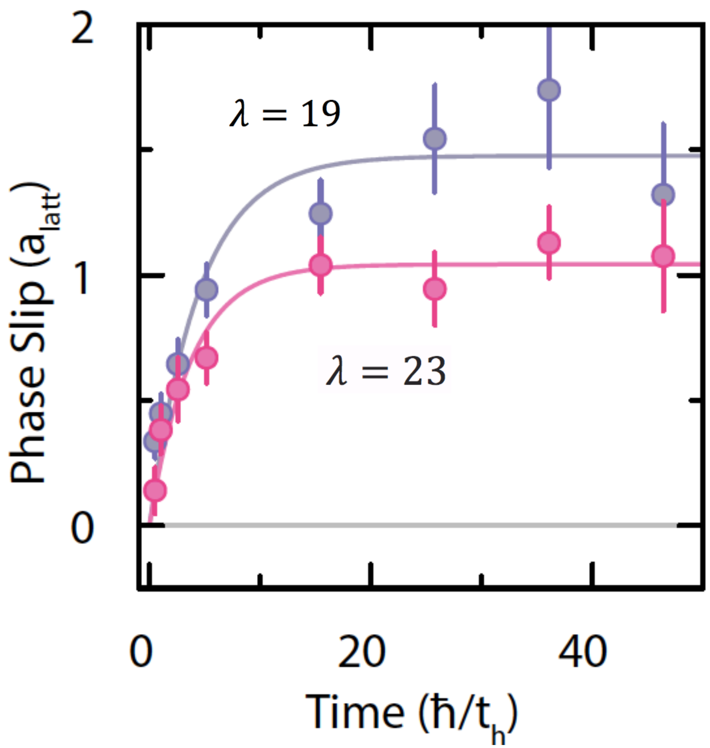

F/t = 1 ; U/t = 4

- System can exchange tilt energy with internal energy to maximize entropy. Internal energy is bounded in single-band lattice system.
- Pattern quickly slips by about 1 lattice site, heating up to infinite temperature in the process.

$$\delta x_c^{\max} \sim \frac{t+U}{F}$$

Reaching local equilibrium: this is a heat diffusion problem!

$$\beta(x,t) \propto \nabla n(x,t)$$

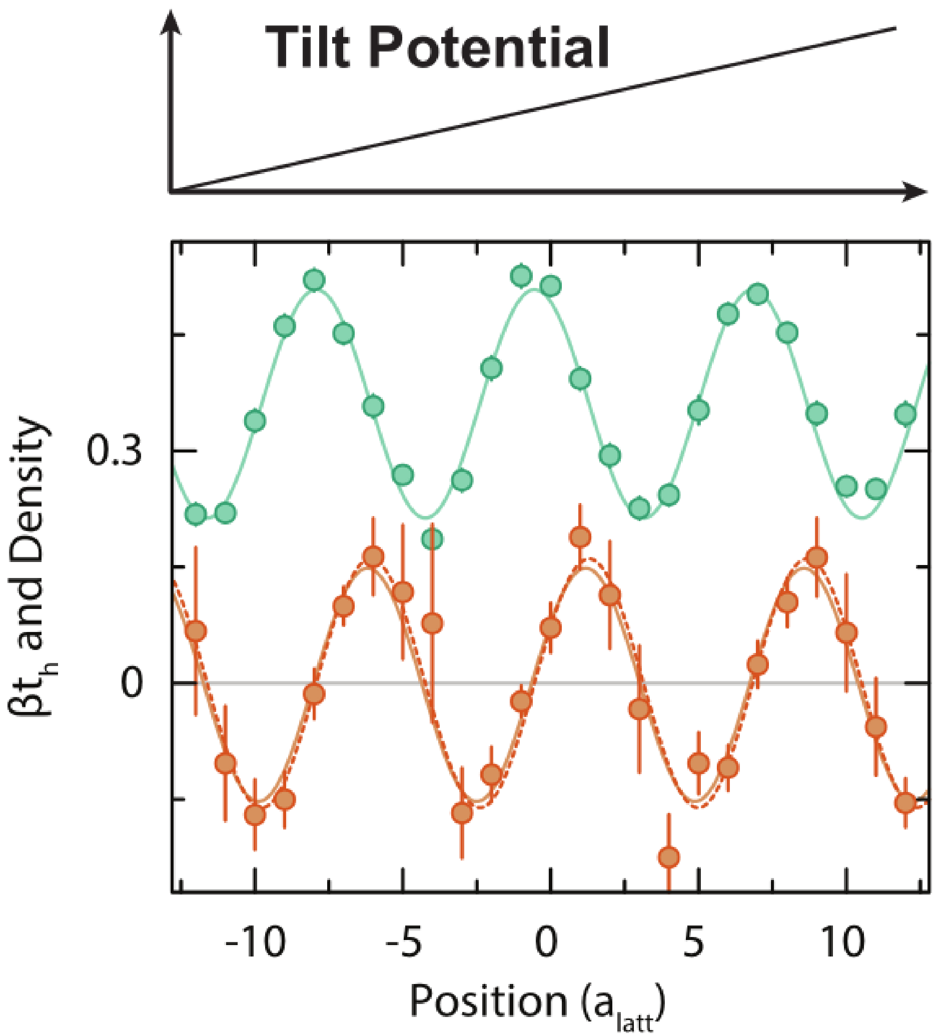

Single component density

Inverse temperature βt

- Local equilibration leads to a modulated inverse temperature shifted by 90 degrees relative to density pattern.
- Verified by measuring singles density and using the atomic limit.

Mandt et. al. PRL 106, 250602 (2011)

Reaching global equilibrium: a hydrodynamic model

- Inverse temperature modulation leads to a diffusive **heat current**

$$j_e = -D_{th} \nabla e$$

"e" is the local internal (non-tilt) energy, can be related to β using a a **high-temperature expansion**.

$$e \sim -\beta \Rightarrow j_e \sim D_{th} \nabla \beta$$

- **Energy conservation**: $\dot{e} = -\nabla \cdot j_e - F j_n$

Strong tilt regime: internal energy change is negligible:

$$j_n \sim -\nabla \cdot j_e \sim -D_{th} \nabla^2 \beta \sim D_{th} \nabla^3 n$$

- **Number conservation**: $\dot{n} = -\nabla \cdot j_n \Rightarrow \boldsymbol{\dot{n} \sim -D_{th} \nabla^4 n}$


QUESTIONS

Outline of today's lecture

- Doped 1D systems (MPQ)
  - Equilibrium: Hidden AF correlations, incommensurate magnetism.
  - Dynamics: Spin-charge fractionalization.
- Single dopant in 2D
  - Equilibrium: Imaging magnetic polarons (MPQ)
  - Dynamics: Formation & spreading of magnetic polarons (Harvard)
- Doped 2D AFMs:
  - String patterns (Harvard)
  - Higher correlations: evolution from polaronic metal to Fermi liquid (MPQ).
- Future directions: extended Hubbard models, novel geometries, tweezers… (mostly Princeton's take)

Excellent review: *Exploration of doped quantum magnets with ultracold atoms,* A. Bohrdt *et al.*, arxiv: 2107.08043 (2021)

Hidden antiferromagnetic correlations in doped Hubbard chains

Around a hole, spins prefer to be anti-aligned!

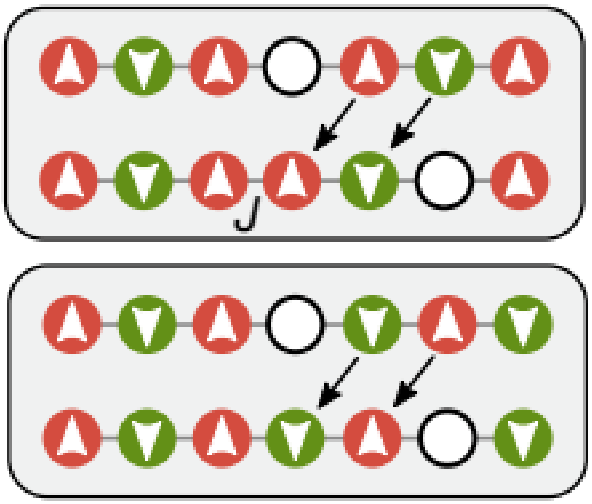

Two ways to bring the correlations back…

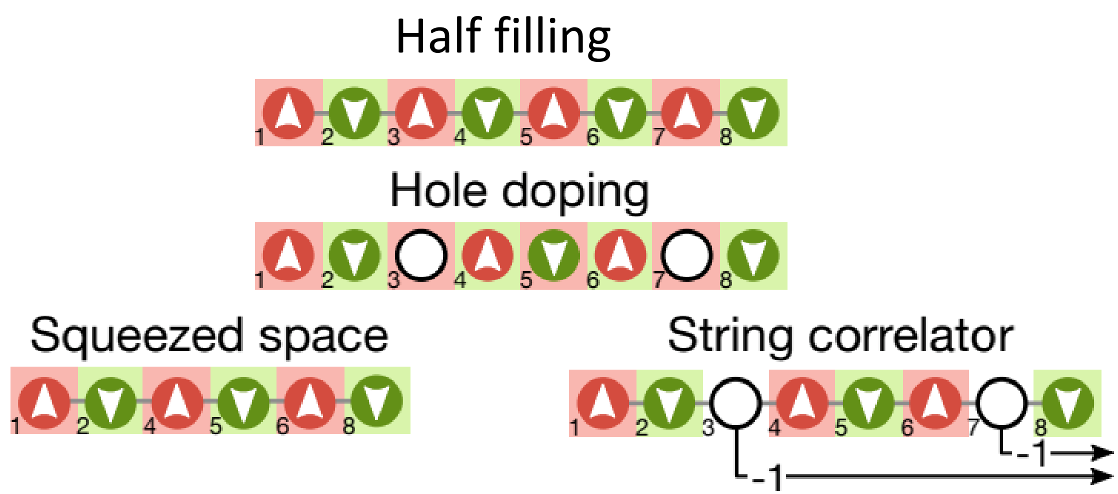

$$C^{\mathrm{str}}(d) = 4 \left\langle \hat{S}^z_i \left(\prod_{j=1}^{d-1} (-1)^{(1-\hat{n}_{i+j})} \right) \hat{S}^z_{i+d} \right\rangle_{\bullet_i \bullet_{i+d}}$$

Hilker … Gross, Science 357, 484 (2017)

Hidden antiferromagnetic correlations in doped Hubbard chains

Around a hole, spins prefer to be anti-aligned!

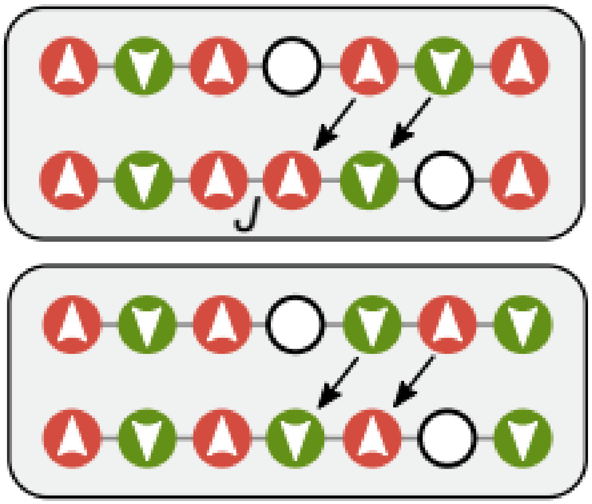

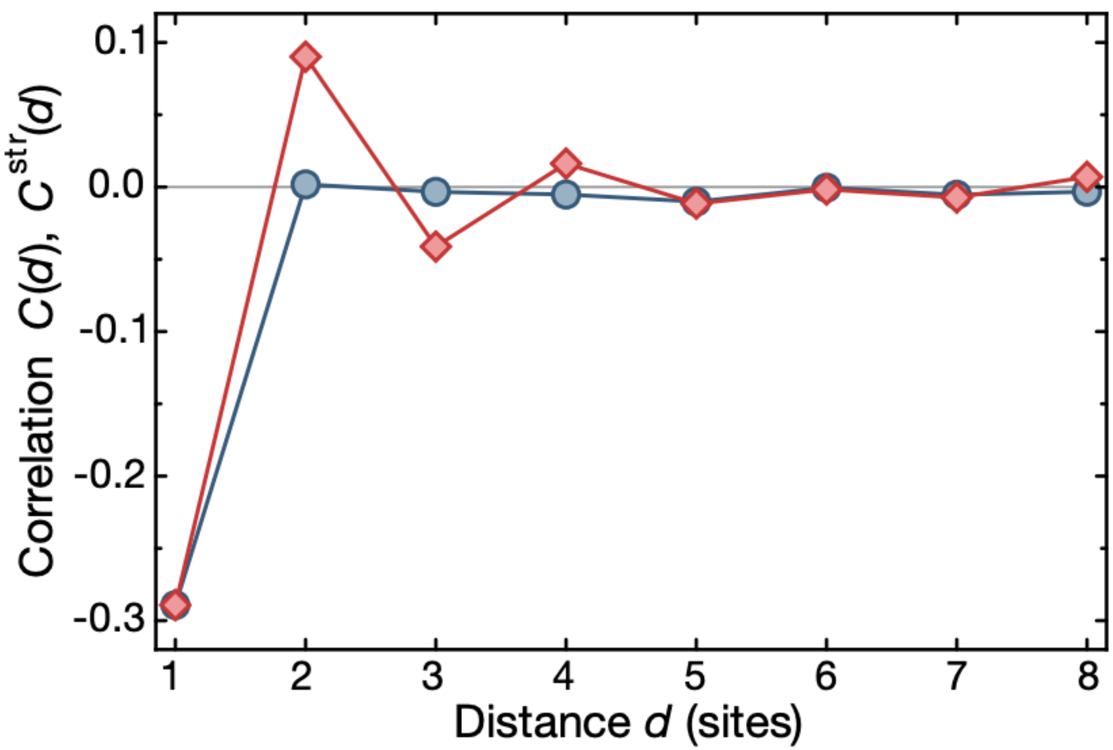

Hilker … Gross, Science 357, 484 (2017)

Incommensurate AFMs

Luttinger liquid theory predictions for doping/spin-imbalance in 1D:

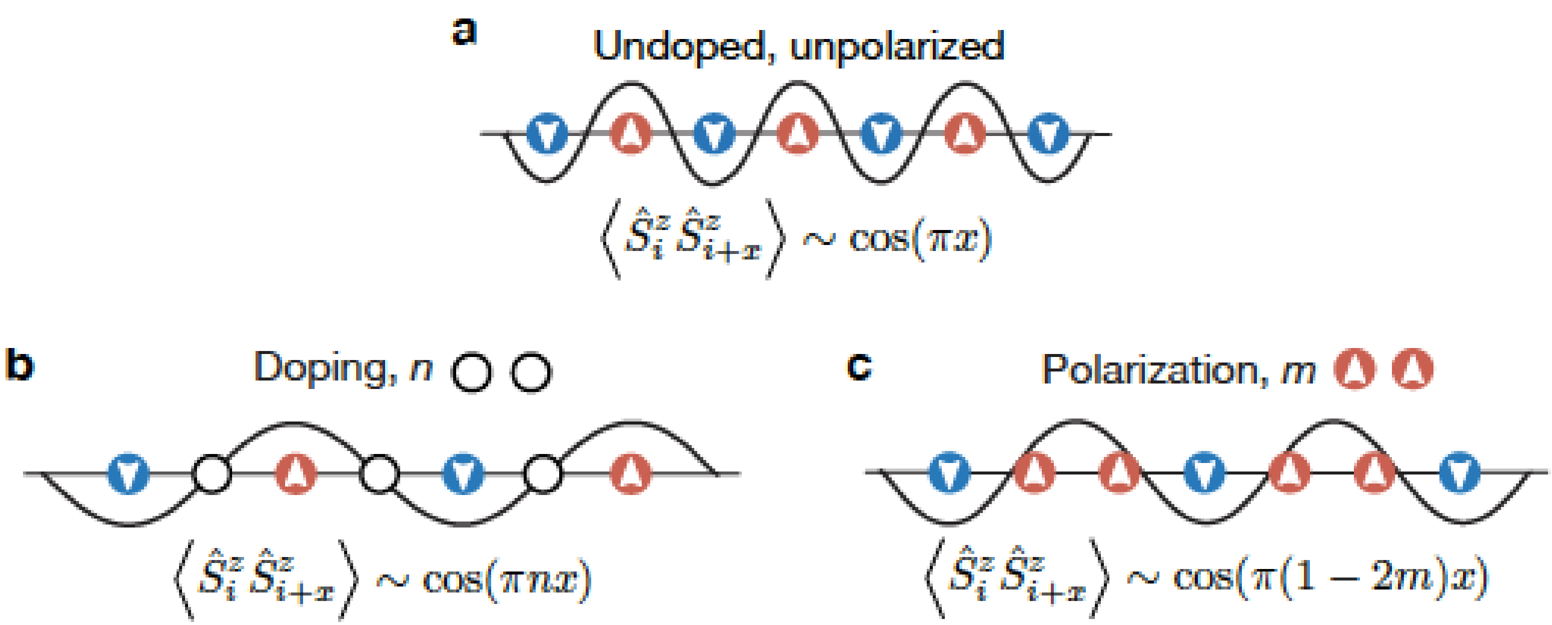

Salomon … Gross, Nature 565, 56 (2019)

Incommensurate AFMs

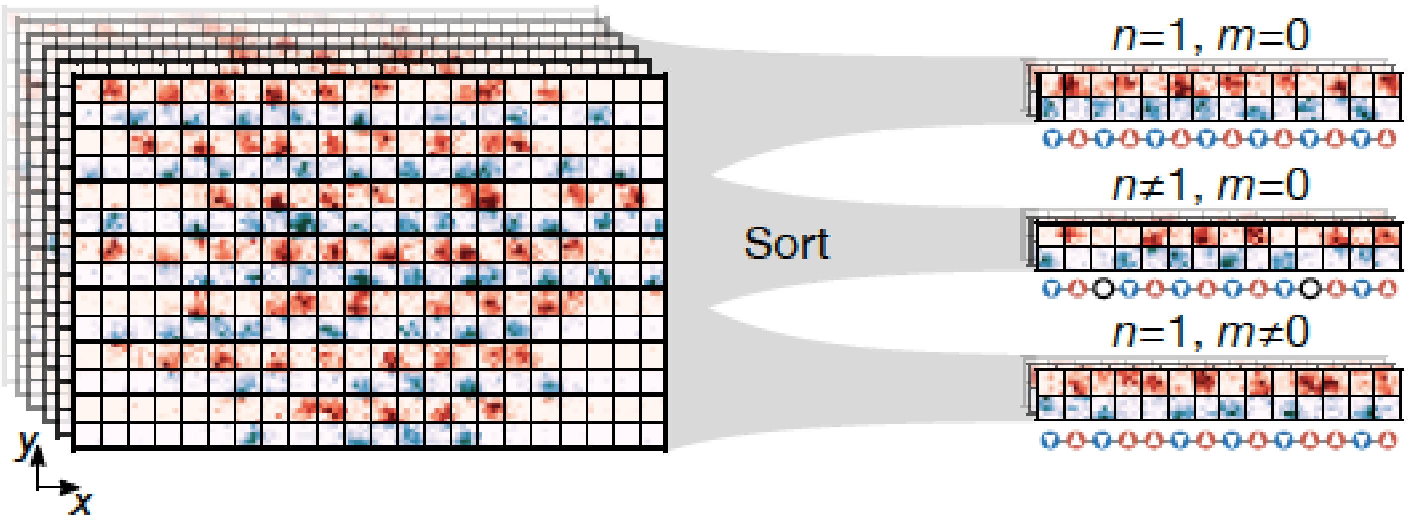

Salomon … Gross, Nature 565, 56 (2019)

Incommensurate AFMs

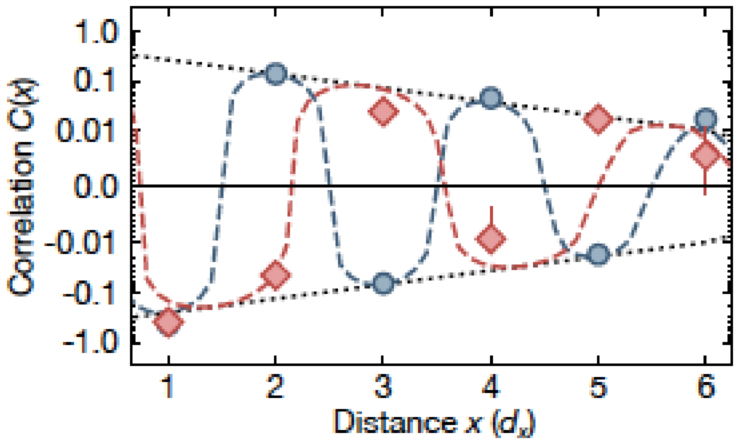

Example of shift in AFM periodicity going from n=1 to n=0.7.

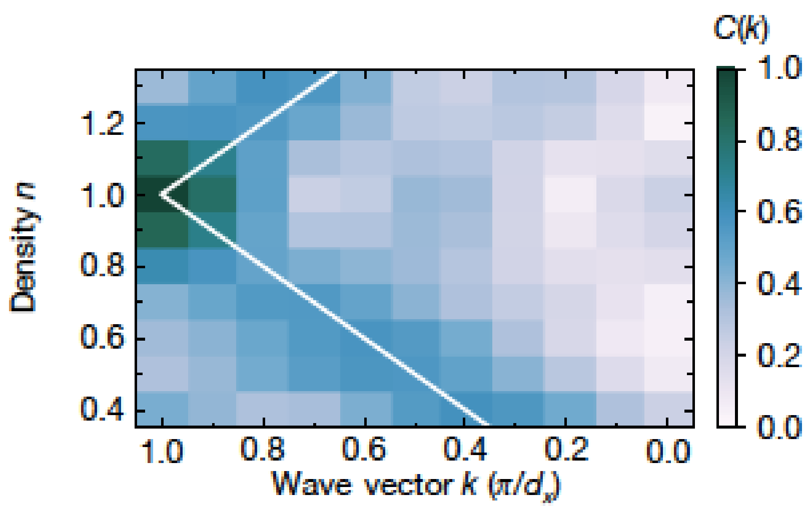

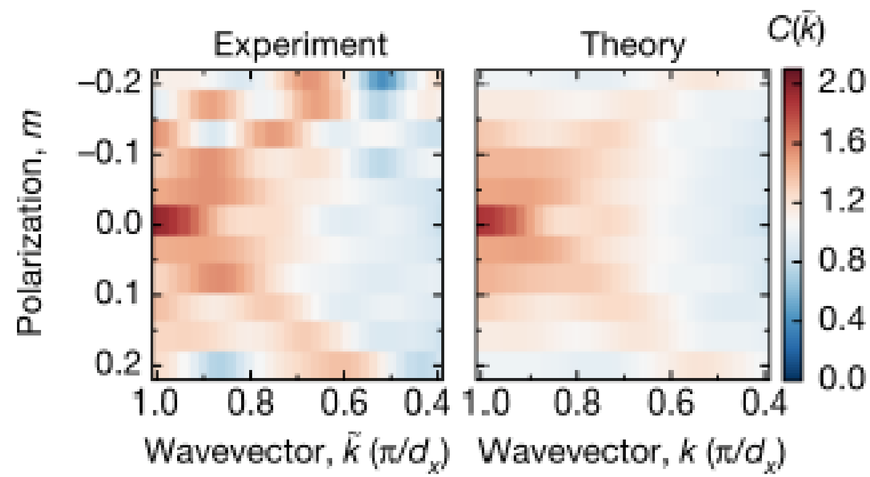

Salomon … Gross, Nature 565, 56 (2019)

Spin-charge separation

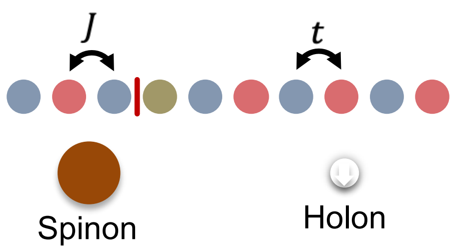

Quasiparticles in 1D Fermi-Hubbard model are holons and spinons, move with different velocities.

Holons/spinons carry fractional quantum numbers:

holon: spin 0, charge 1.

spinon: spin ½, charge 0.

Injected hole decays into holon and spinon (dynamical fractionalization), magnon would decay into two spinons.

Spinon cannot be created by local spin flips but magnon can.

Similar quasiparticles in quantum spin liquids.

Time-resolved observation of spin-charge deconfinement in fermionic Hubbard chains

Jayadev Vijayan[1,2]*†, Pimonpan Sompet[1,2]*, Guillaume Salomon[1,2], Joannis Koepsell[1,2], Sarah Hirthe[1,2], Annabelle Bohrdt[2,3], Fabian Grusdt[2,3,4], Immanuel Bloch[1,2,5], Christian Gross[1,2]

Science **367**, 186–189 (2020)

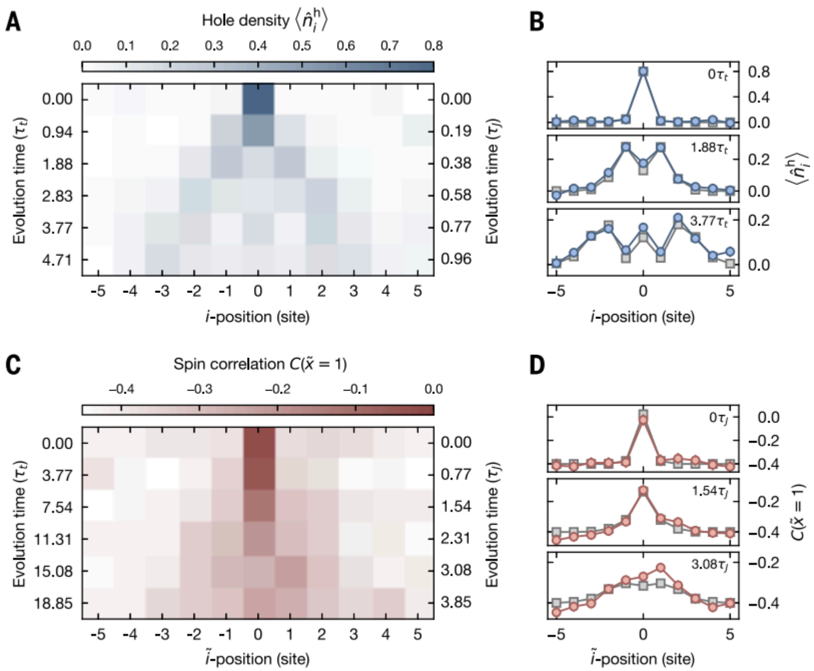

Fig. 2. Time evolution of spin and charge excitations. (**A**) Hole density distribution $\langle \hat{n}_i^h \rangle$ as a function of time

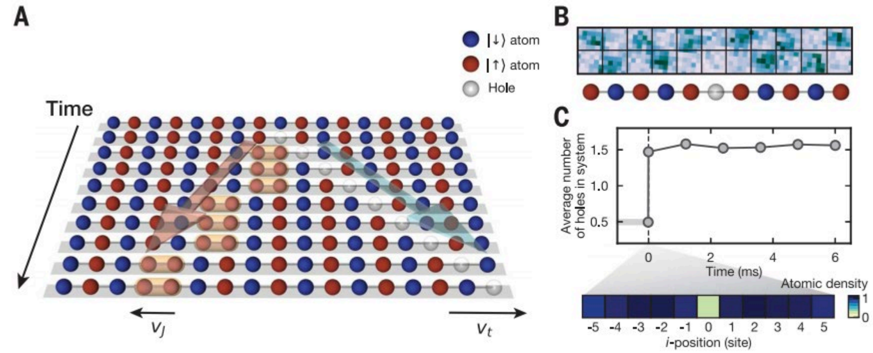

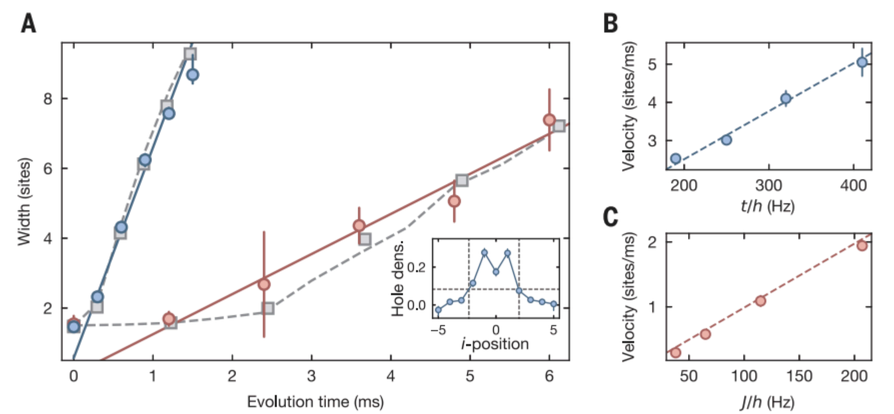

Fig. 3. Quasiparticle velocities of spinons and holons. (**A**) Time evolution of the widths of the hole density

Local spin fluctuations around spinon

$$\hat{\Sigma}_{\tilde{j}}^2 = \left(\sum_{\tilde{i}} \hat{S}_{\tilde{i}}^z f_{\tilde{j}}^\sigma(\tilde{i}) \right)^2 \qquad f_{\tilde{j}}^\sigma(\tilde{i}) = \exp\left(-\frac{(\tilde{i}-\tilde{j})^2}{2\sigma^2} \right)$$

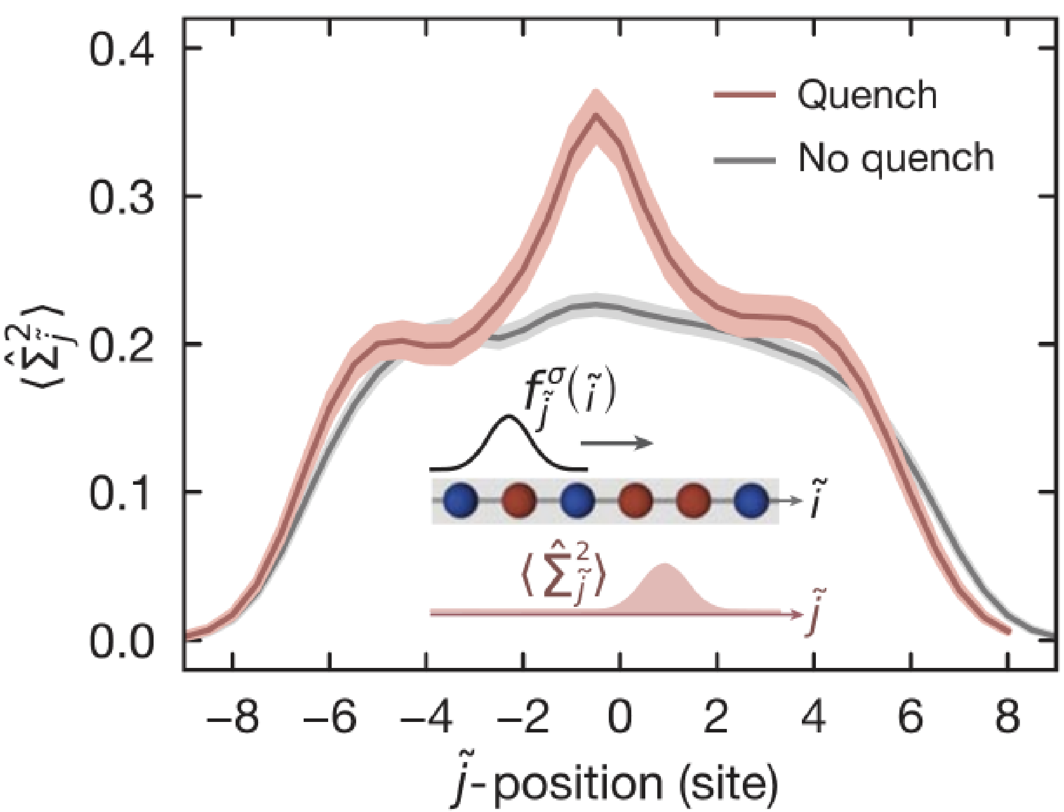

Vijayan … Gross, Science 367, 186 (2020)


QUESTIONS

Single dopant in 2D: Magnetic Polarons

A single doublon in 2D – simple intuition

Delocalizing a doublon in an AFM background

$$|\Psi\rangle =$$

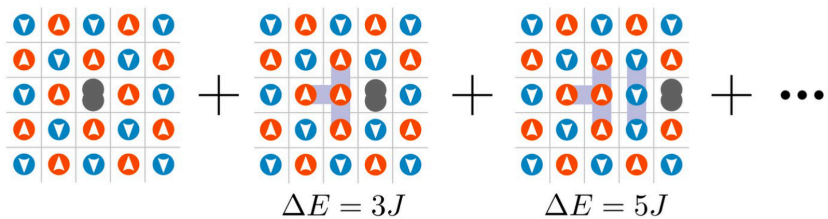

Delocalization costs magnetic energy!

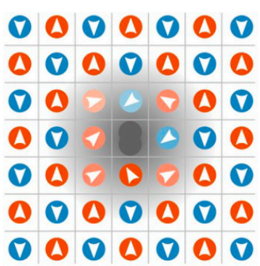

- **Localized distortion** of magnetism around doublon

→ The "inner structure" of a polaron in real space

Schmitt-Rink et al., PRL 1988 | Shraiman + Siggia, PRL 1988 | Sachdev, PRB 1989 | Kane et al. PRB 1989 | Dagotto et al., PRB 1989 | Martinez + Horsch, PRB 1991 | Barnes et al., PRB 1989

Slides courtesy C. Gross

Magnetic Polarons

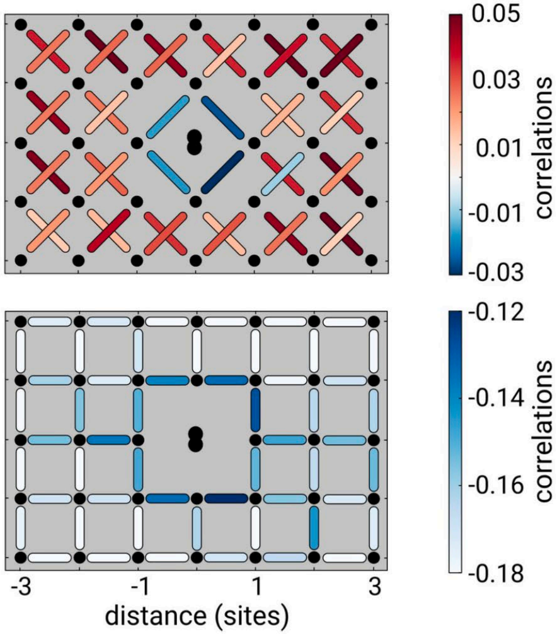

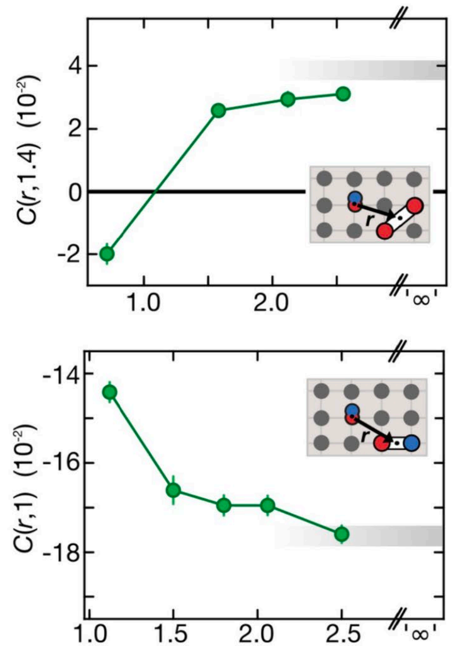

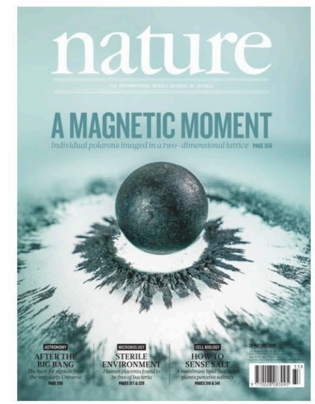

Koepsell et al.,
Nature **572**, 358 (2019)

Polaron size ≈1-2 sites

Slides courtesy C. Gross

M. Greiner and group

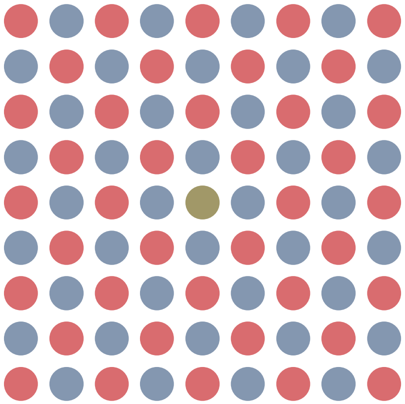

Dopant dynamics scheme

1. Prepare system in equilibrium
2. Suddenly shut off hole confinement
3. Wait for variable time
4. Image

M. Greiner and group

Long-time delocalization

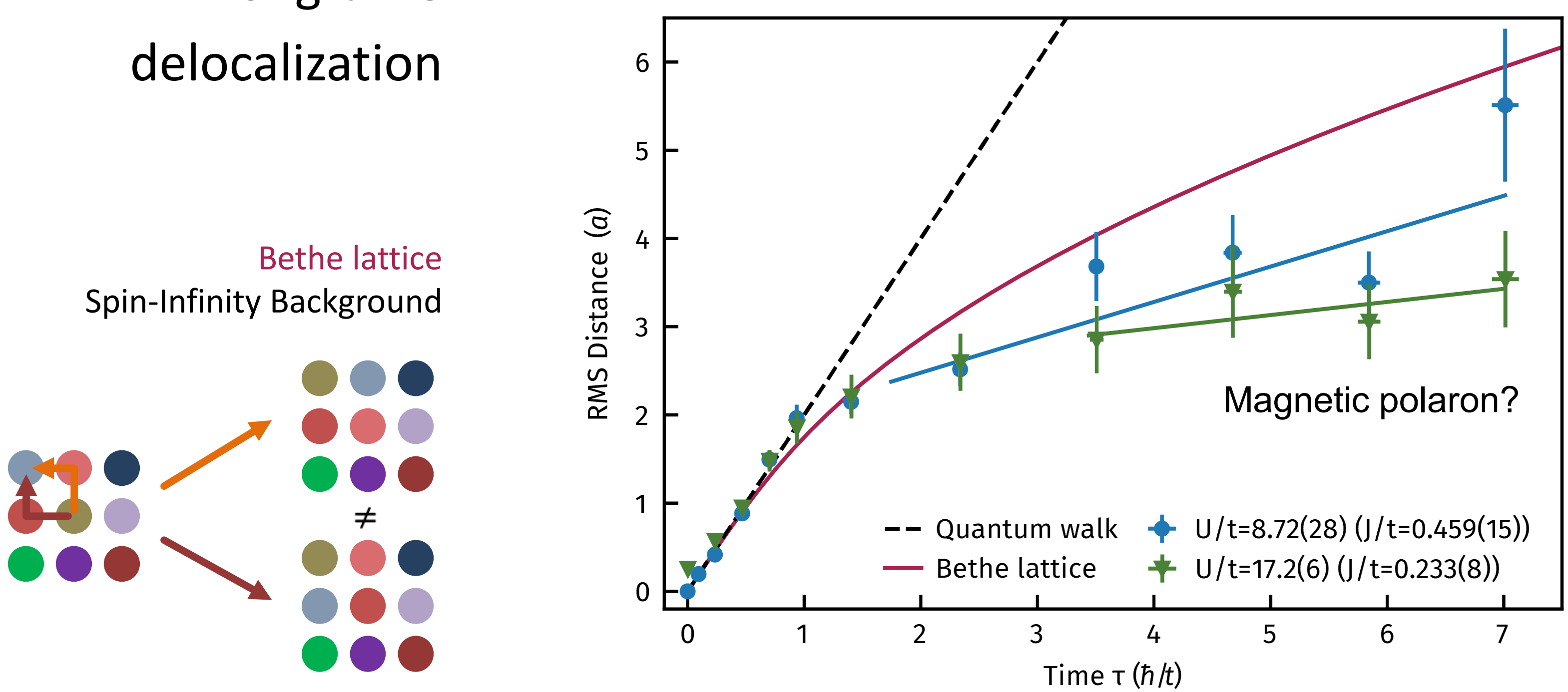

G. Ji et al., Phys. Rev. X 11, 021022 (2021)

String patterns in the doped Hubbard model

Christie S. Chiu[1], Geoffrey Ji[1], Annabelle Bohrdt[2,1,3], Muqing Xu[1], Michael Knap[2,3], Eugene Demler[1], Fabian Grusdt[1,3], Markus Greiner[1*], Daniel Greif[1]

Science **365**, 251–256 (2019)

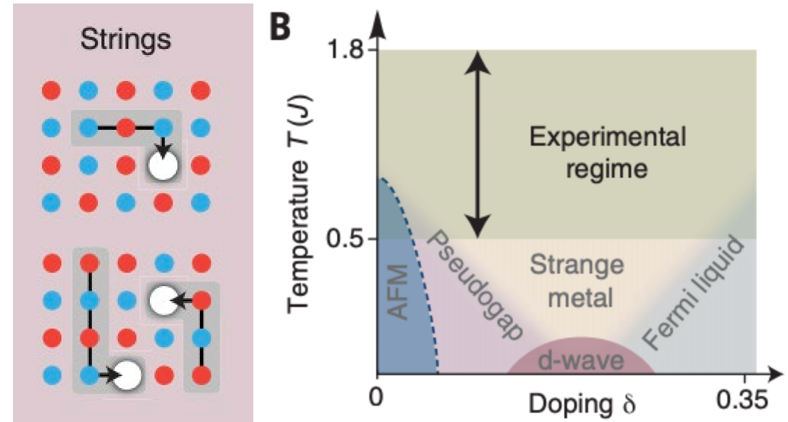

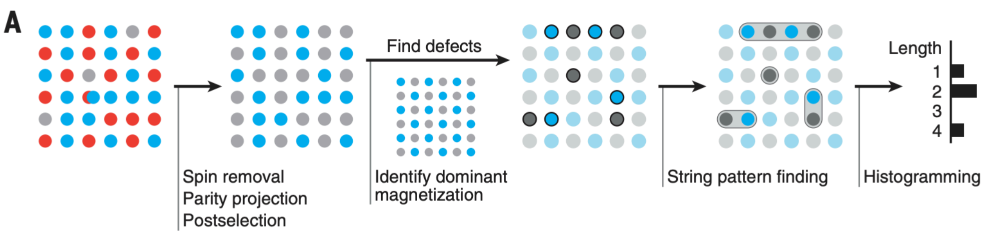

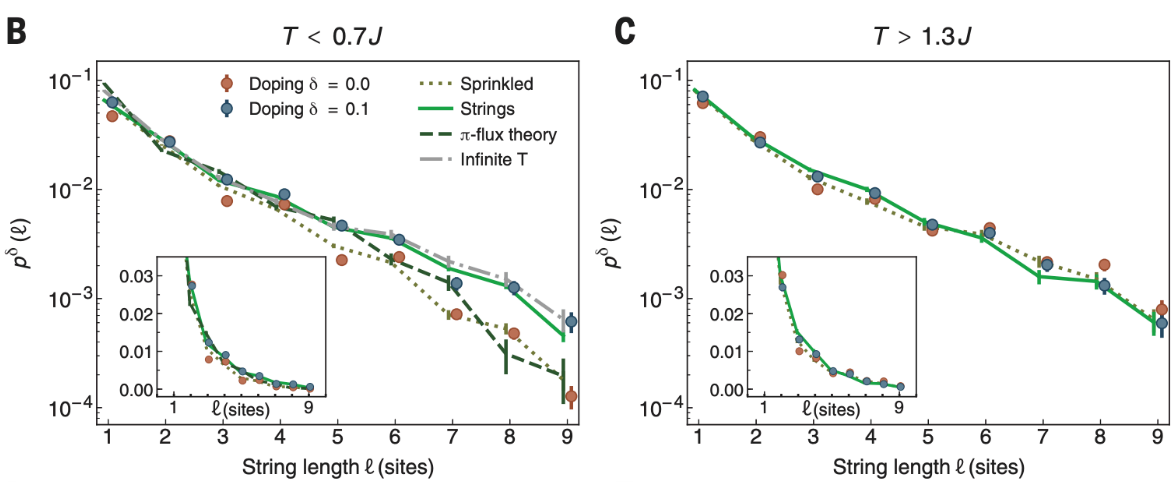

Microscopic evolution of doped Mott insulators from polaronic metal to Fermi liquid

Joannis Koepsell,[1,2,*] Dominik Bourgund,[1,2] Pimonpan Sompet,[1,2] Sarah Hirthe,[1,2] Annabelle Bohrdt,[2,3] Yao Wang,[4,5] Fabian Grusdt,[2,6] Eugene Demler,[4] Guillaume Salomon,[1,2,7,8] Christian Gross,[1,2,9] and Immanuel Bloch[1,2,6]

arXiv:2009.04440

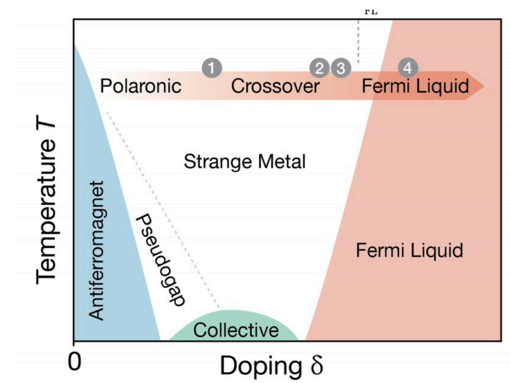

hole - spin/spin correlator

Always negative

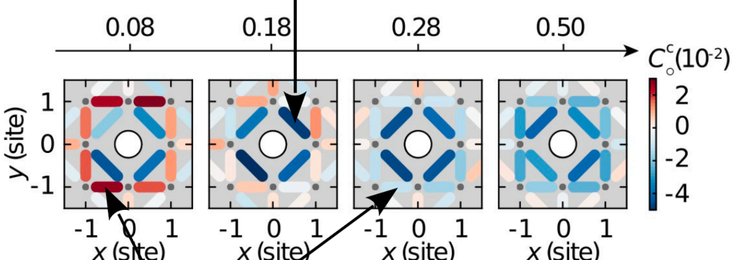

switches sign as a function of doping
(positivity as a signature for the polaron)

Polarons

Fermi liquid

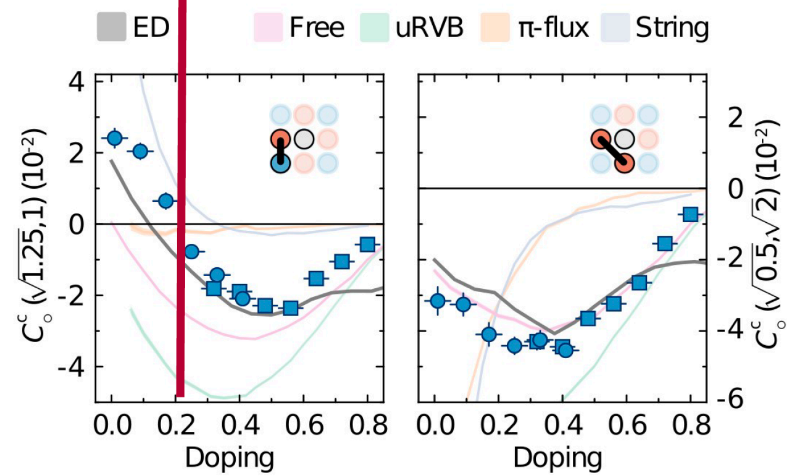


QUESTIONS

Novel Systems, novel techniques

Bakr group:

Rydberg Dressing

t-V model

$$\hat{H} = -t \sum_{\langle i,j \rangle_x} \left(\hat{c}_i{}^{\dagger} \hat{c}_j + h.c. \right) + \sum_{i,j} V_{ij} \hat{n}_i \hat{n}_j$$

Quench Dynamics of a Fermi Gas with Strong Nonlocal Interactions
Phys. Rev. X 11, 021036 (2021)

Elmer Guardado-Sanchez, B. M. Spar, P. Schauss, R. Belyanski, J. T. Young, P. Bienias, A. V. Gorshkov, T. Iadecola, and W. S. Bakr

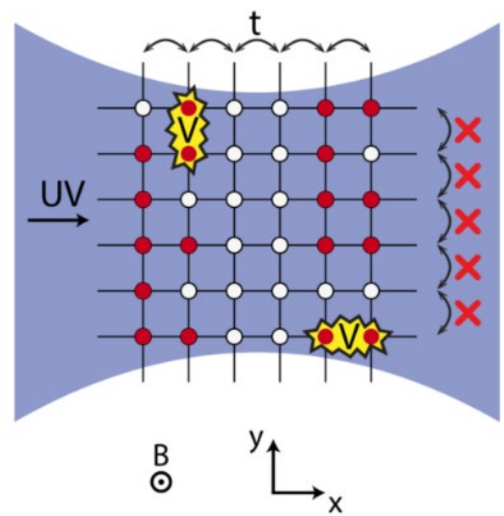

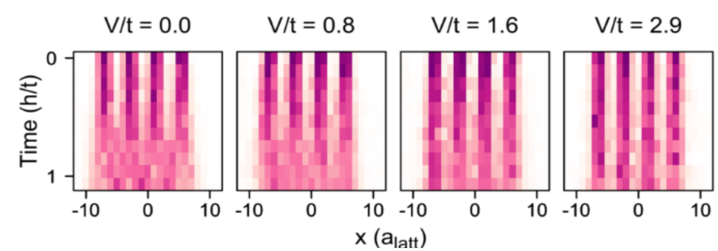

Competing magnetic orders in a bilayer Hubbard model with ultracold atoms

Marcell Gall[1,2], Nicola Wurz[1,2], Jens Samland[1], Chun Fai Chan[1] & Michael Köhl[1]✉ *Nature* **589**, 40–43(2021)

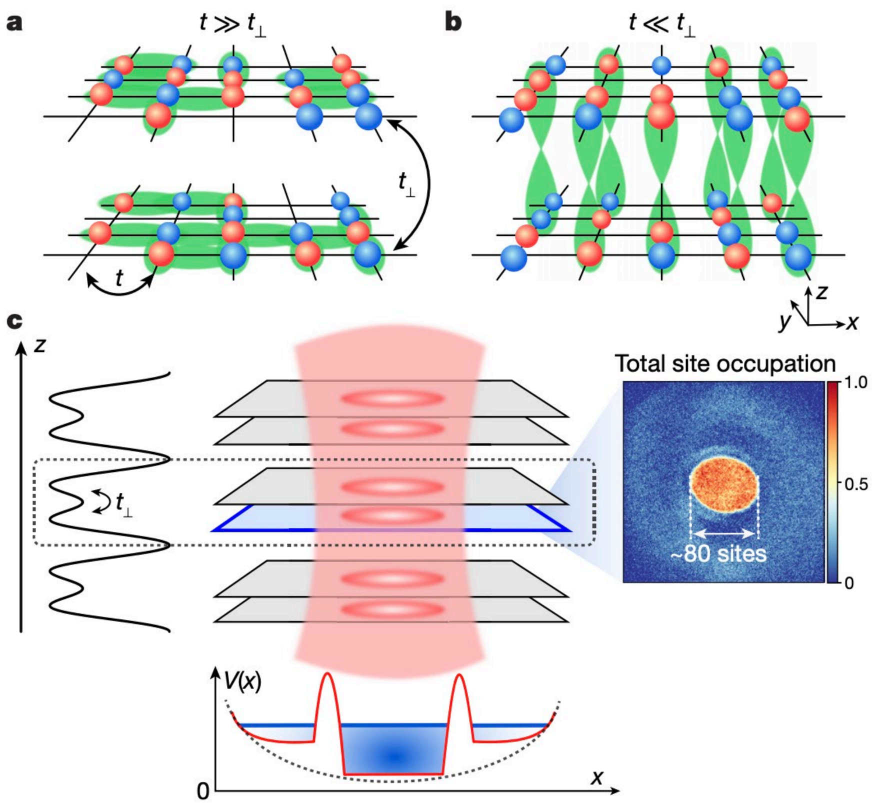

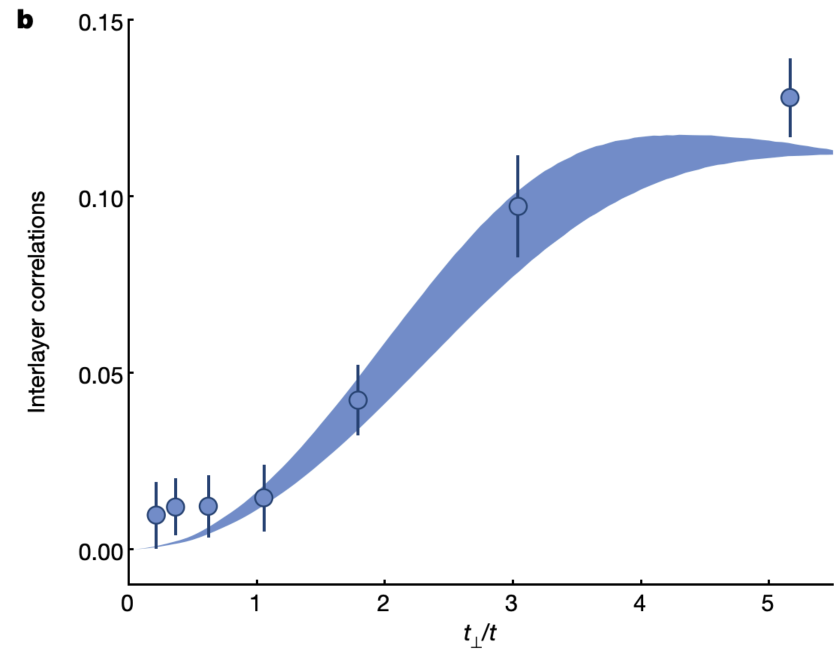

Site-resolved imaging of ultracold fermions in a triangular-lattice quantum gas microscope

Jin Yang,[1,*] Liyu Liu,[1,*] Jirayu Mongkolkiattichai,[1,*] and Peter Schauss[1]

PRX Quantum 2, 020344 (2021)

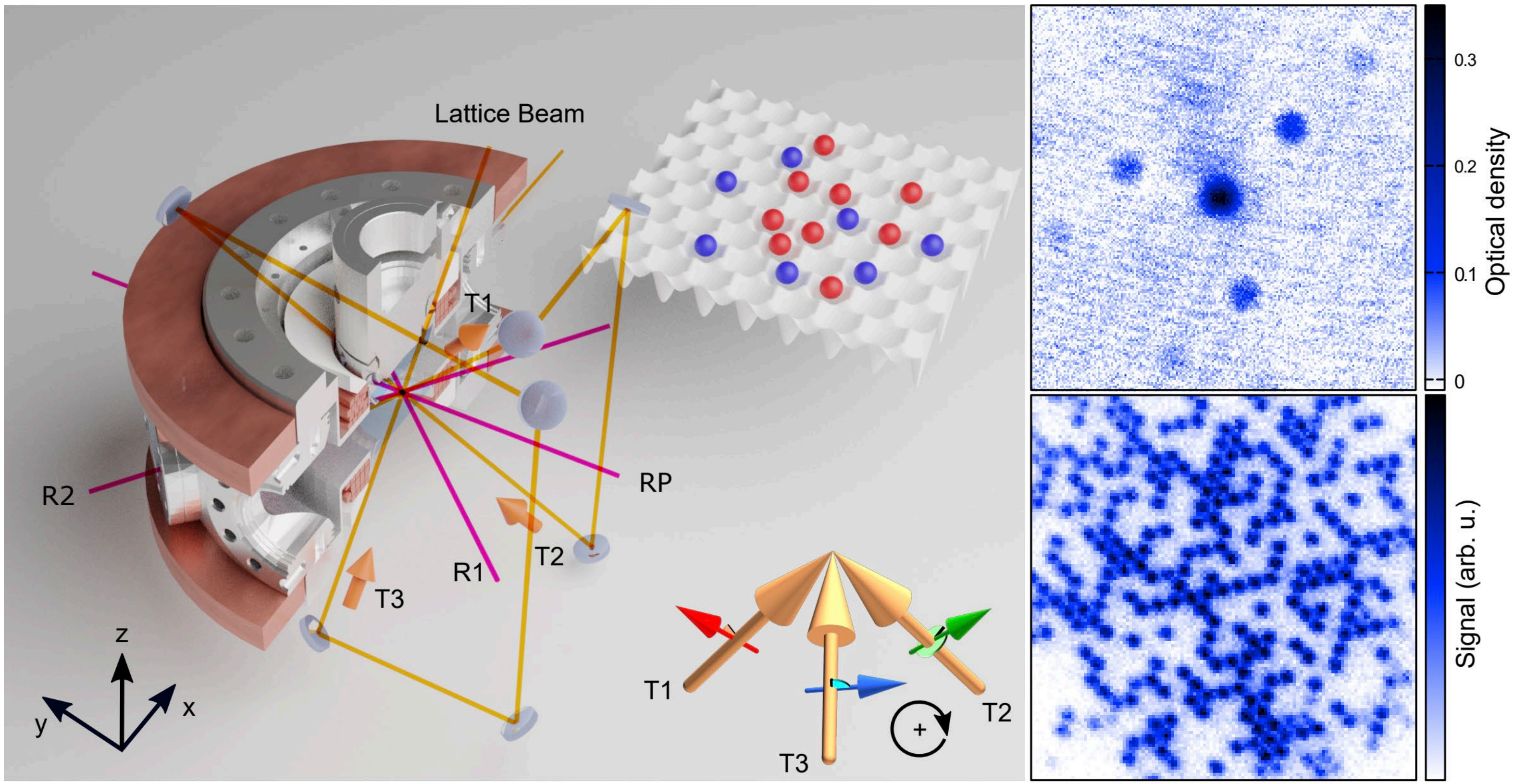

Fermi-Hubbard tweezer arrays

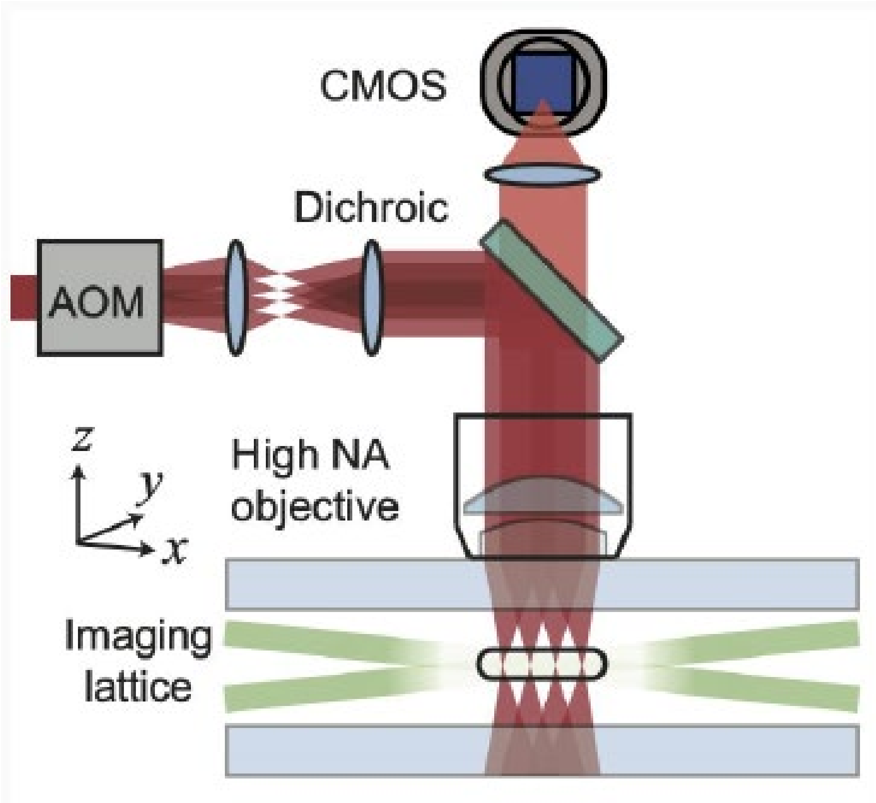

Advantages:
Arbitrary geometry, low entropy.

Experimental setup:

- Load degenerate atoms into tweezers from a dipole trap.
- Combination of magnetic gradient and lowering intensity to get ground state atoms.
- Load into quantum gas microscope for imaging.

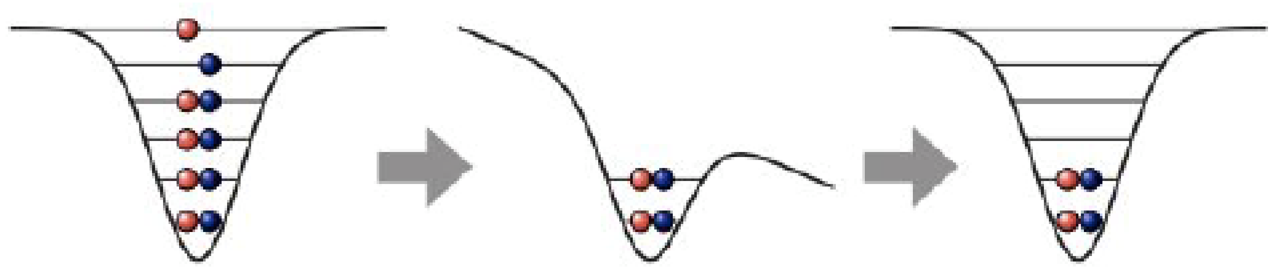

F. Serwane et al, Science 332, 336 (2011).

Fermi-Hubbard tweezer arrays

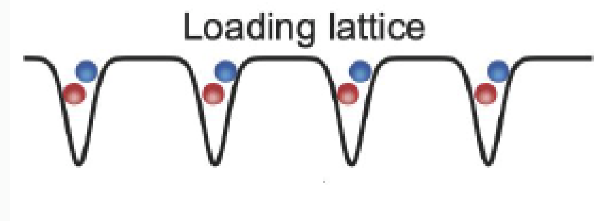

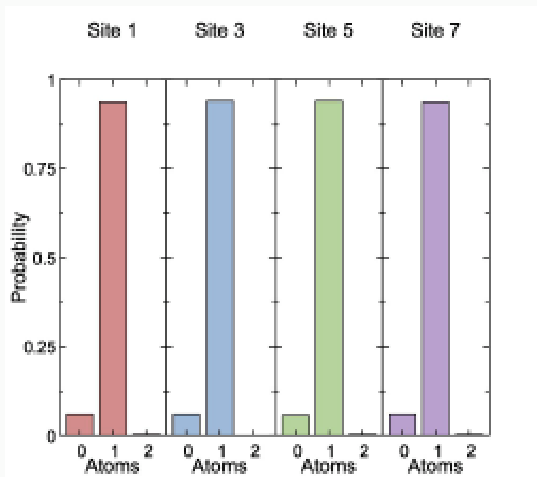

Load odd-numbered sites with 2 atoms per site in ground state.

- Probability of correct state: about 97% (entropy of 0.15 k_B/particle)
- Almost all imperfections 1 atom per site: can be post-selected with full spin/density detection to get zero entropy initial state.

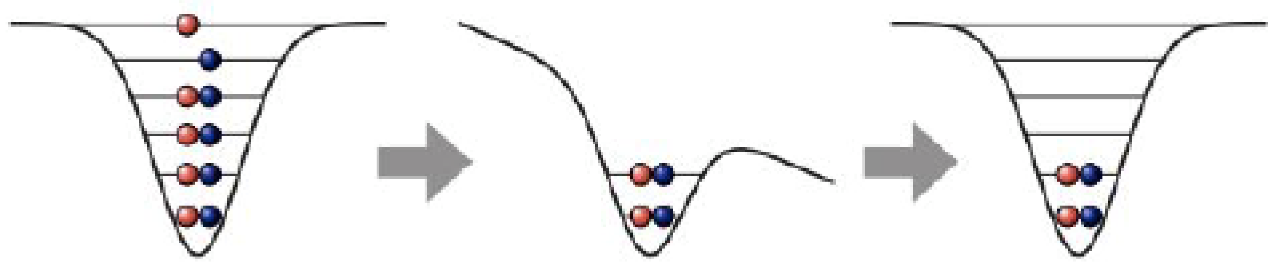

F. Serwane et al, Science 332, 336 (2011).

Fermi-Hubbard tweezer arrays

Main challenge in minimizing disorder in array to better than tunneling (0.5% of tweezer depth).
Use feedback loop on density at U/t = 1.

Adiabatically go to correlated states.

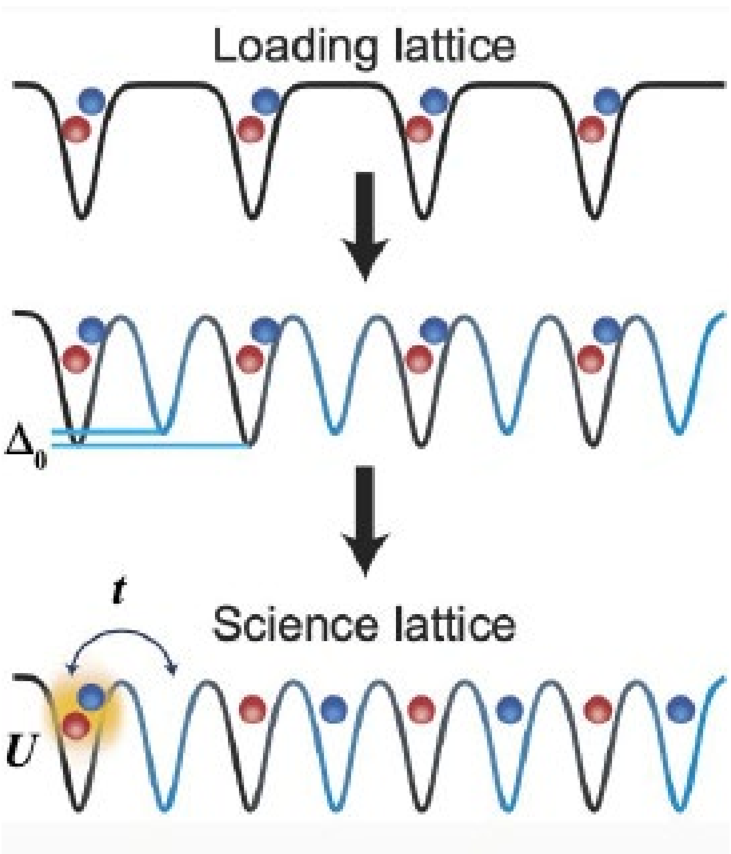

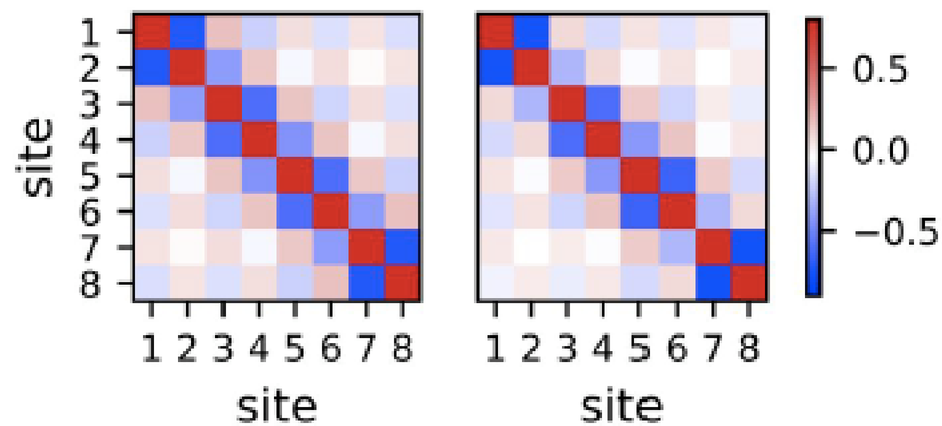

Theory Experiment

Fermi-Hubbard tweezer arrays (dynamics)

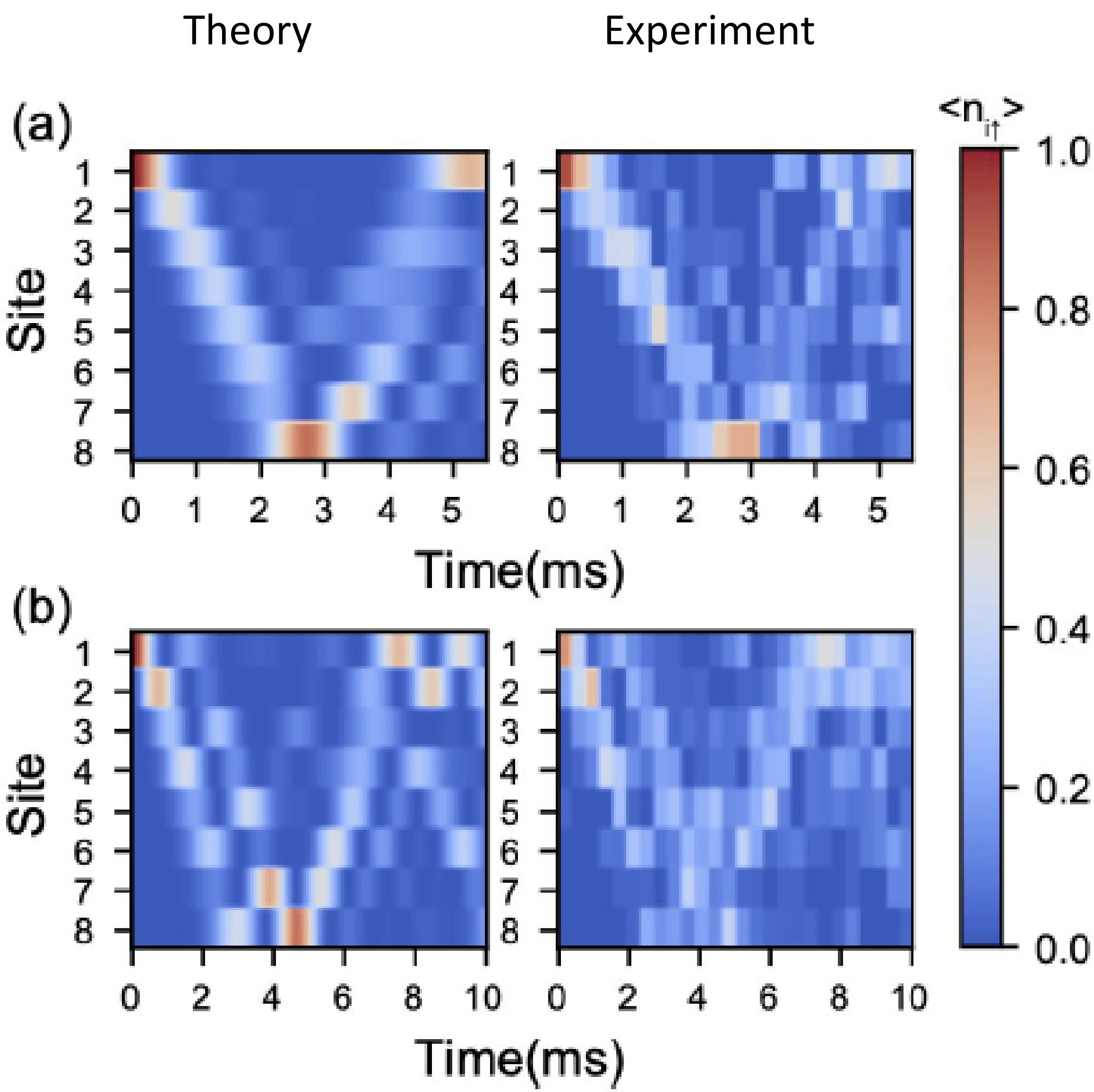

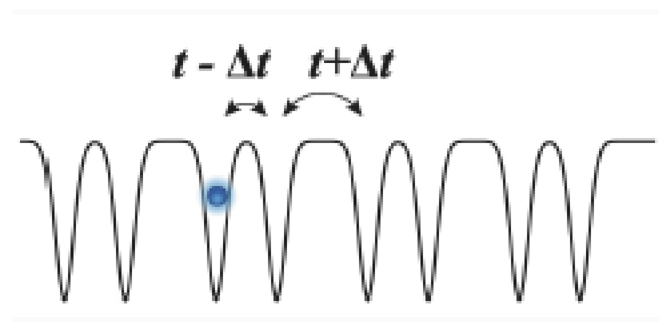

Cold-Atom Fermi-Hubbard Simulators

Exciting developments:

- Transport measurements challenging state-of-the-art theory
- Direct observation of Fermi-Hubbard building blocks, e.g.:
  spin and charge correlations, singlet formation, magnetic polarons, doublon-hole pairing, spin-charge separation in 1D, evidence for strings…
- Reaching lower temperatures
- Novel read-out schemes
- Novel geometries (bilayer, ladder, triangular)
- Novel interactions (long-range, anisotropic, from Rydberg or Molecules)
- Driven Systems

Towards microscopic understanding of Fermi-Hubbard physics

QUESTIONS